
# Geometrical modification of weld lines for high performance plastics in injection molding

**Master-Thesis**

**Andreas Kaufmann, BSc**

Chair of Polymer Processing
Department of Polymer Engeneering and Science
Montanuniversitaet Leoben

in cooperation with

Hoerbiger



| | |
|---|---|
| Supervision: | Dipl.-Ing. Marian Janko, |
| | Ass.Prof. Dr.mont. Thomas Lucyshyn |
| Assessment: | Univ.-Prof. Dr.mont. Clemens Holzer |

Leoben, June 2013

# Affidavit

I declare in lieu of oath,
that I wrote this master thesis and performed associated research myself,
using only the support indicated and literature cited.

| | |
|---|---|
| Leoben, June 2013 | |
| place, date | Andreas Kaufmann |

# Acknowledgements

I have been supported by many people while performing my master thesis and the studies leading to it and I am grateful to have the opportunity to express my gratitude to them.

My thanks go to Clemens Holzer, Head of the Chair of Polymer Processing at the Montanuniversitaet Leoben for giving me the opportunity to compose this thesis.

Special thanks goes to Bernhard Spiegl, Head of R&D and Technology Compressor Soolutions from Hoerbiger, who offered the possibility of performing my thesis. Further thanks to my colleagues at the Hoerbiger Ventilwerke in Vienna for giving technical support in the laboratory, namely Georg Singer, Siegfried Kugler and Ute Kutschera.

Further I would like to express my gratitude to Marian Janko and Thomas Lucyshyn for many fruitful discussions. As my supervisor Marian Janko encouraged me in my work and helped me finding answers to occuring questions, mastering different tasks and giving thought-provoking impulses.

I thank the staff of the Department of Polymer Engineering and Science especially Eduard Leitner for technical support.

Special thanks goes to my study colleagues with whom I worked and studied together in the past five years, especially Patrick Pazour, Michael Kessler, Hans-Jürgen Luger and Filipp Pühringer further to my friends Andreas Winroither, Patrick Allen, Peter Foith and Jörg Guido Schauberger.

My heartful gratitude goes to my family for giving me the opportunity to study as well as financial and mental support.

# Abstract

The aim of this thesis was to improve the mechanical properties of weld lines by two different approaches. On the one hand a variation of processing parameters was performed. On the other hand geometric modifications of the weld lines should enlarge the weld line area created and improve fiber orientation resulting in stronger weld lines.

A double dumbbell specimen mold including a movable flow obstacle for the weld line modification was used. With this mold a specimen with a common weld line and a specimen with a modified weld line can be produced in one shot.

Using a design of experiments the effects and interactions of processing parameters on the mechanical properties of specimens with "commmon" standard and modified weld lines were studied and compared to the results from literature and comparable.

The investigated processing parameters seem to play an unimportant role for the improvement of the weld lines. On the other hand this makes the injection molding process robust and insensitive to minor fluctuations of processing parameters. Only the melt temperature has a significant influence on the weld line strength.

Due to the geometric modification of the weld lines a drastic improvement of flexural properties and a significant increase of the tensile properties was achieved.

Furthermore the structure of the modified weld lines was examined. Using incident light and darkfield microscopy polishes were scanned and a three dimensional model of a modified weld line was created. These investigations show that the weld line area of the modified weld line specimens was delocated from the original position, where the weld line area was expected to be. Furthermore, observations proved that the fiber orientation enhances weld line strength in the modified weld lines.

The influence of five different obstacle head geometries was tested. The head geometries showed to have less influence on the weldline strength but some shapes have advantages in the injection molding cycle.

# Kurzfassung

Ziel dieser Arbeit war die Verbesserung der mechanischen Eigenschaften von Bindenähten durch zwei unterschiedliche Ansätze. Einerseits wurde eine Prozessparametervariation innerhalb eines Versuchsplanes durchgeführt, andererseits sollte die Bindenaht geometrisch modifiziert werden. Bei der Modifizierung sollte die Bindennahtfläche vergrößert und die Faserorientierung verbessert werden.

Für die Versuche wurde ein Werkzeug mit zwei Kavitäten verwendet, welche ähnlich den Normzugprüfkörpern sind. Eine Kavität ist mit einem beweglichen Fließhindernis versehen, welches die enstehende Bindenaht modifiziert. Es können somit pro Schuss zwei Prüfkörper hergestellt werden, einer mit "gewöhnlicher" Bindenaht und einer mit modifizierter Bindenaht.

Der gewählte Versuchsplan enthält einen Zentralpunkt und wurde zur Evaluierung der Effekte und Wechselwirkungen der Prozessparameter auf mechanische Eigenschaften durchgeführt. Die Ergebnisse der Standard-Bindenähte sind mit der Literatur vergleichbar.

Die untersuchten Prozessparameter waren, außer der Schmelzetemperatur, nicht signifikant. Das macht den Spritzgussprozess robust und unempfindlich gegen geringe Schwankungen der Prozessparameter.

Durch die geometrische Modifizierung der Bindenaht konnte eine drastische Verbesserung der Biegeeigenschaften und eine signifikante Verbesserung der Zugeigenschaften erreicht werden.

Weiters wurde die Struktur der modifizierten Bindenähte mittels Auflicht- und Dunkelfeldmikroskopie untersucht und ein dreidimensionales Model der modifizierten Bindenaht erstellt. Die Untersuchungen ergaben, dass die modifizierte Bindenahtfläche von der Position des Fließhindernisses abwich. Durch die Faserorientierung, welche bei der Modifizierung der Bindenaht entstand, wurden höhere Bindenahtfestigkeiten erreicht.

Es wurden fünf verschiedene Geometrien zur Modifizierung getestet und deren Verhalten während der Produktion bewertet. Der Einfluss der Geometrien auf die Bindenahtfestigkeiten war gering, aber manche zeigten Vorteile in der Produktion.

# Contents

# Chapter 1

# Introduction and purpose

Over the past decades polymers began to substitute more and more metal components, an example are valve plates in compressor technology. The conventional steel valve plates in reciprocating compressors were substituted by high performance polymers, which have some advantages.

The standard valve plate by the company Hoerbiger(Fig 1.1a) is produced by cutting the flow passages out of an injection molded full disk, the so called "slug". This process requires more time and nearly twice the material than valve plates produced by injection molding only. The ongoing flow optimizing of the valves made the valve plates complex so these valve plates of the new valve generation (shown in Fig 1.1b) are produced by injection molding.

Unfortunately there is an immutable flaw in these products, resulting from its geometry - the weld lines. Fig 1.2 shows a Moldflow filling simulation of the new generation valve plate, the weld lines are marked with black lines.

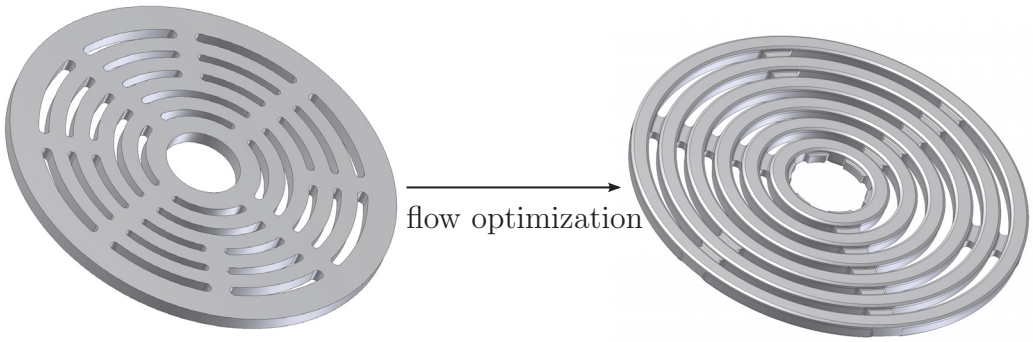


**Figure 1.1:** Evolution of a valve plate. In a) a common valve plate is shown, which is milled out of a slug. Next generation valve plates, shown in b), which is produced by injection molding only, no more milling is required. Images [26].

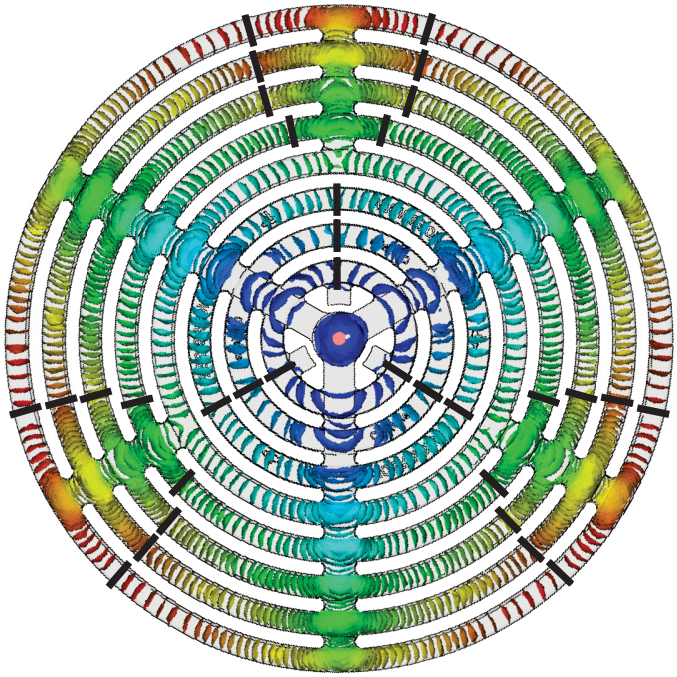


**Figure 1.2:** Filling study of the next generation valve computed with Moldflow. The inlet is in the center of the valve. Colors from blue to red show the melt front at different times during the filling. The weld line positions are marked black. Image [26].

To improve weld lines two possibilities were considered and tested: a) processing parameters and b) a geometric modification of the weld line. It is well known that weld lines decrease the mechanical performance of parts, especially when fiber reinforced polymers are used. For the valve plates a fiber reinforced polyether ether ketone (PEEK) is used which bears the hard working conditions.

To investigate the influence of parameters and test a new weld line modifying system a prototype specimen mold was created with two cavities, for production of dumbbell specimens similar to the requirements of the ISO 178:2003. Several modifications of the mold are possible.

One option is to produce specimens with common (standard) weld lines and specimens with modified weld lines simultaneously. One cavity is modified with a spring loaded, movable, exchangeable flow obstacle, which can be adjusted manually before production. There were five different head geometries of the flow obstacles tested. Due to the obstacle the melt flow is first redirected and then the obstacle is pushed back out of the cavity by the polymer resulting in a different kind of weld line. The modified weld lines have an increased weld line area produced by the movable flow obstacle. Another option is to produce specimens without weld lines by changing the sprue system.

A design of experiments was used to gain information about the dependence of standard and modified weld lines of processing parameters, where melt temperature, holding pressure and injection speed were varied. The mechanical properties of these specimens were compared.

Furthermore, the specimens were inspected using incident light or dark field microscopy. Cuts were made in and perpendicular to the length axis of the specimen. These pictures enable a estimation of the formation of the modified weld line. Even a three dimensional model was compiled to give an idea about the emerged weld line area.

The purpose of this thesis is to identify the influence of processing parameters and the efficiency of a geometrical improvement of weld lines. The system of the movable flow obstacle can be used not only for valve plates but for any other part with a certain geometry in the weld line area, making it suitable for many applications.

# Chapter 2

# Literature Review

The following literature review contains general information about the used material and the benefits of it. The difficulties arising with weld lines are discussed and some solutions and improvements for specific problems are presented. Furthermore, the influence of fillers in a polymer matrix on weld lines is discussed. Finally an overview of the influence of processing parameters is given.

## 2.1 Polyether ether ketone

The first polyether ether ketone (PEEK) was produced by Imperial Chemical Industries (ICI) in the year 1978 [5, 51]. 1979 ICI produced unreinforced PEEK as well as PEEK with 10 and 20 % short glass fibers (GF). In 1981 they started to sell other polyaryl ether ketones (PAEKs) reinforced with 20 and 30 % short carbon fibers (CF) [27]. Today PEEK types are available filled with ceramic, GF, CF or CF and graphite [2]. Blends with Poly(tetrafluoroethylene) (PTFE) give PEEK even better tribological and self-lubricating properties [62]. Furthermore, PEEK is reinforced with endless CFs for manufacturing laminates for a great variety of applications [17, 54].

PEEK is a semi-crystalline thermoplastic material, which has an aromatic backbone with ether and more rigid ketone linkages, the structural formular of PEEK is shown in Fig 2.1. The aromatic backbone reduces chain mobility. These facts result in a high glass transition temperature ($T_g$) of 143 °C and a very high melting temperature ($T_m$) of 334 to 340 °C [19,27]. The continuous operation temperature is up to 260 °C [5,19,27].

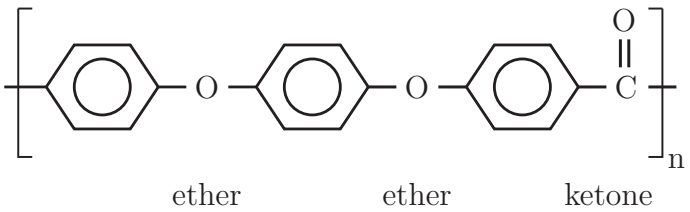


**Figure 2.1:** Structural formular of polyether ether ketone (PEEK). Inspired by [27].

PEEK is highly polar and resists many chemicals, like non oxidizing acids and strong alkalies, as well as hot water and steam, fats, oils and organic solvents. UV light and oxidation are harmful for PEEK. Furthermore, the fire behavior is favorable [27].

PEEK is flame resistant, swells when burning by building char. This char residue is about 70 % of the polymer. While burning the heat release is about 31 kJ/g which is about one eighth of polyethylne (PE). If PEEK is reinforced with GF, the residue is even bigger because the used filler does not burn and heat release is lower. In the case of CF reinforcement the residue is the same, but the heat release rate is different and more gradual [50].

PEEK has a very good mechanical performance at higher temperatures e. g. low creep deformation and good tribological behavior [27]. The crystallinity in injection molded PEEK products is about 25 to 30 % [51], the achievable maximum is at 48 % [19]. The tensile modulus of unreinforced PEEK is 3500 to 4000 MPa. The tensile modulus of GF reinforced PEEK as well as CF and graphite reinforced PTFE PEEK blends is about 11000 MPa. CF reinforced PEEK has the highest tensile modulus up to 25000 MPa [2]. If PEEK is used as a matrix material for laminates the modulus is even higher.

Further on its high toughness and stiffness, advanced tribological properties, chemical, environmental and thermal resistance, physiological inertness as well as good fatigue behavior are favorable. PEEK has a density from 1265 to 1500 kg/m$^3$ depending on crystallinity and filler content [19]. Good adhesion to CF makes it a suitable matrix material for mostly CF reinforced materials and laminates [17]. With increasing CF content thermal conductivity and thermal properties increase. GF have the advantage to improve mechanical properties and reduce thermal expansion [5]. These aspects are considered important in medicine, where PEEK laminates are used as bone plates [54]. In other cases PEEK is used as bearing material, in aerospace engineering as well as in electronic and automotive industry [19, 27, 41].

Another important aspect of materials used in engineering is their performance in case of failure. One aspect is fracture behavior, another aspect is fatigue crack growth. Laminates fatigue behavior of CF reinforced PEEK was investigated and compared to the behavior of CF epoxy systems. The CF PEEK system performed in a better way. These systems did not suffer so much delamination due to good fiber matrix adhesion. The ductility of PEEK as a matrix inhibits the development of local fiber failure and crack growth. Further on this system is nearly inert to hydrothermal aging [17, 41].

## 2.2 Weld lines

### 2.2.1 Introduction, definitions, formation

In many products manufactured by injection molding weld lines occur. Weld lines are also called "knit lines" or simply "welds". They are formed whenever two melt streams recombine creating an area of inferior properties compared to the bulk. The inferiorities can be assessed in monotone, dynamic and impact tests [39]. Malguarnera et al. [34] and Fellahi et al. [20] made literature reviews containing acquired knowledge. Tomari [56] states that within weld lines stronger and weaker parts exist depending on the distance to the part's surface.

Though it is common knowledge it is worth mentioning that there are three main influences on the properties of plastic parts: a) molecular configuration (including additives and fillers / reinforcements), b) processing conditions and c) testing conditions [34].

The term "weld line" is common to everyone working in fabrication of plastics. Nevertheless this term is wrong. The "line" which can be seen on a product surface is just the optical defect of this phenomenon. The correct term would be "weld region", "weld zone" or "weld plane" [13,20,34], see Fig 2.2. Nonetheless the term "weld line" is going to be used here as it is used in literature. The properties of the weld line strongly depend on the shape of the three dimensional area, which is formed when two melt streams (re)unite. Different methods of changing the weld line shape are summarized by Fellahi et al. [20].

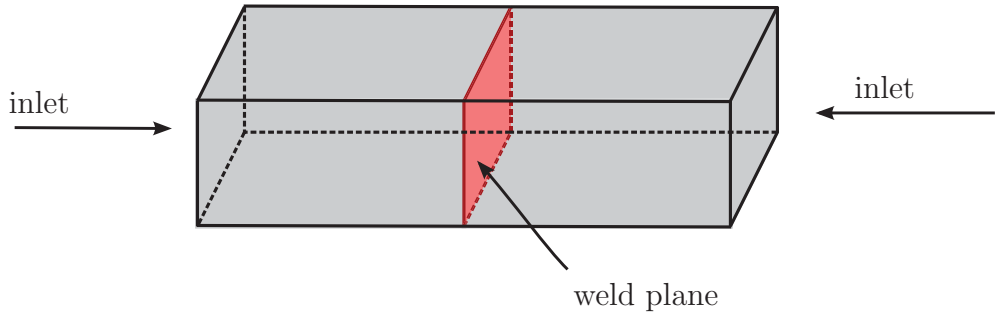


**Figure 2.2:** Schematic sketch of a weld plane which is formed by two colliding melt streams. This "plane" (pictured in red) can have a highly complex three dimensional appearance.

Literature distinguishes between two basic types of weld lines, sketched in Fig 2.3: "cold" or "butt" weld lines and "hot" or "streaming" weld lines [7, 9]. If two melt streams collide and the flow stops a cold weld line is formed. This is the weaker weld line type because no further process helps the streams to (re)unite or improves their molecular entanglement. A typical example for the formation of cold weld lines is multiple gating. A filling study of a cold weld line can be seen in chapter 4 Fig 4.1. Hot weld lines are formed when two melt streams (re)unite and flow on together to fill the rest of the cavity. Hot weld lines are produced by cores, pins or inserts and can not be prevented or eliminated. Whereas cold weld lines can sometimes be improved by changing the cold weld lines into hot weld lines by using a overflow cavity.

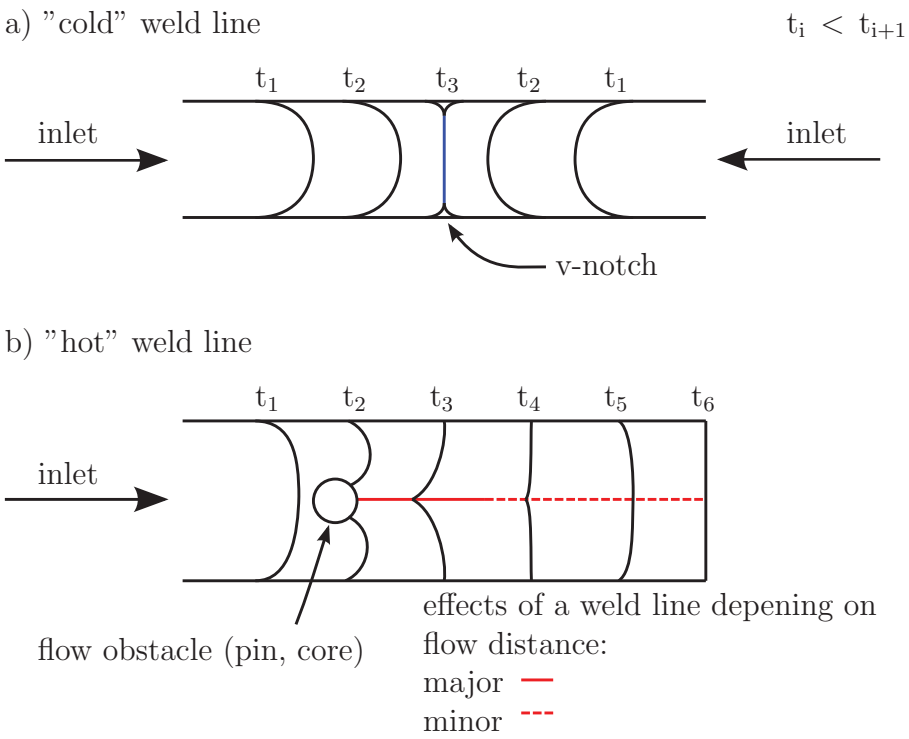


**Figure 2.3:** Two different types of weld lines are reported in literature: a) "cold" and b) "hot" weld lines. In both figures the melt front is pictured at different times $t_1$ to $t_6$.
This shows in a) that the fronts meet at first in the middle of the cavity then filling it completely. If no proper venting system exists in the mold a v-notch emerges more likely, shown in a). A real filling study of the specimen used in this work can be seen in chapter 4 Fig 4.1 in $a_1$ to $a_4$.
In b) the melt front is divided into two streams by a flow obstacle. After it the two melt fronts reunite forming a "hot" weld line. Literature differs concerning the effect of the weld line over the flow distance. In the sketch the effect of the weld line tails off with progressing flow distance. Inspired by [21, 23, 39].

Summing up, there are six possibilities how a weld line can occur:

- multiple gating
- flow obstacles (e. g. cores, pins)
- variable part thickness
- jetting (due to the free surface of the frozen jetting stream)
- inserts
- co-injection molding

The first four reasons are mentioned by many authors [10, 15, 24, 45, 60], inserts as a reason are added by Mennig [39] and the process of co-injection molding by Malguarnera [34].

When a weld line is created melt streams collide under a certain angle. If the angle is 0 ° two streams are colliding head to head. The flow stops and a cold weld line is formed. This angle is influenced by the geometry of the flow obstacle. This was found by Ozcelik et al. [47], who investigated on the best angle for the obstacle to improve weld line properties. Yokoi and Murata et al. [61] claim that there is a vanishing angle for weld lines, which is between 120 to 150 ° for various polymers.

Many papers use the **weld line factor** to compare weld line properties to bulk properties [40]. Non weld line samples are compared to samples inheriting a weld line. This factor is calculated with equation (2.1).

$$\text{weld line factor} = \frac{\text{test result of weld line specimen}}{\text{test result of non weld line specimen}} \tag{2.1}$$

Normally that factor has a value between 0 and 1. Best is 1, meaning no loss of property due to the weld line. Further the material, processing and test settings have to be identical for both specimens with and without weld line. Using this factor makes comparison of different process settings etc. easy [14, 45, 55]. A weld line factor which is determined for one single type of polymer and property is valid for this particular combination only. Criens et al. [15] found out that the weld line factor is not influenced by the diameter of obstacles or the melt temperature concerning the yield point for polycarbonate (PC). But those effect the point of fracture.

### 2.2.2 Reasons causing the problems with weld lines

The reasons of the weakness of weld lines compared to the bulk were investigated by many different scientific groups. Subsequently a list of influences on the weld lines and their effects is summarized.

- Due to the separated melt fronts the molecular entanglement over the weld line is less than the entanglement in the bulk. The fewer molecules are entangled the weaker is the weld line. There is chance of **molecular diffusion**. If many molecules diffuse from one stream to the other weld line strength is better than if there is no diffusion and just adhesion. Furthermore, orientation of molecules in and near the weld lines differs greatly from that in bulk. Molecular diffusion needs time, this is why the weld line factor in hot weld lines improves with increasing distance after passing the flow obstacle (see Fig 2.3b), distance to the cold mold wall, increasing temperature and with decreasing viscosity, shown in Fig 2.4 [12, 20, 24, 34, 35, 40, 45, 56, 58].

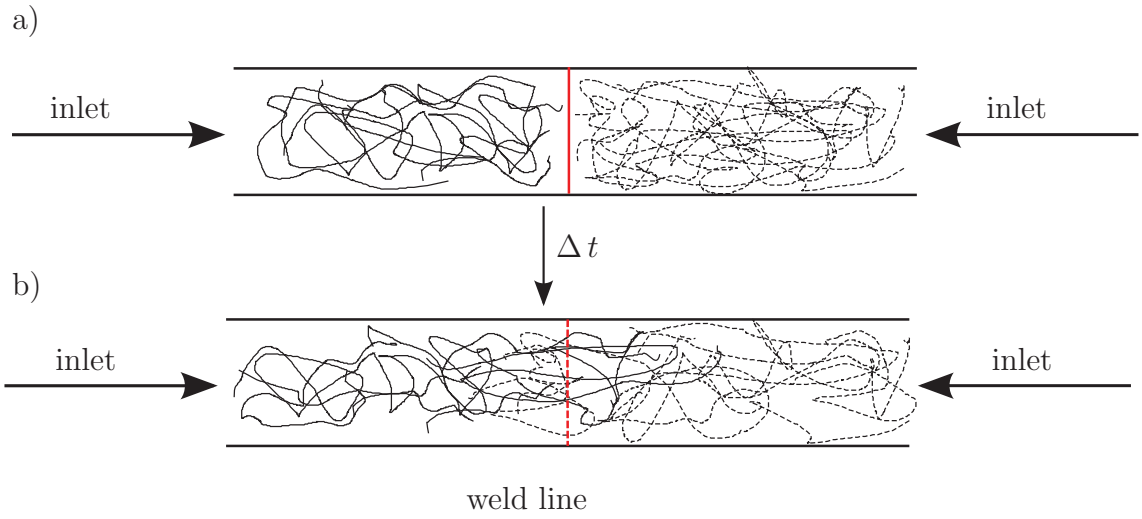


**Figure 2.4:** Diffusion of macromolecules: a) After the polymer fronts meet the molecular diffusion starts. Providing a weld line with temperature and time entanglement of molecules, especially in amorphous polymers, improves. In b) high entanglement of the molecules can be seen. Inspired by [40].

- Similar to the orientation of molecules, **orientation of fillers** differs greatly from weld line to bulk [12, 31, 49]. Fillers, their orientation and effects on weld lines are discussed later in section 2.2.4.

- Molecular orientation and temperature cause differences in weld line **morphology**. It highly depends if the weld line surface or a region behind the weld line is examined. Investigations showed that spherulithes at the weld line grow differently [24]. Generally crystallization of semi crystalline polymers is highly complex and depends on cooling rate and time, nucleating agents, melt and mold temperature and others [34].

- Polymeric blends (as PP/PC, PP/EPDM, HDPE/PA6) show layers of matrix and the incorporated material. The incorporated material is deformed due to shearing and orientated in flow direction, leading to minor propterites of the weld line. This happens due to shearing and deformation caused by fountain flow. This phenomenon was investigated on cold weld lines [20].

- Another reason for weak weld lines are **contaminations**. Normally molds should be clean but often lubricating grease is used to ensure steady production or mold release agents which reduce adhesion of the colliding melt streams weaken the weld line. Also a thermally damaged melt stream surface reduces strength and quality of the weld line. This thermal damage can appear when the "Diesel" effect burns material before the streams unite [12, 39].

- **Microvoids** were observed on the interface of cold weld lines only. They are small in size but nevertheless they are flaws and weaken the weld line [12, 37, 49].

- Finally another well known phenomenon, which has great influence on weld line strength, is the **v-notch**, depicted in Fig 2.3 and Fig 2.5. It is not only an optical

defect but a mechanical one, resulting in stress concentration on the notch root. This favors crack growth and failure at the weld line. A reason for the formation of such a notch can be entrapped air or high polymer viscosity [20, 34]. If the product is a part with high surface-finish requirements, an optical defect is a great problem, especially in transparent polymers.
Kobayashi et al. [31] used aluminum flakes as filler and discovered that these particles are reorientated and turned during the formation of a weld line. There was a strong visual effect produced due to light reflection by the orientated flakes at the weld line.
Hobbs [24] found that the v-notch perishes if the mold temperature is high enough. A high mold temperature means longer cycle times and therefore this method can only be used within limits. Tomari et al. [58] measured the depth and width of v-notches. According to their work the depth of v-notches is up to 0.3 mm for polystyrene depending on the holding pressure. The width of the notch increases with fiber content, because more fibers result in higher anisotropy and then the weld line properties differ stronger from the bulk due to different fiber orientation [37]. Further on cooling time, injection pressure and mold temperature have some, but melt temperature the greatest influence on the v-notch's width. Low melt temperature results in small width for high density polyethylene (HDPE) [12].

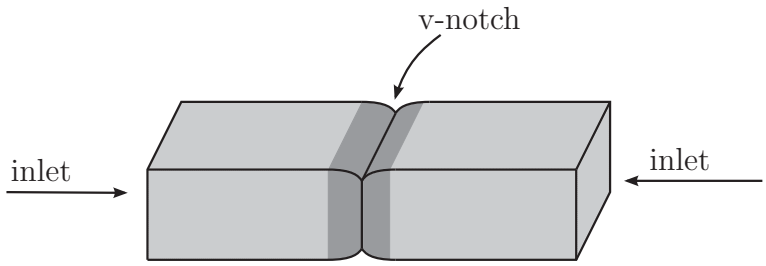


**Figure 2.5:** V-notch at a cold weld line.

### 2.2.3 Improvement of weld lines

Due to the shape, product complexity and functionality of most injection molded parts it is not simply possible to avoid weld lines. This leads to the idea of improving the behavior of the occurring weld lines. There are four main actuating variables which have to be considered [35, 44]:

- polymer type
- geometry
- processing conditions
- the kind of loading

Generally amorphous materials are less influenced by a weld line than semi crystalline thermoplasts or blends. For brittle thermoplasts weld lines are more critical

than for ductile thermoplasts [45]. As already mentioned the morphology of weld lines differs greatly from the bulk [24], this affects semi crystalline polymers stronger than amorphous ones. Polymeric materials like polystyrene (PS) are blended to improve properties like impact resistance. The modifiers can have positive as well as negative effects on the weld line factor, depending on the property examined [38]. Subsequently a list containing several improvement possibilities for weld lines is presented:

- In the past the **prediction** of weld lines could only be done by trial and error in complex geometries. Since the last decade computer performance improved significantly. Now it is possible to predict certain aspects of weld lines by **simulation**. Today different software tools can be acquired on the market. The computed models are not reality and so they work only within limitations. Whereas the location and even the strength of a weld line can be predicted, these results depend on mesh size. The location is accurate and varies within millimeters, but the weld line strength varies over a broader range [16]. By time software improved and most results are very close to reality now [11, 47]. This makes simulation a fast tool for testing different geometries. Often experimental results and simulation differ, but the tendency shown by simulation is more often correct. This positive aspect of simulation makes it crucial to every plastic product development process. But here the fact has to be recalled that every simulation depends on material and processing data. If the data is unsatisfactory the simulation results will be as well [16, 30].

- If a simulation predicts a weld line in a critical part of a product a **geometric change** can improve the situation. Different options are listed below:

  - A possibility is to improve **wall thickness** where the melt streams meet. The relative weld line strength is independent from wall size, so a thicker wall makes the weld line carry a higher maximum load [13].
  - If increasing the wall thickness is no option the **position of the gating** can be varied. Due to that the weld line can be moved to a less critical position of the product. This might improve the parts performance, but it does not eliminate the problem of the existence of weld lines [34].

- Another improvement in weld lines is a proper **mold ventilation system**. The venting shall transport all air and low molecular material entrapped out of the cavity when it is closed and being filled. This is important, because entrapped air can cause the "Diesel" effect and favors the formation of v-notches [10, 13, 34, 35, 49].

- Experiments resulted in the fact that **obstacle geometry** and **size** as well as the distance of flow to the obstacle influence weld line quality. Unfortunately literature disagrees in the significance of these aspects.

  Early researches showed that obstacle geometry seems to be not significantly important. The only thing that influences weld line strength is the width of the obstacle perpendicular to the melt flow: The greater this distance the weaker the weld line [38]. Mosle and Dick [46] stated that in perforated plates the hole

diameter is the primary factor influencing mechanical properties, whereas Liu et al. [33] found out that circular geometries with the same pheripherical length as square geometries performed better. They discovered that the weld line quality improved with increasing obstacle size. Despite that Ozelik et al. [47] stated that the obstacle shape also has an influence, which is even greater than that of mold or melt temperature because the molecular orientation is influenced by the obstacle geometry.

Fisa et al. [21] concluded that neither the distance of flow, nor the obstacle diameter influenced the weld line strength significantly. He mentioned filler content as main variable that has to be considered when considering weld line strength.

The distance of flow after the obstacle seems not to be important. Nevertheless after a flow distance of 60 mm for amorphous acrylonitrile butadiene styrene (ABS) the negative effects of the weld line were negligible small and the sample nearly had bulk strength again. This distance could only be changed within a small range varying processing conditions [38]. The possibility of "forgetting" an obstacle like a pin or insert is an ability for unfilled and single phase polymers only. In filled systems the fiber orientation is disadvantageous and does not change with the distance to the obstacle or flow length [37]. This length is substantially longer for fiber reinforced thermoplasts. The fibers need more time respectively flow length to reorientate after the weld line. This length is between 20 to 40 cm. It cannot be varied by processing parameters and even filler concentration or pin diameter have no influence on this distance [52].

- The **choice of material** is another main factor. If a product contains weld lines a polymer with a high weld line factor should be chosen for usage. If this is not possible other methods have to be used for optimization. The main parameters of a material influencing weld line strength and quality are density and viscosity as well as the pvT behavior [16].
  Furthermore, filler type and content as well as orientation have to be taken into account. This is discussed separately in section 2.2.4.

- Using **special processing techniques** enables improvement of weld line properties.

  - A number of authors [11,23,28,48,57] claim that the **push-pull technique/ method** works satisfactory, especially for (fiber) reinforced systems because the fillers/fibers are reorientated in flow direction. This method works with two injection units at different gates. Both inject molten plastic until the mold is filled. Then one injection unit uses higher holding pressure than the other one and pushes material towards the other injection unit. Then the pressure difference can be changed and the material is pushed the other way. This cycle can be repeated several times. Especially when the part is thicker this system works well. In the best case the strength of the modified weld lines can be doubled. After a single push the weld line forms a "tongue profile", which has the best effects on the weld line. After that a change of pressure difference forms a "tooth profile". Using more strokes a "complex tooth profile" is formed, but the weld line strength does not improve any

more [11]. This dislocation of the weld line is sometimes called "back flow" [23, 57].
Hamada et al. [23] produced this phenomenon with only one injection unit using an unbalanced multi cavity mold, where one cavity has two inlets. Holding pressure was asymmetrical in that cavity producing an improved weld line. Tomari et al. [57] found out that the weld line strength amongst other properties depended on the deviation length. This length means the distance a weld line is dislocated, measured from its original point to the point dislocated furthest. The longer the deviation length the higher the weld line strength.

  - Another idea of improving weld lines is to use a **heated pin or core**. The higher local temperature shall lower the viscosity and minimize the frozen layer. Furthermore increased temperature allows molecules to entangle more easily. These effects shall lead to better weld line properties. Following two problems were reported: If a polymer is fiber reinforced the fibers conduct too much heat away from the emerging weld line and the desired effects vanish. The second problem appears when using more power to encounter the first problem. This results in too high temperature, which leads to unfavorable changes in morphology, namely bigger spherulites, which decrease mechanical properties. This concludes that amorphous unfilled materials perform better and are more suitable for this process [22].
  - As mentioned before molecular entanglement across the weld line is not as it would be favored. Often higher temperatures are used to achieve better entanglement. Recently a new method was presented, an **ultrasonic sonotrode** was used for performing in-mold oscillation experiments. Two experimental arrangements were tested: a) placing an ultrasonic horn on the mold to make the whole surface vibrate and b) placing it into the mold. Here only a small area, around and on the weld line was affected. Method b) showed better results and experiments concerning processing parameters were performed. Too high holding pressure has negative effects, a maximum temperature exists, above which the sonotrode has no more significant influence. Furthermore, oscillation time has an optimum after which the effects seem to be reversed. A reason for that can be dropping temperature during oscillation time due to cooling [32].

- **Processing parameters** influence properties of every injection molded part. This is valid for weld lines, too. Wu et al. [60] found out that unfortunately there is just a minor effect of the processing parameters on the weld line at least for tensile strength.
  The processing conditions were already the field of many researches and are discussed separately in section 2.2.5.

- **Annealing** is a certain temperature treatment of injection molded parts after production. This can be used to reduce residual stresses. Annealing has a positive effect on the morphology of weld lines if a semi crystalline polymer is not additionally nucleated. Due to nucleation the polymer forms more and smaller

crystallites, which perform mechanically better. Annealing would induce growth of the crystallites and so reduce mechanical properties [36].

### 2.2.4 Fillers and their influence on weld lines

Many different filler types are available and used today to reach the required performance or to reduce costs of polymeric products. There are many different kinds of fillers leading to even more different features of the produced compound. Following the different types of fillers and their aspect ratio are described. Further the effect of fiber content and fiber orientation in injection molded parts especially their influence on weld lines is summarized.

A classification of **filler types** can be made between natural and artificial fillers or between different geometries. Examples are fibers of different length (one dimensional), flakes (two dimensional) and cuboids or spheres (three dimensional), view Fig 2.6. Beside the aspect ratio the polymer to filler adhesion is very important. It should be big enough to transfer the load from the polymer to the filler [18].

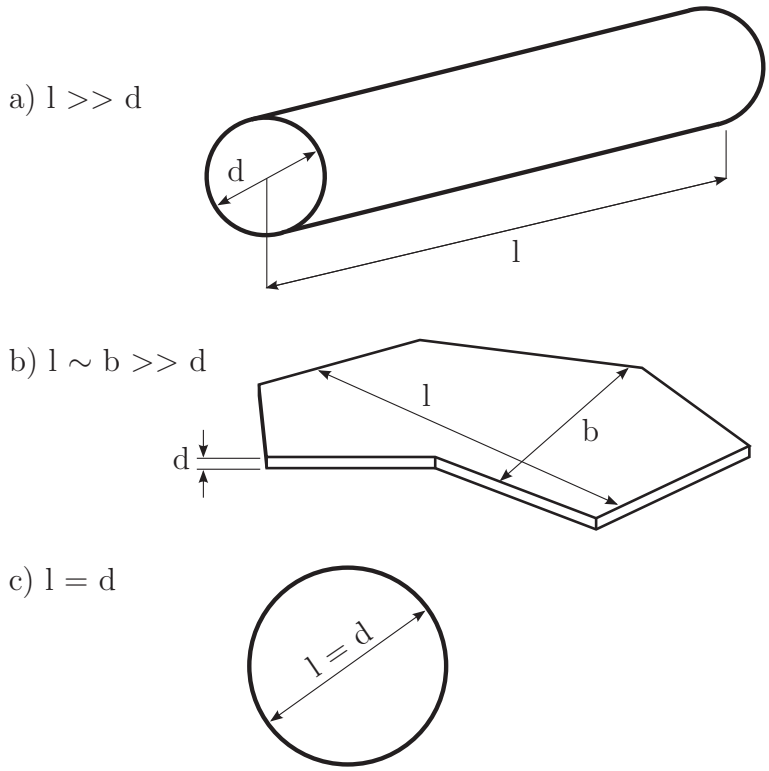


**Figure 2.6:** Filler types distinguished by geometry: a) one dimensional (fibers), b) two dimensional (flakes) and c) three dimensional (spheres).

A very common characteristic is the **aspect ratio** of a filler. It means the ratio of length (l) to diameter (d), often written as l : d, for instance a glass sphere has an aspect ratio of 1 : 1, length and diameter are equal. Fillers which have an aspect ratio of greater than 20 : 1 seem to be the optimized reinforcement. The higher

aspect ratio leads to higher orientation and to the anisotropic nature a filled polymer has. Bulk strength in flow direction increases with fiber orientation, fiber strength, fiber content and aspect ratio. Unfortunately the weld line factor decreases with these factors increasing, meaning more strength loss due to a weld line [13, 21, 53, 55, 59]. Another negative side effect of the increasing aspect ratio is that v-notches become deeper [52].

Polymers tend to build layers of different fiber orientation when filling the mold and cooling down at the same time. There are different **layer models**, but they agree on the fact that fiber orientation is different in their layers. The first model presented here is speaking of three layers (skin - core - skin) [21,49,52,59] the second one of five layers (skin - shell - core - shell - skin) [1]. Kenig [29] speaks of nine layers and explains the different types of flow, which result in the layered structure. He names the following four types of flow: a) spreading radial flow, b) converging flow, c) elongation flow and d) shear flow. Where a) results in transversal fiber orientation the others align the fibers in flow direction.

In the core fibers are orientated randomly, giving the core nearly isotropic properties. All models agree on that. The first model claims that the skin inherits highly orientated fibers. The second model mentions that the skin for polyamides and polypropylenes is 5 to 7 % of the sample thickness and this does not change with processing parameters. The core varies between 20 to 60 %, depending on the processing parameters, the rest is shell. In the skin and core layer fibers are orientated nearly randomly. Whereas in the shell the fibers are orientated in flow direction [1]. This phenomenon gives parts with thinner walls a higher relative strength in flow direction because a higher percentage of fibers is orientated in the same (flow) direction. If a sample has a fixed wall thickness the core thickness can be influenced by the processing parameters. The thicker a specimen the more core exists resulting in less strength because of less fiber orientation [1, 49].

There is a relationship between **fiber orientation**, concentration and layered structure. Orientation of fibers results from fountain flow of the melt in the mold. Fiber orientation depends on the layer of the part, the flow direction and on the existence of a weld line. Generally fiber orientation results in anisotropy. Mostly dumbbell specimens are tested, which have excellent properties in flow direction. If tensile specimens are milled out of a plate the results of anisotropy can be easily acknowledged by testing specimens in and perpendicular to the flow [8, 63].
Considering fiber orientation in the layered structure following facts come to interest. 75 % of all fibers in the skin are orientated $\pm 15\,^{\circ}$ to the flow direction. In the core only 45 % have this orientation, which means they are randomly oriented there [59]. There is a general drop in fiber content from core to skin. This drop is between 5 to 15 % depending on the method of measurement [1].

Considering the results of Vaxman et al. [59] it is easy to follow the findings of Fisa et al. [21]: They tested the strength of weld lines with a load applied perpendicularly to the weld line, but also in direction of the weld line. In the second testing arrangement they found the weld line to have higher strength than the bulk. The reason for that is the high fiber orientation parallel to the weld line over all layers. Another research found that the above described fiber orientation in the weld line effects shrinkage of

specimens. The weld line was measured and found to be thicker than the rest of the part because shrinkage was hindered due to fiber orientation [37, 52]. This statement is true for the investigated specimens of this work, see section 5.3.2.

Finally **filler content and filler distribution** are considered. It is commonly known that filled polymers inherit greater strength than unfilled compounds especially when fibers are used as fillers. An interesting fact is that the influence of processing parameters decreases with increasing filler content [13]. Fisa et al. [21] declared weld line strength to be a function of fiber content only. A reason for that is worse polymer-polymer melding at the weld line due to fiber content and fiber orientation at the weld line [59]. Although fiber orientation in weld lines differs drastically from the rest of the bulk, fiber content at the weld line does not, according to investigations of Meddad et al. [37], this group contradicts others in their paper. No concentration gradients could be located by Sanschagrin et al. [52].

If fiber length and fiber distribution are examined, higher fiber contents have the disadvantage of having a greater amount of smaller fibers. The shortening of fibers happens in the dosing phase [48].

### 2.2.5 Processing parameters and their influence on weld lines

There are a lot of processing parameters which have influence on the quality of produced parts. The same parameters influence weld lines. One has to keep in mind that all these parameters interact with the polymer and its modifiers and fillers. Afterwards the most important parameters (according to literature) are named. The influence of a parameter depends on the property observed as well as the testing methods. Literature does not agree completely in the importance of the single processing parameters, therefore the ranking starts with the parameter found most frequently:

- **melt temperature**
  With increasing melt temperature, molecular entanglement and diffusion speed rise and the "healing" effect of a weld line is improved. The disadvantages of an increased melt temperature are a higher cycle time [39] and a higher energy consumption. This factor is considered to be highly influential by [9, 10, 12, 15, 20, 33, 35, 36, 43, 46, 55, 60]. Another interesting fact is that non weld line samples have higher strength at lower melt temperatures because of higher molecular orientation. The orientated molecules have not enough time above the glass transition temperature to relaxe. Higher orientation means higher strength [15, 43, 45].

- **mold temperature**
  Considering mold temperature it is crucial to know if the used polymer is amorphous or semi crystalline and whether nucleating agents are used or not. High mold temperatures are preferred by [9, 12, 33, 35, 36, 60]. It was found that with higher mold temperature the width of the weld line decreases [60]. Selden [55] and Bown [10] found that depending on the material, especially for semi crystalline polymers e. g. polyphenylne sulfide (PPS), high mold temperatures can have negative effects. Due to higher temperatures crystallinity and the size of

crystals increases making the part without weld line more brittle, which results in less strength than a part with weld line at low mold temperatures. Other authors like Mosle and Dick [46] found the mold temperature to be of no importance for the weld line strength.

- **holding pressure**
  Concerning this parameter the literature also differs. Several authors claim that a higher holding pressure improves weld lines [9, 32, 55, 58], others neglect the importance of this parameter [34, 60]. Hamada [23] states that it depends on the cavity, especially for multi cavity molds higher holding pressure is beneficial. Especially in unbalanced multi cavity molds this can lead to pressure differences in the holding pressure phase, where the weld line is dislocated similarly to the push-pull technique.

- **injection speed**
  Again it depends on the polymer and filler (type and content). The optimization direction can be to higher or lower injection speed [12, 23, 35, 36, 55, 60]. Liu et al. [33] concluded that injection speed is a rather negligible factor.

- **Injection acceleration**
  Wu et al. [60] consider this parameter to be unimportant.

The differences in the literature result from the fact that many different polymers with different fillers are tested. This makes a comparison difficult and an investigation for a specific material necessary.

The material used for this thesis is a 30 weight% CF filled PEEK. This high perfomance material is necessary to bear the hard working conditions of the valve. Unfortunately no literature concerning weld lines of PEEK specimens was found.

The literature review describes the emerging of weld lines and their disadvantages and also points out which countermeasures can be taken. Unfortunately the high fiber content of the used material leads to the assumption, that processing parameters will play a minor roll in the improvement of weld line properties. The geometry of valves cannot be changed drastically, so a modification of the weld line itself shall facilitate a breakthrough.

# Chapter 3

# Material and machines

## 3.1 Material

For all experiments the material VICTREX PEEK 650CA30 from the company Victrex was used after four hours predrying at 150 °C . This PEEK is filled with 30 weight% CF. Further information about the material and recommended prozessing parameters are shown in Tab 8.1 to Tab 8.4 in the Appendix (page 91 to 93).

## 3.2 Machines

### 3.2.1 Injection molding machine

An injection molding machine of the type Engel e-motion 940 / 280, company Engel Austria GmbH, Austria, with 2800 kN clamping force and a screw diameter of 55 mm was used.

### 3.2.2 Tensile and flexural testing

For all tensile and flexural tests a standard testing machine of the type Zwick Roell Z010, company Zwick GmbH & Co. KG, Germany, was used with a 10 kN force sensor, precision class 0.05 %. For tensile testing a clamping system and a displacement transducer were used.

### 3.2.3 Microscopy

Then the polished samples were investigated in a microscope type Leica CTR6000 or Leica M205 A, both with a camera system named Leica DFC425, company Leica Microsystems GmbH, Germany.

## 3.3 Mold

The mold concept is a simple weld line specimen mold with two cavities and a special installation in one of the specimen cavities in form of a spring loaded movable flow

obstacle. The specimens are slightly modified from the specimen of the ISO 178:2003 to get closer to the valve plate ring shape. The width is 7 mm and the thickness is 5 mm (original ISO specimen: 10 x 4 mm). Fig 3.1 shows the shape of the two specimens and especially the shape of the flow obstacle in one of the specimens. The weld line specimen without flow obstacle is used to compare the standard with the modified weld line [25].

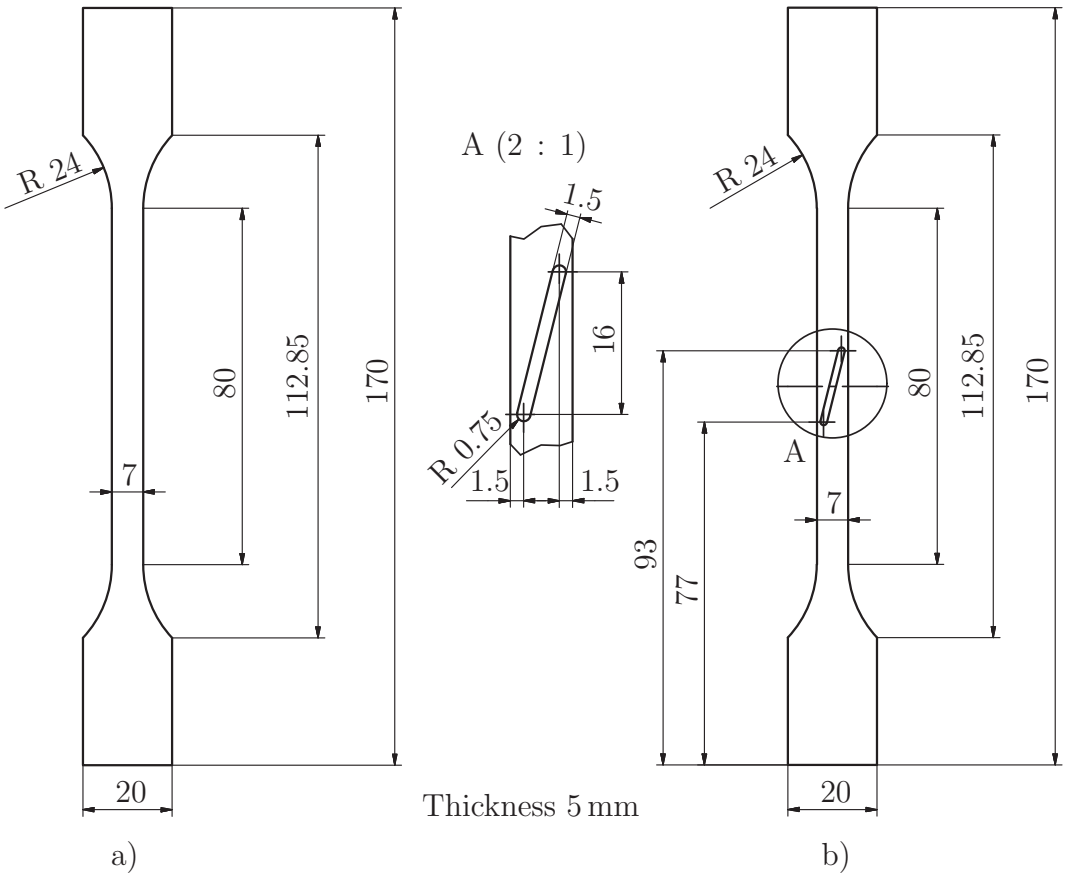


**Figure 3.1:** Geometry of weld-line specimens: a) standard weld lines and b) modified specimen with obstacle geometry. The difference to ISO 178:2003 specimens is the middle part which is here 7 mm x 5 mm instead of 10 mm x 4 mm (ISO). Inspired by [25].

The cross section of the ejector side (ES) of the mold is shown in Fig 3.2 to Fig 3.4. The changeable mold-insert with the contour-close generously dimensioned venting system can be seen. Fig 3.2 also reveals some information about the spring system on the outside of the mold. Details are pictured in Fig 3.3 to Fig 3.4, showing the movable stamp with the flow obstacle. At the end position the obstacle head lies flat in the mold surface. The stamp is connected to a lever that transfers the forces of the outer spring to the stamp. The immersion depth of the flow obstacle in the unfilled state is adjustable via the nut and counter-nut. The flow obstacle protruding into the cavity is shown in Fig 3.4. Under melt pressure the flow obstacle is pressed out of the cavity against the spring load and to a variable limit. The cavity surface was chosen to be

the limit of the stamp. This results in a little mark on the article surface, which is comparable with an ejection mark [25].

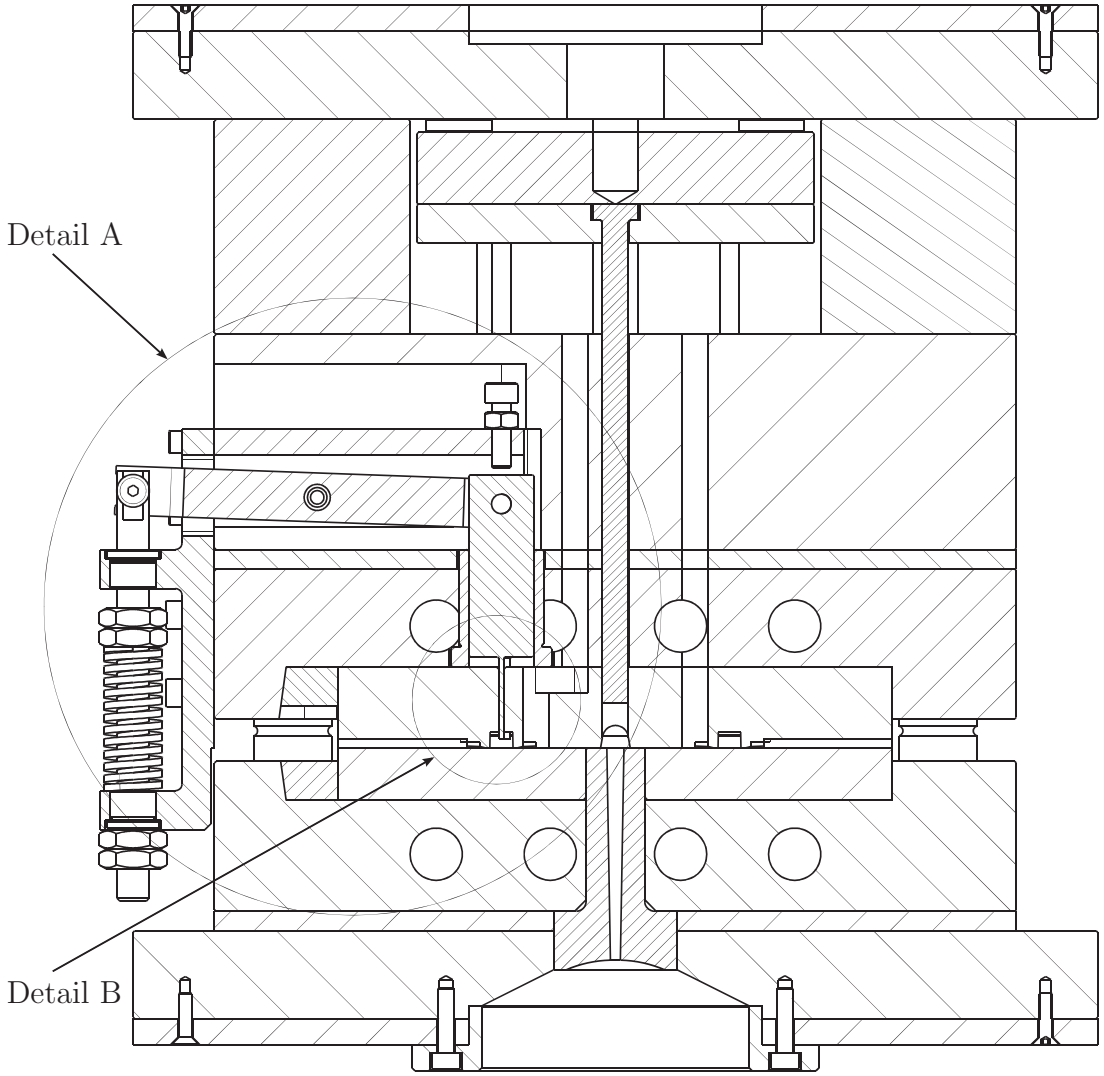


**Figure 3.2:** Cross section of the spring system which creates modified weld line specimens. Details A and B are shown in Fig 3.3 and 3.4. Inspired by [25].

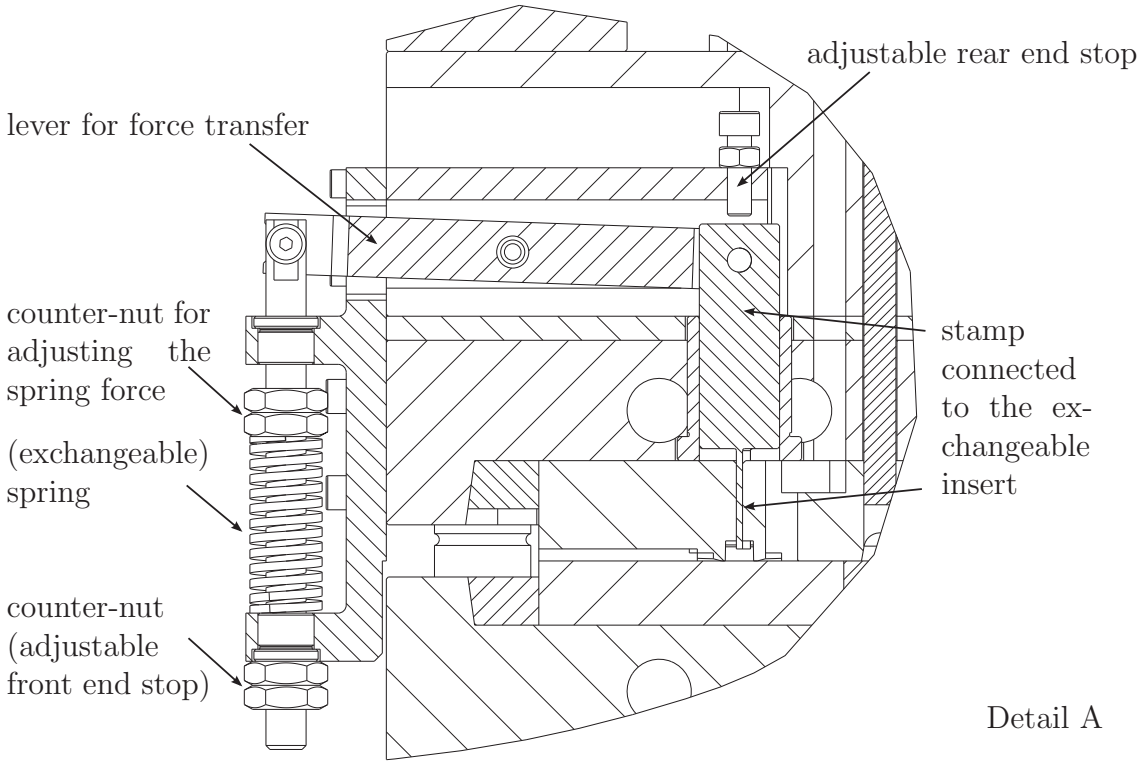


**Figure 3.3:** Detail A of the cross section of the spring system. Inspired by [25].

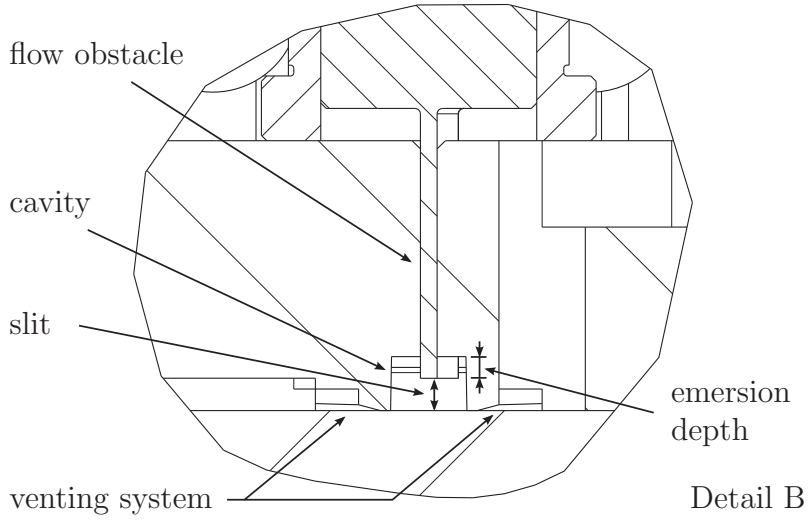


**Figure 3.4:** Detail B of the cross section of the flow obstacle and the cavity. The generously constructed venting system can be seen to both sides of the cavity. The flow obstacle is at an intermediate position. The slit can be adjusted manually for the plain insert. For all other flow obstacles (see Fig 3.7) no slit is required. Inspired by [25].

The mounted mold is shown in Fig 3.5 a) and b). The additional pneumatic cylinder which is necessary to relieve the spring load from the specimen when the mold is opened is shown in Fig 3.6 [25].

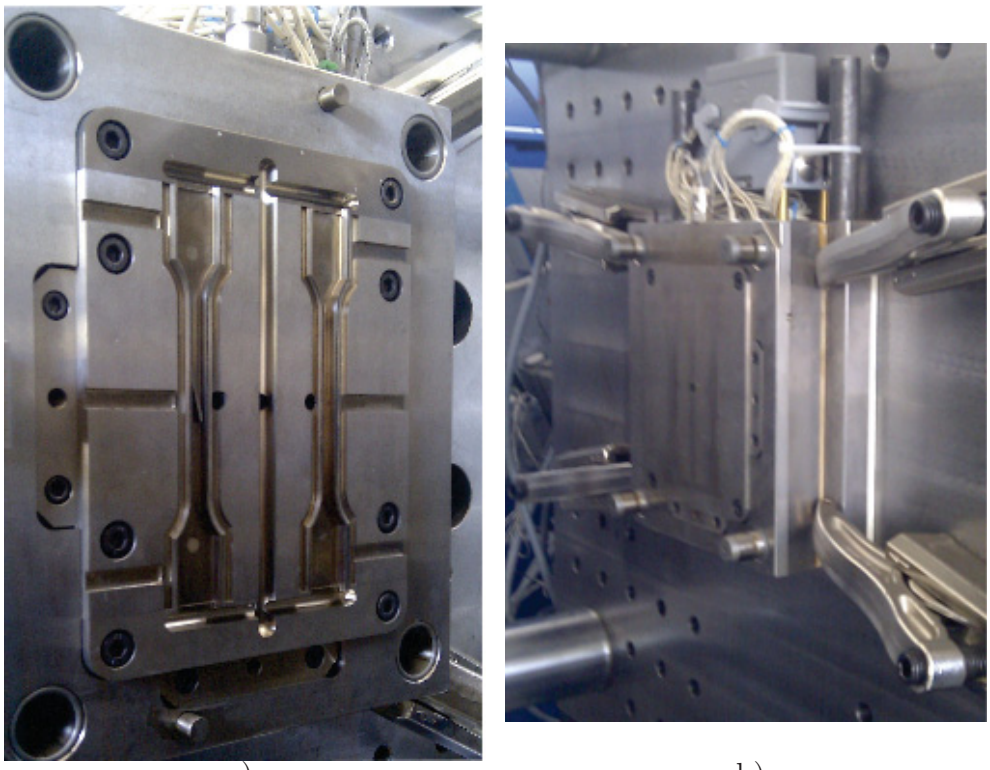

a) b)

**Figure 3.5:** Mounted mold. Ejector side is shown in a), nozzle side in b) [25].

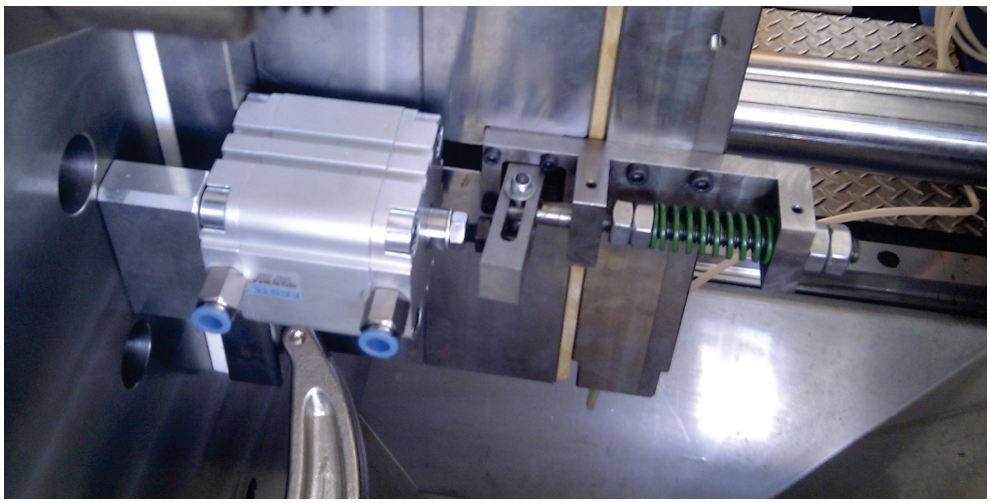

**Figure 3.6:** Spring system and pneumatic cylinder (to relieve the force from the flow obstacle) [25].

The movable flow obstacle is exchangeable. To investigate the influence of the insert head geometry on the weld line five different shapes were tested, which are shown in Fig 3.7. Geometric details are summarized in the Appendix 94.

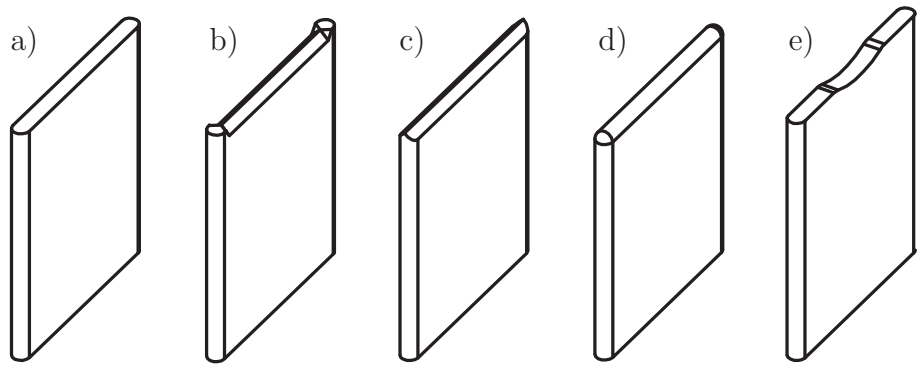


**Figure 3.7:** Different inserts with varied head geometries used as movable flow obstacles: a) plain, b) halfblade, c) blade, d) round and e) hole. The upper side points into the cavity. Inspired by [25].

# Chapter 4

# Experimental

The aim of this thesis is to investigate the influence of processing parameters on standard and modified weld lines in dumbbell specimens made out of PEEK 650AC. Further the differences between standard and modified specimens are evaluated and different head geometries are investigated. To gain data efficiently a design of experiments (DOE) was carried out and all different head geometries were tested concerning their effect on the tensile and flexural properties as well as their applicability for production.

## 4.1 Design of Experiments

In section 2.2.5 the main effects of processing parameters on weld lines are explained. Out of this literature review and preliminary runs three processing parameters were selected for the DOE: melt temperature, holding pressure and injection speed. A three factor two level ($2^3$) DOE including a center point was chosen for the investigation of effects. The center point is used to find nonlinearities in the dependences of mechanical properties from processing parameters. The high and low levels of this design were chosen in such a way that the whole DOE would produce fault free parts. All parts were filled up to approximately 98 % before applying holding pressure avoiding the maximum injection pressure limitation of 1800 bar. Furtheron no mold breathing and burr formation was accepted, which limits the holding pressure to 800 bar, view Tab 4.1.

**Table 4.1:** Levels of varied processing parameters of the DOE including a center point.

| **Processing parameter** | **level** | | |
|---|---|---|---|
| | **low** | **center point** | **high** |
| melt temperature | 410 ° C | 420 ° C | 430 ° C |
| holding pressure | 600 bar | 700 bar | 800 bar |
| injection flow rate | 15 $cm^3/s$ | 25 $cm^3/s$ | 35 $cm^3/s$ |

All other processing parameters and geometric modifications were held constant for the DOE. Their values were tested and evaluated before the DOE was set up.

Tab 4.2 shows the constant processing parameters and Tab 4.3 the geometric and spring settings.

**Table 4.2:** Constant processing parameters for the DOE.

| **Processing parameter** | **level** |
|---|---|
| dosing volume | $90\,cm^3$ |
| switch over point (volume dependent) | $32\,cm^3$ |
| dosing profile | constant $0.2\,cm^3\,s\,m^{-1}$ |
| back pressure | 110 bar |
| specific injection pressure limitation | 1800 bar |
| clamping force | 500 kN |
| cooling time after holding time | 30 s |
| mold temperature ejection side | 210 ° C |
| mold temperature nozzle side | 210 ° C |
| ejector position | 90 − 104 mm |
| cavity height | 316 mm |
| nozzle force | 10 kN |
| decompression after dosing | $10\,cm^3$ |

**Table 4.3:** Constant geometric and spring parameters for the DOE

| **Geometric modification** | **level** |
|---|---|
| spring constant | 2.8 N/mm |
| spring length released | 32 mm |
| spring length installed | 18.2 mm |
| spring force installed | 38.6 N |
| insert type | halfblade |
| immersion depth | 5 mm* |
| weld line (Yes/No) | Yes |

Melt temperature was varied as seldom as possible because changing the melt temperature is very time consuming. So a non randomized DOE was performed, see Tab 4.4. There were no replicates produced for this DOE for the same reason. For every level at least 20 specimens were produced. At least four specimens were tested in tensile testing and bending testing.

As the measurement of the melt temperature was not possible, the nozzle temperature was varied in the DOE, in Tab 4.4. Nevertheless the term "melt temperature" is

*5 mm are the cavity depth, which is used as end stop

used in this thesis. The settings of the zones of the cylinder temperature can be seen in Tab 4.5. The holding pressure from Tab 4.4 was held for 10 seconds and then reduced to 110 bar within the following 5 seconds. A constant profile was used for the injection rate. To finish the DOE within the shortest possible amount of time and to work cost efficient, it was necessary to change melt temperature as little as possible resulting in a non randomized DOE.

**Table 4.4:** Full factorial $2^3$ DOE including a center point (setting D5). Tab 4.5 contains the exact cylinder temperatures.

| **test setting** | **processing parameters** | | |
|---|---|---|---|
| **name** | **melt temperature** | **holding pressure** | **injection rate** |
| | in ° C | in bar | in $cm^3/s$ |
| D1 | 430 | 800 | 35 |
| D2 | 430 | 800 | 15 |
| D3 | 430 | 600 | 35 |
| D4 | 430 | 600 | 15 |
| D5 | 420 | 700 | 25 |
| D6 | 410 | 800 | 35 |
| D7 | 410 | 800 | 15 |
| D8 | 410 | 600 | 35 |
| D9 | 410 | 600 | 15 |

**Table 4.5:** Cylinder temperatures set for varying melt temperature. The first column shows the nozzle temperature, which is defined as melt temperature. All other zones are aligned from nozzle to feeder.

| **nozzle** | **zone 1** | **zone 2** | **zone 3** | **zone 4** | **feeder** |
|---|---|---|---|---|---|
| all temperatures in ° C | | | | | |
| 430 | 425 | 420 | 410 | 400 | 60 |
| 420 | 415 | 410 | 400 | 395 | 60 |
| 410 | 410 | 405 | 395 | 385 | 60 |

## 4.2 Interpretation of the design of experiments

Whenever the melt temperature was changed at least ten specimens were rejected after emptying and refilling the barrel when the cylinder temperature reached the prefered temperature. This procedure should remove all degenerated material from screw and cylinder and provide constant melt temperature.

Between two settings of the same melt temperature only one shot was rejected because holding pressure and injection speed are easily and instantly adjusted by the injection molding machine. There is no need to reject more parts because no time lagging influences on the injection molding process have to be considered compared to a change of temperature. This is the reason why all specimens with high or low temperature level were produced in a row.

Additionally to the DOE, a series of the setting D5 was produced without weld lines with a single gated mold insert. This specimens were used for the comparison of properties between the standard weld line, the modified weld line and the specimens without weld line. This series was perfomed on another day after changing the gating system.

As mentioned before experiments were made with different geometric modifications presented above in Fig 3.7. Before a new set of specimens with another insert head geometry was produced a filling study was performed. As an example the filling study of the insert "blade" is compared with a filling study of a standard weld line specimen in Fig 4.1. Two melt streams flow towards each other until they collide. In $b_1$ there is no difference to the "a" series because no flow obstacle hinders the flow. In $b_2$ to $b_3$ the shape of the obstacle becomes visible, showing that some melt also streams through the small gap between insert and mold. This weld line is going to be called "side weld line" and will show up in destructive testing and microscopy.

Proof that the inserts do not move until the cavity is filled is given in Fig 4.2, where two examples are pictured.

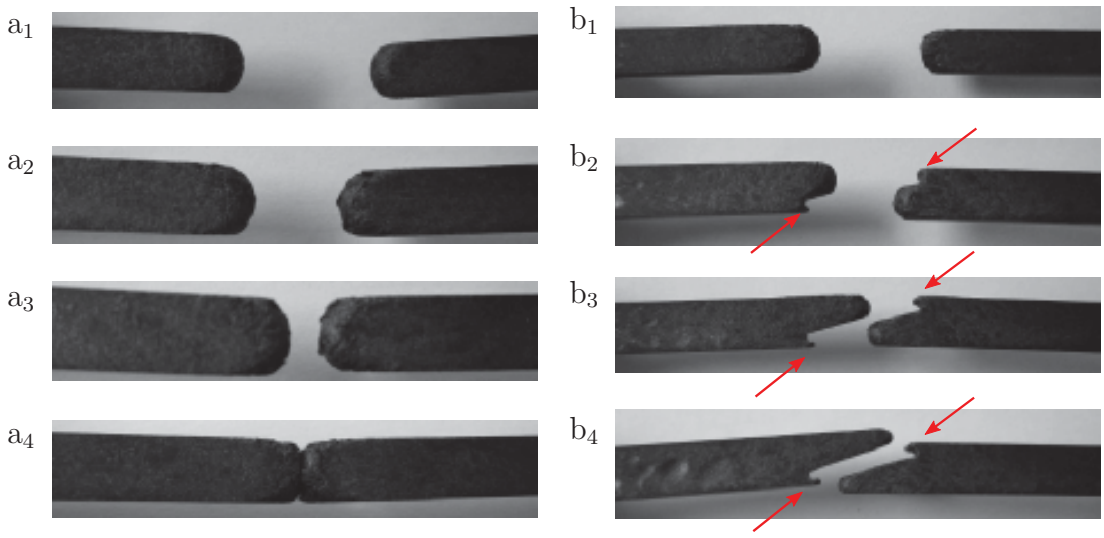


**Figure 4.1:** Filling study of a standard (a) and modified weld line of the insert type "blade" (b) with four consecutive points of time $a_1$ to $a_4$ and $b_1$ to $b_4$ respectively. The side weld line formation is marked with red arrows.

a)

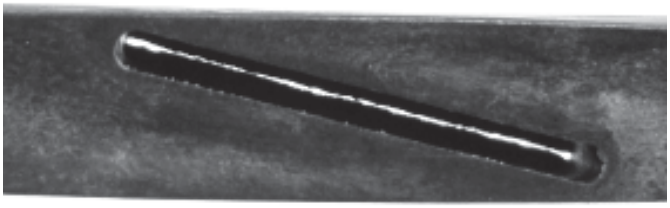

b)

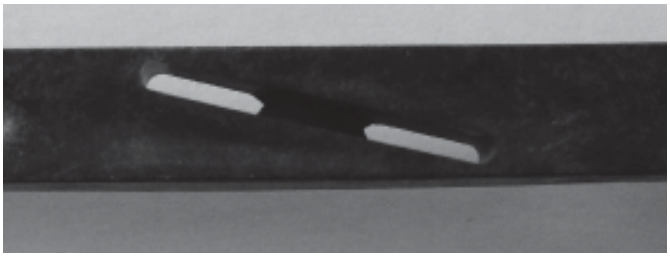

**Figure 4.2:** Proof that the inserts do not start to move until the rest of the cavity is full. These specimens were obtained by turning off holding pressure and filling the cavity to approximately 99 %, the insert has not moved at this point.
The modified specimen with a) insert blade and b) insert hole are pictured. In b) the hole which is provided by the insert is already filled. Applying more pressure would trigger the inserts. The other inserts show similar behavior.

## 4.3 Preparation of the specimen

Specimens for the mechanical tests were prepared in the following manner. Specimens without and with a standard weld line were cut off their sprue with a band saw and had no further preparation, see Fig 4.3. Specimens with modified weld lines were cut of their sprue as well and lapped to remove all the protruding material at the insert location. The protruding material was produced by the geometry of the insert head, see Fig 4.4. Lapping removed these surface defects and should reduce scatter of results. Although the lapping was performed carefully the specimen surface was partly influenced by this procedure, but it was assumed that this procedure did not have significant influence on the further testing. For tensile testing the specimens were deburred at the cutting position to guarantee proper clamping. Testing of specimens was performed with a minimum delay of 24 hours after injection molding.

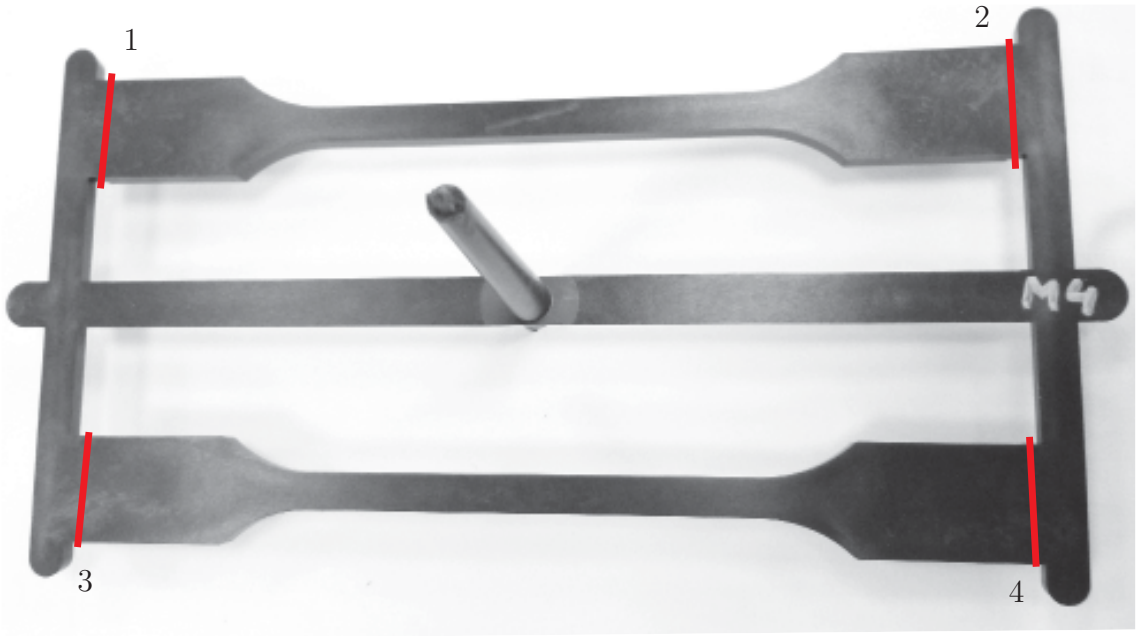


**Figure 4.3:** Specimens with sprue. The red marks show where the sprue was cut off before testing. For tensile specimens the cut surfaces were deburred.

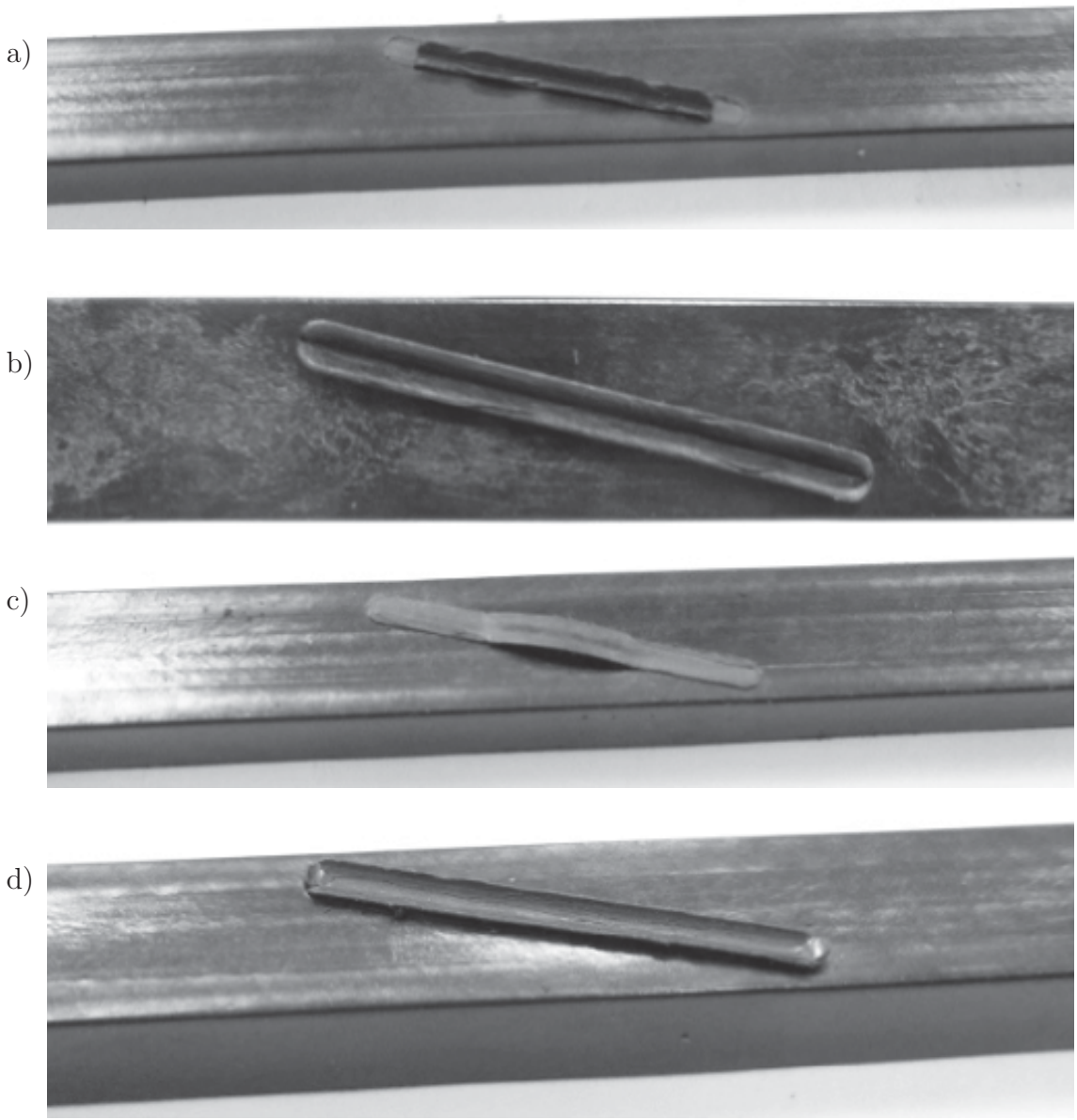


**Figure 4.4:** Protruding material of modified specimens: a) half-blade, b) blade, c) hole and d) round. The protruding material was lapped off before testing to guarantee equal testing conditions for modified weld line specimens, standard weld line specimens and specimens without weld line. Standard weld lines and the plain head geometry did not leave protruding marks.

### 4.3.1 Tensile testing

The tensile modulus was tested using an extensiometer. The extensiometer arms were set to ±30 mm from the middle of the specimen to measure the displacement during tensile testing, see Fig 4.5. This kind of measurement was used to gain more accurate data than from displacement measurements at the cross beam. Using an extensiometer has the advantage that it is not influenced by the deformation of the testing machine.

The specimens are inserted, clamped and the displacement transducer is positioned, then the measurement is started. The testing parameters are shown in Tab 4.6.

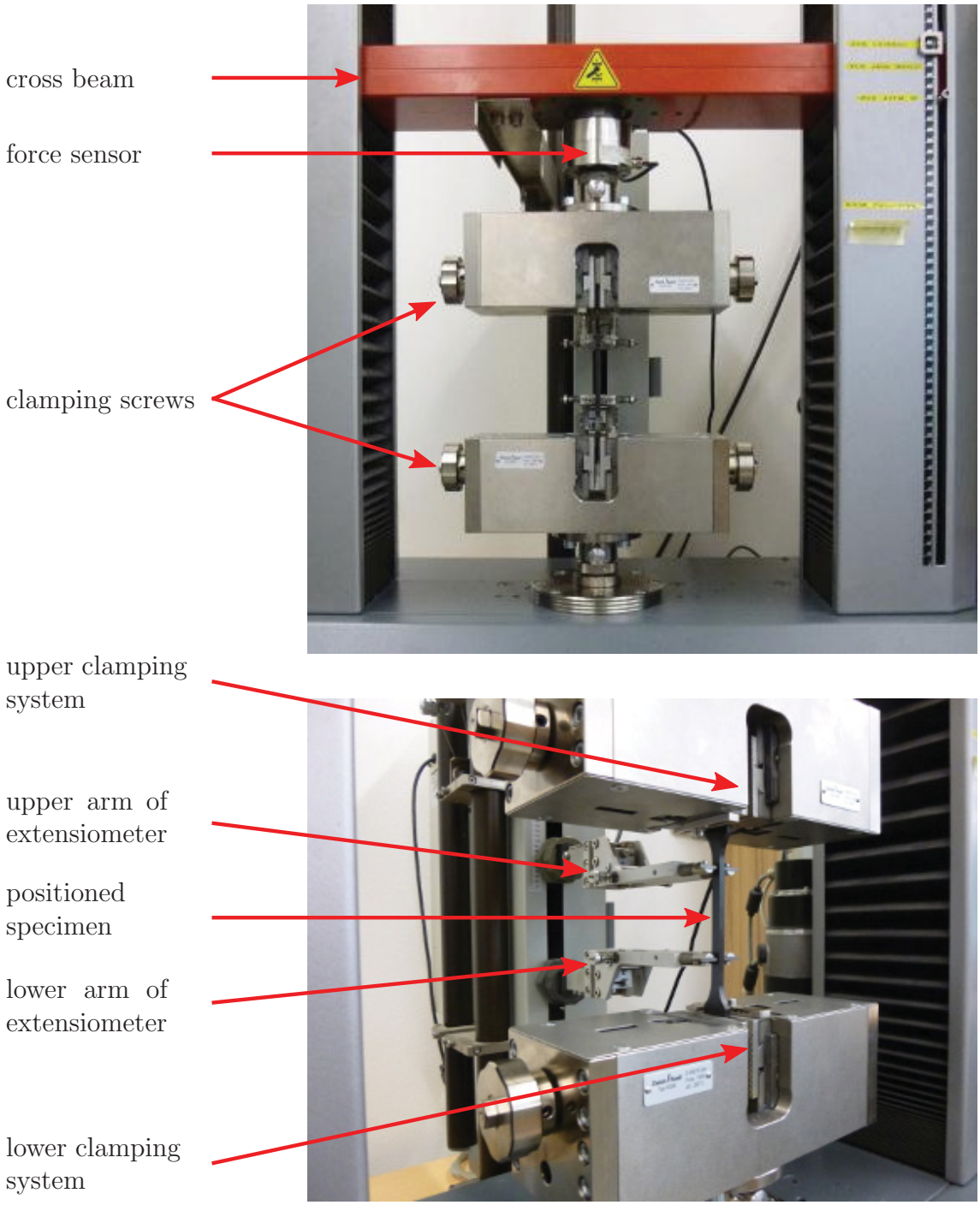


**Figure 4.5:** Measurement of tensile properties with an extensiometer. The upper picture gives an overview of the measurement setup. Below the arms of the displacement transducer can be seen.

**Table 4.6:** Testing parameters for tensile testing.

| parameter | value |
|---|---|
| clamping length | 125.6 mm |
| strain rate | 1 %/min = 1.26 mm/min |
| extensiometer starting length | 60 mm |
| initial load | 20 N |
| type of regulation | position control |
| temperature | 23 °C |
| rel. humidity | 50 % |

### 4.3.2 Flexural testing

For testing the flexural properties the weld lines of the specimens were positioned exactly under the stamp. In case of the modified specimens the middle of the modified weld line was positioned under the stamp. The configuration of the specimens in the flexural tests was ejector side up, if not otherwise declared, see Fig 4.6. A three dimensional scheme of the different testing configurations with a modified specimen can be viewed in Fig 4.7. The testing parameters are shown in Tab 4.7. Photos of the measurement setting are shown in Fig 4.8.

Ejector side up is the only used setting for the DOE, while the differences between ejector and nozzle side up is discussed later in 5.2.1.

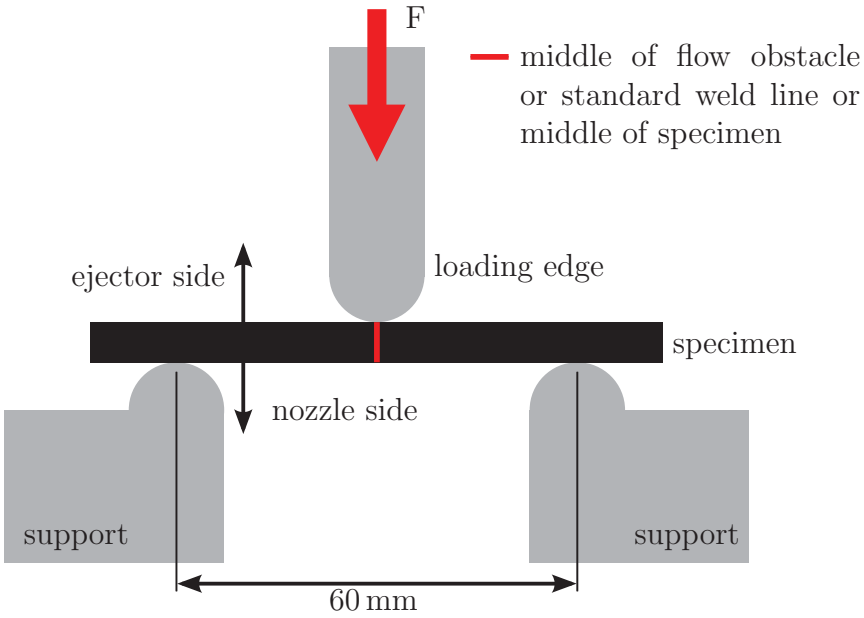


**Figure 4.6:** Schematic flexural test configuration. The prop is positioned directly on the middle of the specimen, where the standard weld line and the middle of the modified weld line is. This position is marked with a red line. The ejection side is up, if not declared otherwise.

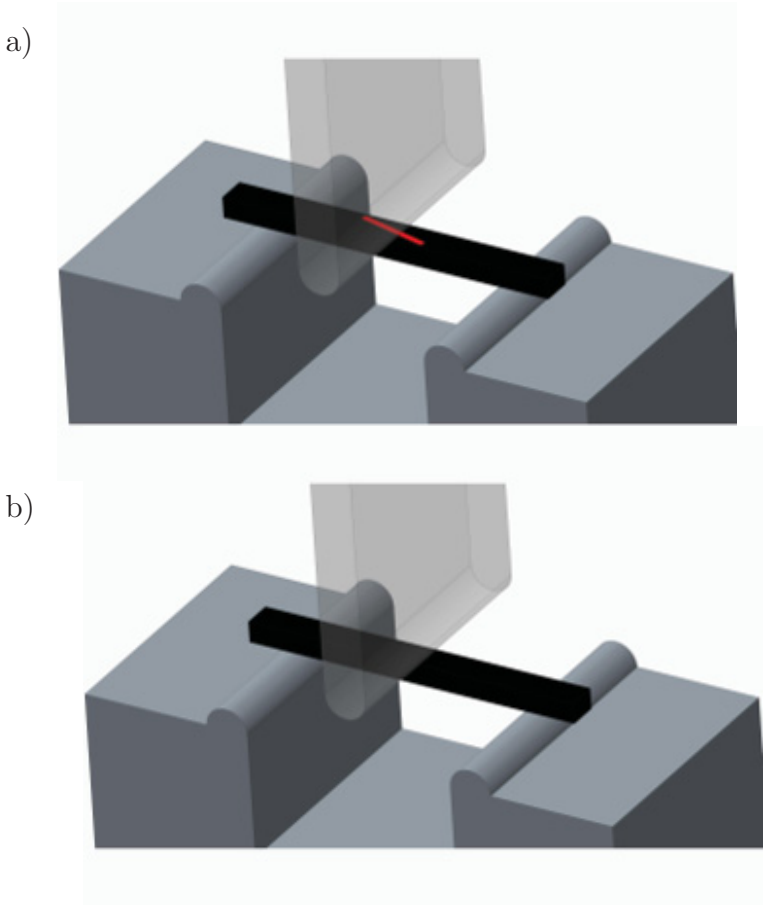


**Figure 4.7:** Three dimensional scheme of flexural testing. In a) ejector side is up, so the mark of the modifying insert can be seen (here marked red). In b) nozzle side is up. Inspired by [25].

**Table 4.7:** Testing parameters for flexural testing

| **parameter** | **value** |
|---|---|
| support length | 60 mm |
| testing speed | 20 mm/min |
| initial load | 10 N |
| type of regulation | position controlled |
| standard specimen orientation | ejection side up |

For the flexural test the specimen was placed on two fixed supports with a distance of 60 mm between them. The tests were carried out with the ejection side up, exceptions (nozzle side up) are marked in the results.

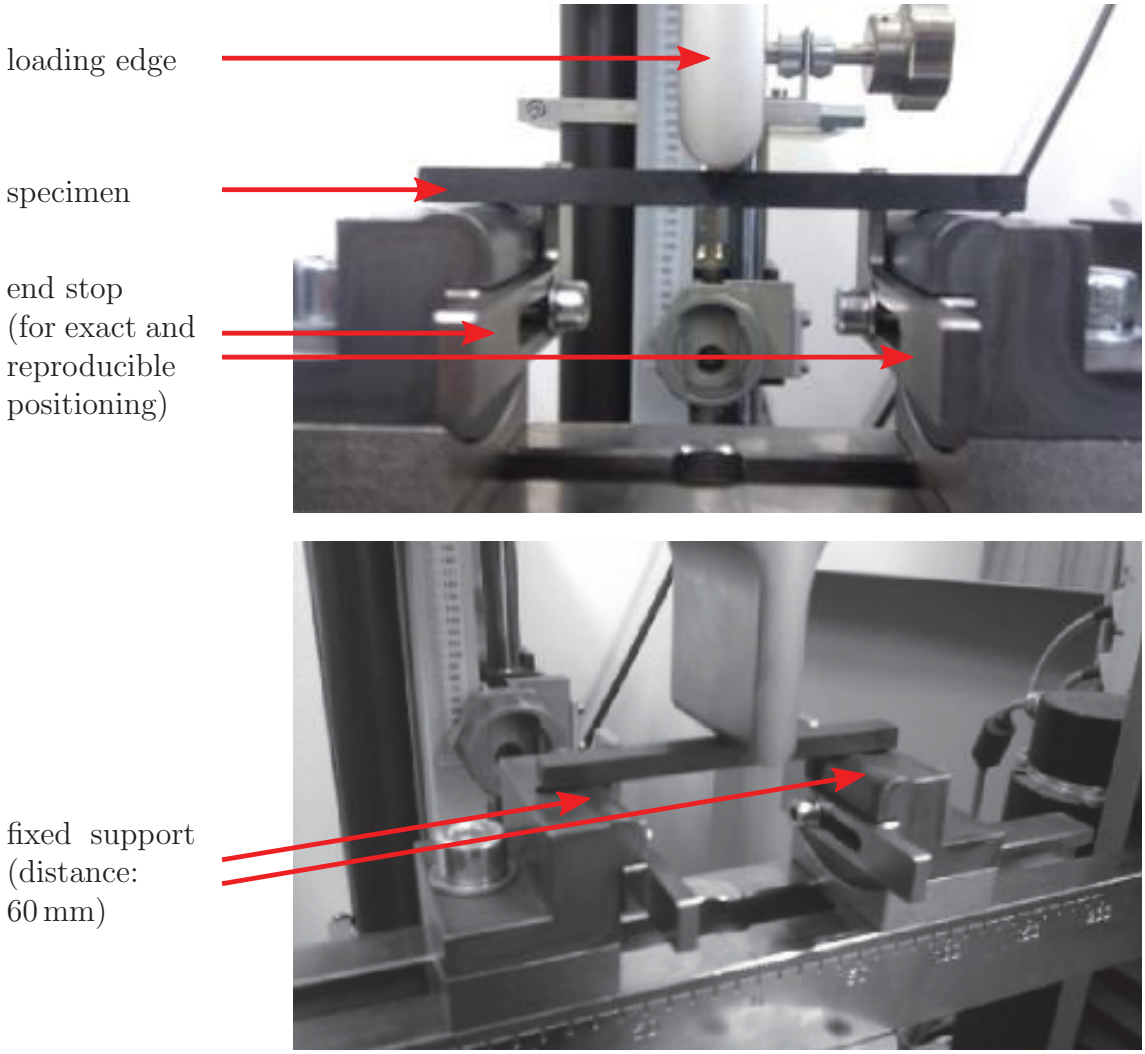


**Figure 4.8:** Test setting for the measurement of flexural properties. Photos [25].

### 4.3.3 Data preparation

After flexural or tensile tests had been performed all data were exported from the measurement program and further converted and processed in Matlab to gain suitable data to compile graphs in Origin.

By means of Matlab flexural and tensile data were processed. Out of the tensile testing data the tensile stress ($\sigma_t$) and the strain ($\epsilon_t$) were calculated from the measured load and displacement with an extensiometer ($\delta_t$), see equation (4.1) and equation (4.2). $l_0 = 60\,\text{mm}$ is the distance between the arms of the extensiometer. $B$ is the width and $H$ the height, see Fig 4.9.

In case of flexural properties the flexural stress ($\sigma_b$) and the edge fiber elongation / strain ($\epsilon_b$) were calculated from the measured load ($F$) and displacement ($\delta$) at the maximum load. The equations for that are shown subsequently and their origins are in the ISO 178:2003, see equation (4.3) and equation (4.4). $L_0 = 60\,\text{mm}$ is the distance between the fixed supports.

$$\sigma_t = \frac{F}{B \cdot H} \tag{4.1}$$

$$\epsilon_t = \frac{\delta_t}{l_0} \cdot 100 \tag{4.2}$$

$$\sigma_b = \frac{3 \cdot L_0 \cdot F}{2 \cdot B \cdot H^2} \tag{4.3}$$

$$\epsilon_b = \frac{600 \cdot \delta \cdot H}{L_0^2} \tag{4.4}$$

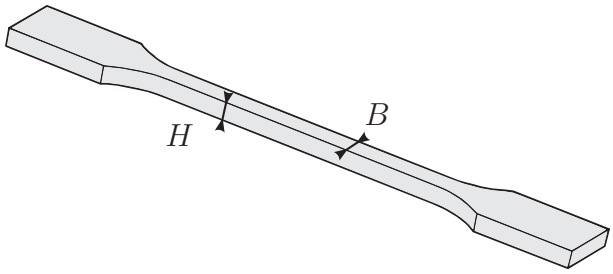


**Figure 4.9:** Height $H$ and and width $B$ for tensile and flexural testing.

## 4.4 Microscopy

For microscopy sample preparation the specimens were cut with a saw (type: Sectom-10, company: Struers) and embedded in a cold hardening matrix system called VariDur 3000 from company Buehler consisting of two components, one solid the other one fluid. These phases are mixed 2 : 1 (solid : fluid). This system consisting of methyl metacrylate and styrene hardens completely within one hour at room temperature. Then the samples were polished on a polishing machine of the type TegraPol-21 produced by Struers. The polishing program can be viewed in Tab 4.8. Some specimens were notched diagonally in direction of the modification to detect the exact location in the polished cross section for location determination, see Fig 5.23 in section 5.3.1.1.

**Table 4.8:** Polishing program

| **Polishing material** | **Grain size** † | **Polishing time in minutes** |
|---|---|---|
| abrasive paper | P320 | 4 ‡ |
| abrasive paper | P800 | 3 |
| abrasive paper | P1200 | 4 |
| abrasive paper | P2400 | 5 |
| abrasive paper | P4000 | 5 |
| NAB B1 Dia Pro SiC/diamond suspension | 1 $\mu$m | 10 |

Then the polished samples were investigated and pictures were made with incident light or using dark field microscopy. The software option "multistep" puts several photos together to one large picture. So information about the whole sample can be collected in one single picture. Although a shading correction was performed in some of the composed pictures, the single photos of which the whole picture consists can still be identified.

†or ISO/FEPA grit designation (P numbers)

‡This step is repeated until the desired distance is ground off.

# Chapter 5

# Analysis, results and interpretation

In this chapter the gained data are analyzed and the results for tensile and flexural tests are interpreted. First the analyzing methods are explained for the DOE, to gain the effects and interactions of processing parameters. Furthermore, the tensile and flexural tests are examined for specimens with modified, standard and without weld line. For standard weld lines the process scatter is inspected to gain additional information for interpreting the DOE correctly.

Additionally, the fracture behavior and fracture surfaces of the tested specimens were analyzed to gain information about the failure behavior of the different specimens under tensile and flexural load. Finally standard and modified weld lines are investigated by microscopy. Out of the inspection of fiber orientation a three dimensional model of the modified weld surface was created.

## 5.1 Tensile and flexural properties

### 5.1.1 Analyzing methods

The DOE delivers information about the size of effects and interactions of processing parameters. Due to the high costs of the investigated material, the quantity of the experiments was limited. No replicates of the DOE were manufactured and only four specimen were tested for each test run, whereas ISO 527 recommends at least five specimens [3]. This recommendation states as well that depending on the required precision of the mean value more specimens should be tested. The more specimens are tested the better the standard deviation can be evaluated. Furthermore, all specimens which break near the grip have to be rejected. This did not occur at this investigation, because specimens with weld lines (modified or not) had a flaw in the middle part and broke there.

The statistical analysis was performed with the program Minitab. At the beginning the mean values of four specimens per test were calculated and then used for analysis. To gain more significant information two to three analysis runs were needed. In the first run all main effects and second order interactions as well as the center point were considered. Then the p-values of the main factors were analyzed and rated.

The p-value is defined as smallest level of significance that would lead to rejection of the null hypothesis. The null hypothesis states that the mean values of two test runs

are equal [42]. This means that the smaller a p-value the more significant the factor of the DOE is. Usually a p-value below 0.05 is used as an indication for significance. This corresponds to an $\alpha$ level of 5 %, which is the probability of committing a type I error, which means that the null hypothesis is rejected even if it is true.

In the second analysis run the main factor with the least significant p-value was chosen for reduction of interactions, if it was above the 5 % $\alpha$ level. The interactions of this main factor were no more considered. If a main effect had a p-value higher than 0.8 it was no more considered. This removal meant that the analyzed data now consisted of 2 replicates of the other two main factors. Subsequently is an example with an explanation for this procedure which was performed for all testing combinations of stress, strain, standard weld line and modified weld line, see Fig 5.1 and Tab 5.1 and Tab 5.2. The two tables (Tab 5.1 and Tab 5.2) show the effects and interactions of the processing parameters. Only melt temperature is significant for modified weld line specimens.

In Fig 5.1 Pareto charts of the standardized effects are shown. This diagram type compares the relative magnitude and the statistical significance of main and interaction effects [4]. The effects are plotted in decreasing order. All effects which have significant influence have a beam which overtop the red line. This red line marks the 5 % level described above. The position of the red line depends on the number of replicates and further on the degrees of freedom for the data analysis and of course on the $\alpha$ level. The pareto chart only shows the absolute value of an effect, but not the algebraic sign. To gain information if an investigated property in- or decreases with an enhaced processing parameter the sign of the effect has to be regarded, see Tab 5.1 and Tab 5.2, in the column effect. The p-values from the second run of Tab 5.1 and Tab 5.2 are compared in Tab 5.9 concerning flexural stress of standard and modified weld line specimens [4].

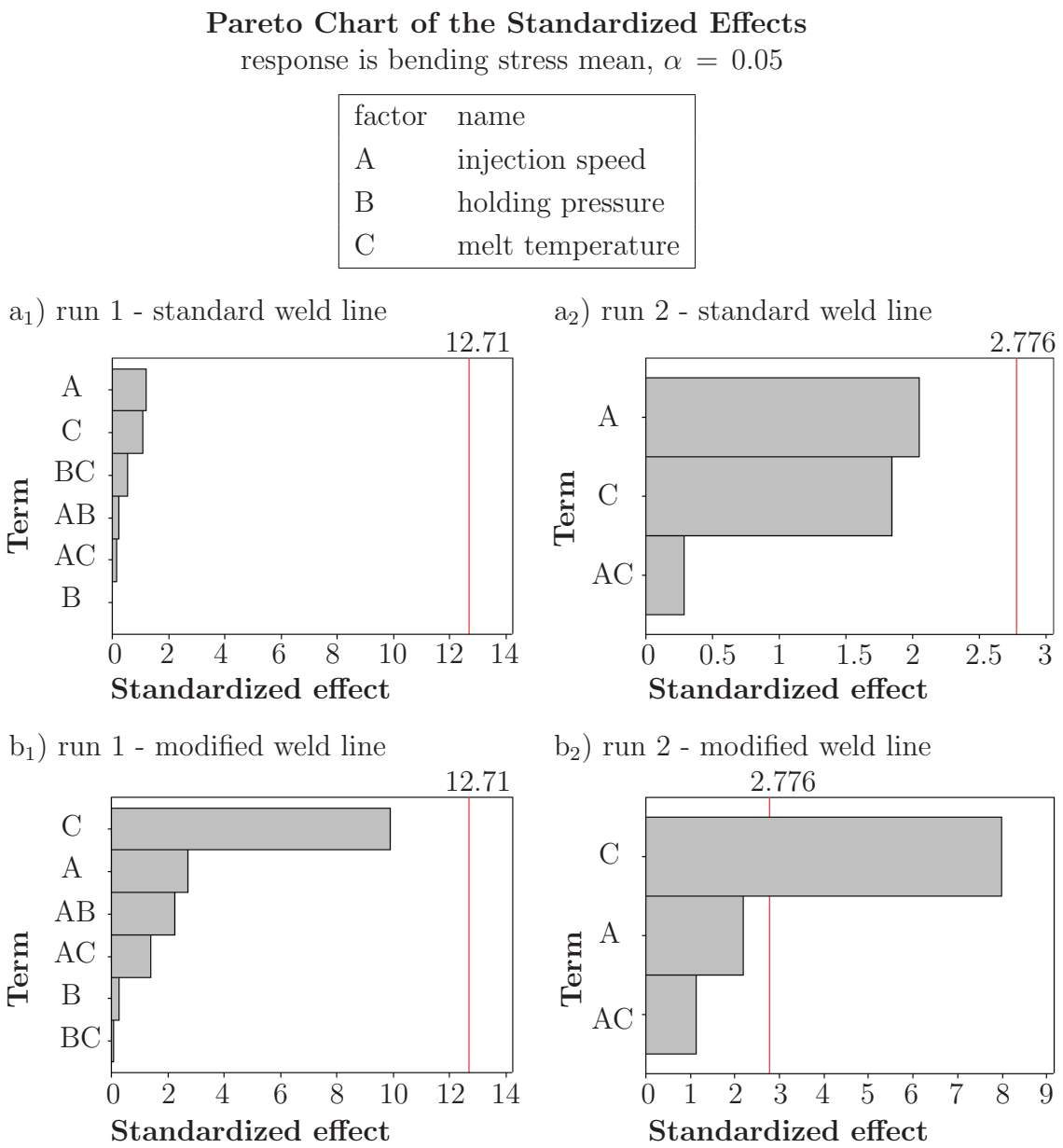


**Figure 5.1:** Pareto charts of standardized effects. The first two $a_1$) and $a_2$) come from the analysis of flexural stress tests of standard weld lines. In $a_1$) the holding pressure has a p-value of 1.0, which is bigger than 0.8 and means that the holding pressure is far away from being significant. In $a_2$) the analysis was repeated without the factor holding pressure and its second order interactions. In this case the reduction does not make a real difference because the other main effects still remain not significant. But with a higher degree of freedom the level for significance decreases from 12.71 to 2.776.

In example $b_1$) and $b_2$) the analysis was performed analogously to the first. Here the reduction of a main factor (holding pressure) and its interactions results in one significant factor: melt temperature. This results from a greater amount of data, which is now used for the determination of significance. By reducing the calculated results from six main effects and interactions to three the initially unreplicated $2^3$ factorial design is projected into a $2^2$ factorial design with one replication.

**Table 5.1:** p-values for the example in Fig 5.1 for the standard weld line. Here non of the examined processing parameters is significant.

| **run 1 and run 2 of standard weld line flexural stress** | | | |
|---|---|---|---|
| **term** | **effect** | **p-value run 1** | **p-value run 2** |
| injection speed | 5.152 | 0.443 | 0.109 |
| holding pressure | −0.000 | 1.000 | x |
| melt temperature | 4.630 | 0.477 | 0.138 |
| injection speed*holding pressure | −1.043 | 0.849 | x |
| injection speed*melt temperature | 0.717 | 0.895 | 0.789 |
| holding pressure*melt temperature | −2.348 | 0.682 | x |
| center point | | 0.924 | 0.847 |
| * sign for second order interaction of the two mentioned factors | | | |

**Table 5.2:** p-values for the example in Fig 5.1 for the modified weld line. In the second run, considering flexural stress, melt temperature becomes significant, this is marked bold.

| **run 1 and run 2 of modified weld line flexural stress** | | | |
|---|---|---|---|
| **term** | **effect** | **p-value run 1** | **p-value run 2** |
| injection speed | −4.270 | 0.225 | 0.094 |
| holding pressure | 0.454 | 0.821 | x |
| melt temperature | 15.618 | 0.064 | **0.001** |
| injection speed*holding pressure | 3.538 | 0.267 | x |
| injection speed*melt temperature | 2.215 | 0.394 | 0.32 |
| holding pressure*melt temperature | 0.152 | 0.939 | x |
| center point | | 0.213 | 0.080 |
| * sign for second order interaction of the two mentioned factors | | | |

### 5.1.2 Results of the tensile testing

Tensile properties were examined to find out which effects and interactions the processing parameters show. Insert type halfblade was used in the DOE.

#### 5.1.2.1 Design of experiments

For every setting of the DOE including the center point eight specimens were tested, four standard weld line specimens and four modified weld line specimens. As an example Fig 5.2 shows the results of the process parameter setting D4. To compare all

settings of the DOE all stress-strain curves of the tested specimens are printed into one diagram, see Fig 5.3. It can easily be seen that there is no great difference between a "best" and "worst" adjustment of the different settings of the DOE.

All standard weld line specimen settings broke at an average tensile stress of 100 to 105 MPa. The standard deviation for these settings is greater than the difference of mean values for the standard weld line specimens. The standard deviation for the settings is 3 MPa at a maximum. This leads to the conclusion that processing parameters alone cannot improve weld line quality satisfactorily.

For the modified weld line specimens the average stress for the settings varied between 115 and 134 MPa. The standard deviation for one setting is 9 MPa at a maximum, in the average 3.4 MPa. Further there is an increase in tensile strain. Modified weld line specimens strain up to 1 % where standard weld line specimens strain about 0.7 %.

Additionally to the DOE specimens without weld line were produced at the center point level of the DOE for comparison, see Fig 5.4. The negative effects of weld lines can be seen here easily. These specimens break at a stress of approximately 233 MPa and elongate twice (1.95 %) as much as the specimens with modified weld lines.

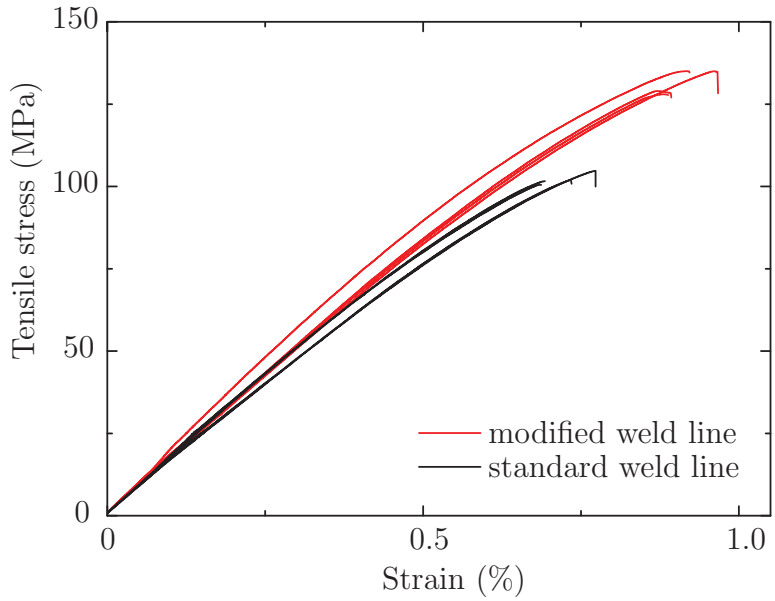


**Figure 5.2:** Tensile testing of setting D4. There is certain scatter of data, but modified weld lines performed better than the standard weld lines of the setting.

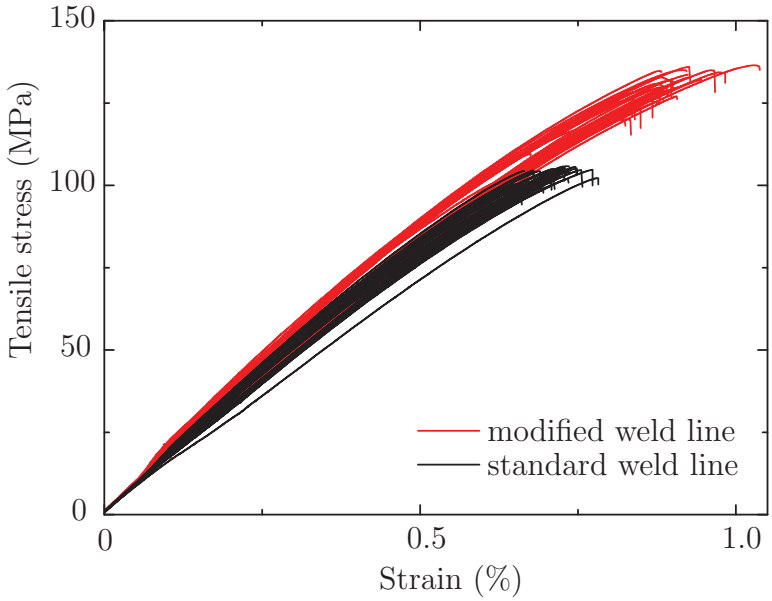


**Figure 5.3:** All data from the tensile testing of the DOE. Obviously modified weld line specimens perform better than standard weld line specimens. Processing parameters do not seem to have great influence, there is no big difference between a best and worst set of processing parameters.

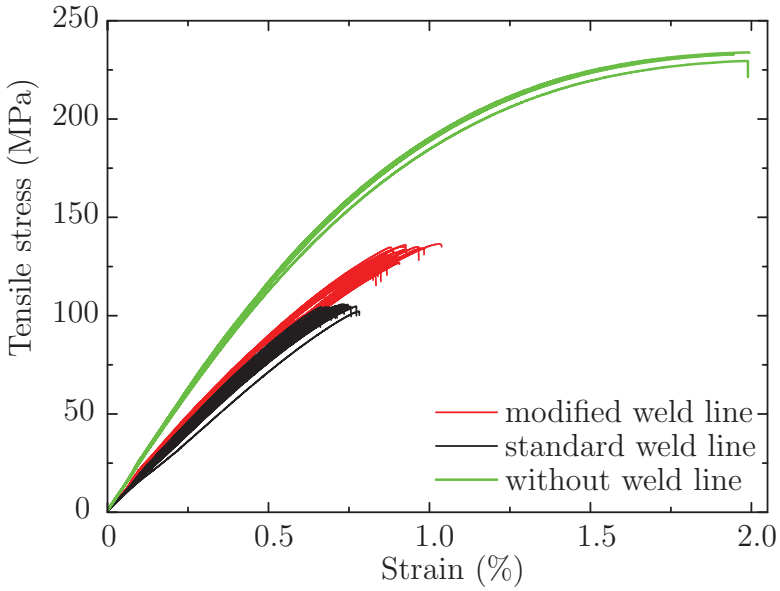


**Figure 5.4:** Comparison of specimens without and with standard or modified weld line. The tensile strength is reduced to 45 % for standard weld line specimens and to 57 % for modified weld lines (100 % is the strength of specimens without weld lines, 233 MPa).
Elongation at break is reduced drastically, for further information take a look at the weld line factors in Tab 5.6. The results from non weld line specimens is in agreement with the material data in Appendix A Tab 8.3.

The performed statistical analysis of tensile testing resulted in the p-values in Tab 5.5, if below 0.05 the value is marked bold. Melt temperature is the only significant processing parameter for modified weld lines. Melt temperature is not significant due to this analysis for standard weld line specimens.

The mean values of tensile strength is shown in Tab 5.3 and the mean values of tensile strain is shown in Tab 5.4. These tables contain the data for the calculation of the p-values in Tab 5.3. In both tables D1 to D4 are the high temperature levels, D5 is the center point and D6 to D9 are the low temperature levels. The maximum values from the high melt temperature setting are used for weld line factor calculation in section 5.1.2.2, these values are marked bold.

**Table 5.3:** Tensile strength mean values comparison of standard and modified weld lines of the DOE. The maximum values from the high melt temperature setting are used for weld line factor calculation, the values are marked bold. Melt temperature improves weld lines while increasing. D1 to D4 are the high temperature levels, D5 is the center point and D6 to D9 are the low temperature levels.

| **setting** | **std weld line** | **mod weld line** |
|---|---|---|
| | in MPa | |
| D1 | **105** | **134** |
| D2 | 104 | 130 |
| D3 | 104 | **134** |
| D4 | 103 | 132 |
| D5 | 100 | 124 |
| D6 | 101 | 115 |
| D7 | 103 | 126 |
| D8 | 103 | 127 |
| D9 | 101 | 126 |

**Table 5.4:** Tensile strain at break mean values comparison of standard and modified weld lines of the DOE. The maximum values from the high melt temperature setting are used for weld line factor calculation, the values are marked bold. D1 to D4 are the high temperature levels, D5 is the center point and D6 to D9 are the low temperature levels. Concerning strain of standard weld lines the processing parameter are not significant, hardly any changes can be recognized between the different settings.

| **setting** | **std weld line** | **mod weld line** |
|---|---|---|
| | in % | |
| D1 | 0.70 | 0.90 |
| D2 | **0.73** | 0.88 |
| D3 | 0.70 | **0.95** |
| D4 | **0.73** | 0.93 |
| D5 | 0.68 | 0.85 |
| D6 | **0.73** | 0.73 |
| D7 | 0.68 | 0.85 |
| D8 | 0.70 | 0.85 |
| D9 | 0.70 | 0.88 |

**Table 5.5:** The p-values for tensile testing of the DOE for all three processing parameters are listed. The posed data are acquired by the method explained in section 5.1.1. The p-values below 0.05 are marked bold.

| | **type** | **melt temperature** | **holding pressure** | **injection speed** | **center point** |
|---|---|---|---|---|---|
| **stress** | STD | 0.102 | 0.677 | 0.423 | 0.126 |
| | MOD | **0.039** | 0.284 | x | 0.402 |
| **strain** | STD | 1 | 0.460 | 1 | 0.245 |
| | MOD | **0.049** | 0.116 | 0.469 | 0.710 |

In tensile testing only one processing parameter has significant influence on the tensile properties of the modified weld line specimens, whereas standard weld line specimens cannot be influenced significantly by processing parameters. This concludes that on the one hand injection molding process is robust on the other the change of processing parameters does not significantly change the tensile properties of the specimens.

#### 5.1.2.2 Improvement by weld line modification

If the mean values of stresses and strains are compared, it can be noticed that the modification by the flow obstacle improves the weld line quality significantly, see Fig 5.2 to Fig 5.4 as well as Tab 5.3 and Tab 5.4. Due to the fact that melt temperature is the only significant processing parameter for modified weld lines further investigations were made considering the influence of melt temperature. The maximum stress of modified specimens (134 MPa) is reached with high melt temperature and is approximately 30 % higher than that of standard weld line specimens. The optimization of processing parameters achieved only 5 % for standard weld lines.

All investigations were performed analogously for standard weld lines for comparison. In Tab 5.3 the tensile strength of standard and modified weld line specimens is compared. The maximum values (acquired at high melt temperature) are used for the calculation of the weld line factors. The same procedure is performed for tensile strain in Tab 5.4. All weld line factors calculated are shown in Tab 5.6.

**Table 5.6:** Weld line factors concerning stress and strain of standard and modified weld line specimens. The max values from Tab 5.3 and Tab 5.4 are used for the calculation of the weld line factors, using equation (2.1). The improvement from standard to modified weld lines is significant.

| property | standard weld line | modified weld line | without weld line |
|---|---|---|---|
| stress | 0.45 | 0.58 | 1 = 233 MPa |
| strain | 0.37 | 0.49 | 1 = 1.95 % |

### 5.1.3 Results of flexural testing

Analogously to the analysis of tensile results the data of flexural tests is discussed in this section. Insert type halfblade is investigated.

#### 5.1.3.1 Design of experiments

Four modified weld line specimens and four standard weld line specimens were tested for each setting of the DOE. As an example setting D4 is chosen to show the stress-strain curves of one setting of the DOE, see Fig 5.5. There is a drastic improvement of the weld line flexural properties when the weld line is modified. This is valid for the whole DOE, see Fig 5.6. All stress-strain curves of standard weld lines are close together, seeming independent from changes of the processing parameters. Also for modified weld line specimens no big difference can be seen between the different settings of parameters.

In Fig 5.6 the average strain of standard weld lines is 1.40 %, where modified weld line specimens strain 2.44 % in average. flexural strength improves from 178 MPa to 301 MPa, these are the maximum values achievable for standard and modified weld lines, accomplished with setting D4. This is an improvement of 41 %. The standard deviation for flexural strength is in the range of 2 to 3 % of the mean value for modified and standard weld lines.

To compare the results of the DOE with specimens without weld lines, see Fig 5.7. The specimens without weld lines were produced at the center point level. Noticeable is that modified weld line specimens elongate like specimens without weld line, but break at lower stresses. Specimens without weld lines break at an average flexural stress of 366 MPa and strain for 2.42 % in average. For the weld line factors look at Tab 5.10.

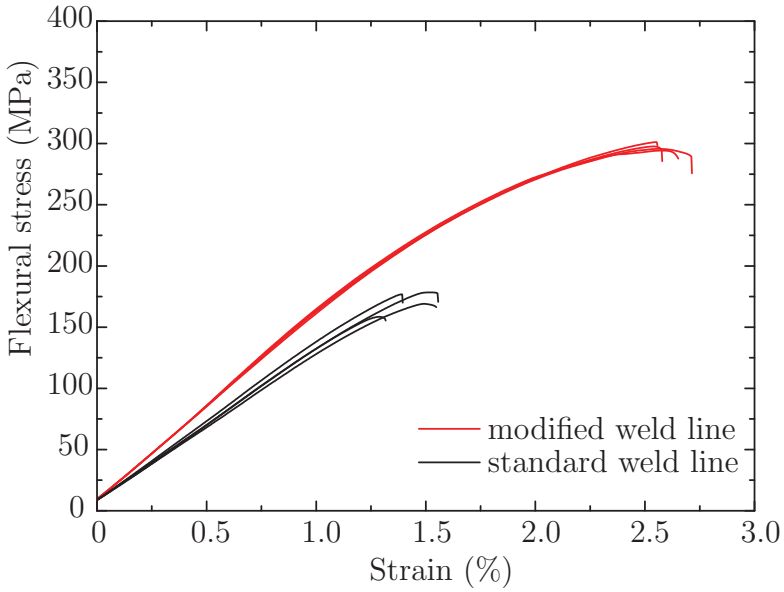


**Figure 5.5:** Flexural testing of setting D4. The performance of modified weld lines is far better than that of standard weld lines. For this setting the scatter for the modified specimens is remarkably low.

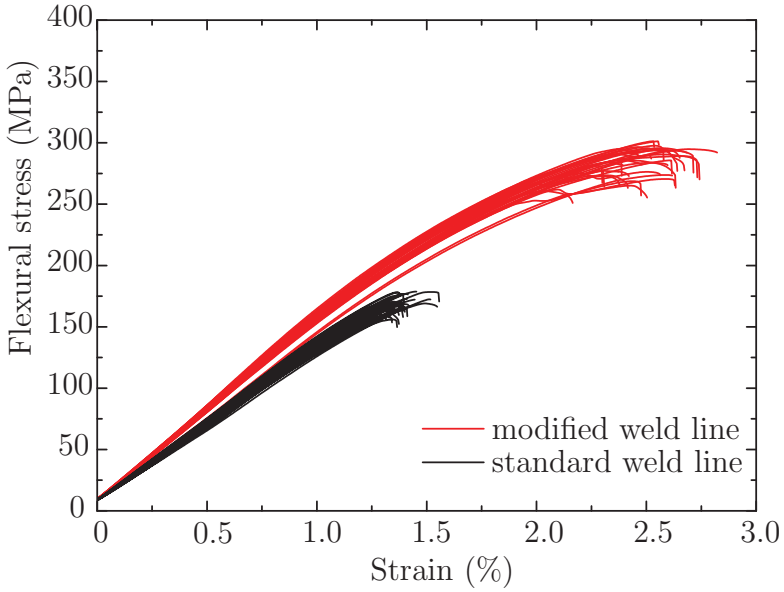


**Figure 5.6:** Comparison of all standard and modified weld line specimens tested for the DOE. The scatter of data is similar to that of tensile testing. Due to the modification the improvement is 41 % for the flexural strength and 43 % for the flexural strain.

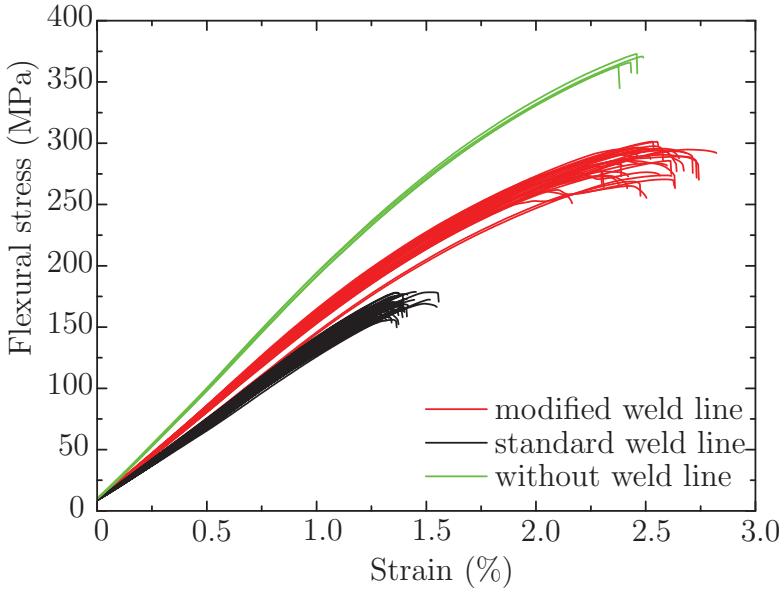


**Figure 5.7:** Comparison of stress and strain from specimen without weld line and standard and modified weld line specimens. Remarkable is the elongation before break at modified weld line specimens: regarding the strain they perform like specimens without weld lines.

Statistical analysis of flexural tests resulted in the table of p-values, see Tab 5.9. If the p-value is below 0.05 it is marked bold. The only significant processing parameter is melt temperature for modified weld line specimens concerning flexural stress, the rest is not significant.

The mean values of tensile strength is shown in Tab 5.7 and the mean values of tensile strain is shown in Tab 5.8. These tables contain the data for the calculation of the p-values in Tab 5.7. In both tables D1 to D4 are the high temperature levels, D5 is the center point and D6 to D9 are the low temperature levels. The maximum values from the high melt temperature setting are used for weld line factor calculation in section 5.1.3.2, these values are marked bold.

**Table 5.7:** Flexural stress mean values comparison of standard and modified weld lines from the DOE. The maximum stresses achieved are marked bold and used for calculation of the weld line factors.

| setting | std weld line | mod weld line |
|---|---|---|
| | in MPa | |
| D1 | 174 | 296 |
| D2 | 166 | 297 |
| D3 | 177 | 286 |
| D4 | **178** | **301** |
| D5 | 164 | 265 |
| D6 | 170 | 281 |
| D7 | 167 | 277 |
| D8 | 164 | 276 |
| D9 | 156 | 286 |

**Table 5.8:** Flexural strain mean values comparison of standard and modified weld lines from the DOE. The maximum strains achieved are marked bold and used for calculation of the weld line factors.

| setting | std weld line | mod weld line |
|---|---|---|
| | in % | |
| D1 | 1.31 | 2.42 |
| D2 | 1.42 | 2.48 |
| D3 | 1.42 | 2.39 |
| D4 | **1.50** | 2.53 |
| D5 | 1.42 | 2.42 |
| D6 | 1.42 | 2.31 |
| D7 | 1.33 | 2.31 |
| D8 | 1.42 | 2.48 |
| D9 | 1.33 | **2.64** |

**Table 5.9:** p-values of the DOE for all three varied processing parameters for flexural testing. The posed data is acquired by the method explained above in section 5.1.1. The p-values below 0.05 are marked bold.

| | type | melt temperature | holding pressure | injection speed | center point |
|---|---|---|---|---|---|
| stress | STD | 0.138 | x | 0.109 | 0.847 |
| | MOD | **0.001** | x | 0.094 | 0.08 |
| strain | STD | 0.638 | 0.430 | x | 0.416 |
| | MOD | 0.166 | 0.079 | 0.577 | 0.987 |

#### 5.1.3.2 Improvement by weld line modification

Again an optimization of the mechanical properties can only be achieved by geometric modification of the weld lines. Additionally, flexural properties of modified specimens can only be improved by a hotter melt, see Tab 5.7 and Tab 5.8. The increase of the weld line properties due to modification can be seen in Tab 5.10 showing weld line factors for stress and strain of the best setting for standard and modified specimens.

**Table 5.10:** Weld line factors concerning stress and strain of standard and modified weld lines for high melt temperature settings. The maximum values for calculation are from Tab 5.7 and Tab 5.8. Here the enormous improvement concerning strain can be noticed. The modification makes specimens break at even higher strains compared to the ones without weld lines. The improvement due to modified weld lines is significant.

| property | standard weld line | modified weld line | without weld line |
|---|---|---|---|
| stress | 0.49 | 0.82 | $1 = 366\,\mathrm{MPa}$ |
| strain | 0.62 | 1.09 | $1 = 2.42\,\%$ |

### 5.1.4 Different insert geometries

The previous section shows that the manufactured weld lines are not very sensitive to changes in processing parameters. So for further experiments the processing parameters of the center point were chosen.

After the DOE had been performed inserts with different head geometries (shown in Fig 3.7) were tested to investigate their behavior in the injection molding process. Furthermore, the performance of the produced specimens under mechanical load was investigated.

To gather more statistical information (about the mean value, standard deviation of other inserts etc.) at least six specimens were tested for the following inserts: "blade", "hole" and "round". For the other inserts ("halfblade" and "plain") a minimum of four specimens were tested.

In Fig 5.8 and Fig 5.9 the measured maximum tensile or flexural stress is shown for each measurement of every insert. After drawing the measured points into the graph a normal distribution plot was added and the mean value of the tests included. With the normal distribution curve the difference of the settings can be compared in a better way than with mean values only. If the areas of the curves are placed close together and there is an overlapping over a great range, there will be no significant difference. If the curves just overlap at their edge area or not at all the difference will be significant. To check that also an analysis of variance (ANOVA) was performed, which is discussed in section 5.1.5.1.

For all following comparisons only stresses are used because strains are in a range which is near the resolution limit of the testing equipment.

For tensile strength there is a difference between the insert geometries. Blade and halfblade perform in a better way than the other inserts. The inserts round and plain achieve only 90 % of the approximately 127 MPa, which are achieved by blade. Nevertheless this difference has to be analyzed with the process scatter in consideration, which is performed in section 5.1.5.

For flexural strength the results show less difference between the different head geometries of the inserts. Insert plain performs best with approximately 280 MPa flexural stress. Insert hole has the least flexural stress mean value with approximately 270 MPa, which is a difference of only 3.5 %.

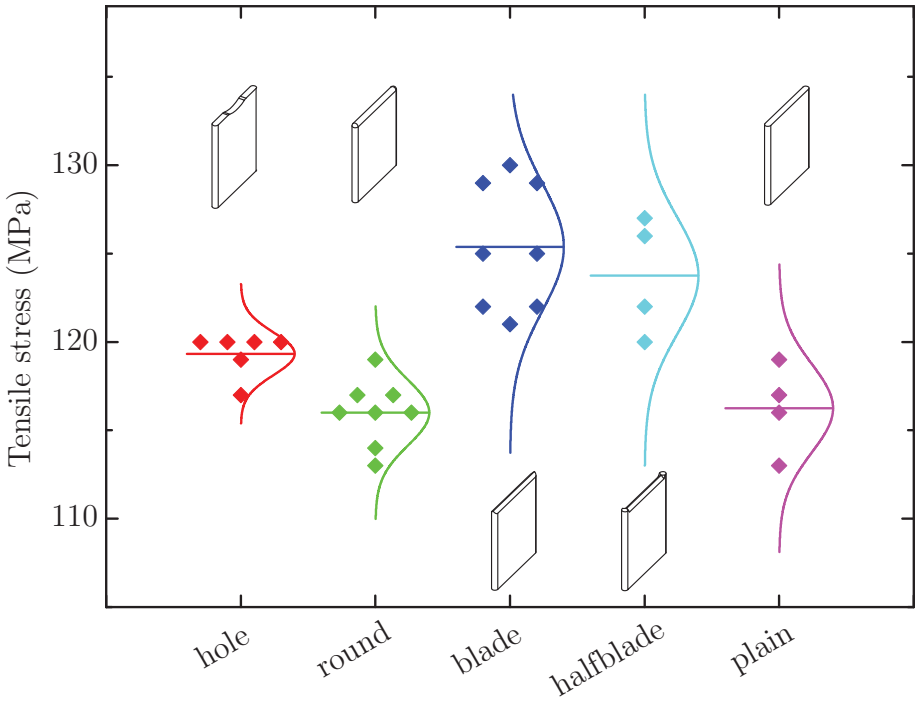


**Figure 5.8:** Tensile strength of modified weld lines with different modification, names according to Fig 3.7.

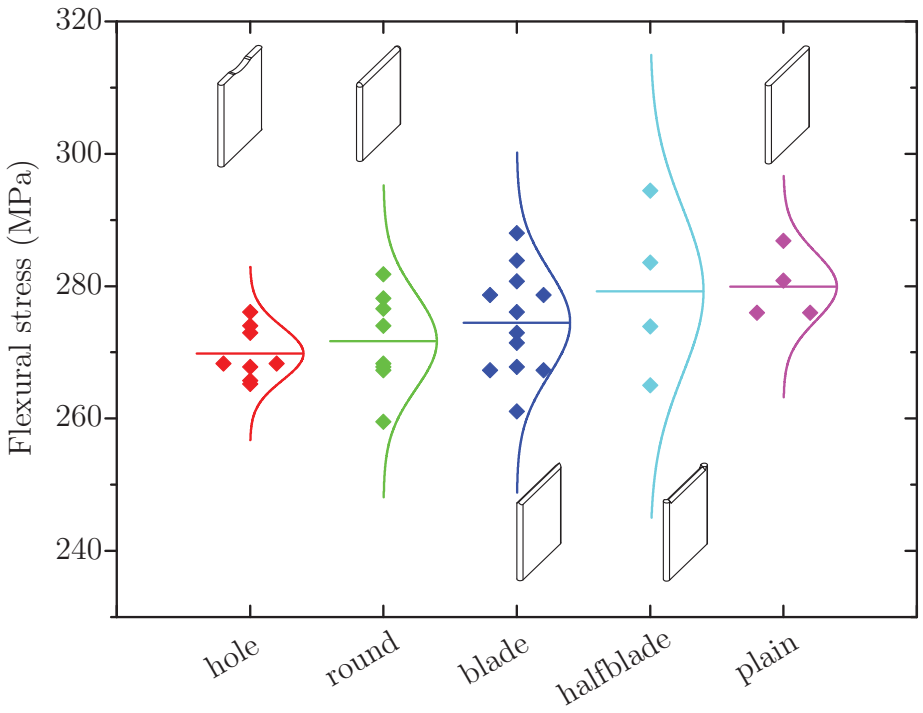


**Figure 5.9:** Flexural stress of modified weld line specimens with different modification, names according to Fig 3.7. The normal curves show that there is no big difference between the different inserts.

### 5.1.5 Process reliability

Together with the modified weld line specimens there were always standard weld line specimens produced. These specimens were used for analyzing the process reliability and process scatter. The great sum of specimens gives information about the statistical behavior of standard weld lines.

In Fig 5.10 the tensile stress and in Fig 5.11 the flexural stress of the standard weld line specimens are shown. In the last column all standard weld line testing results are shown to represent the mean value over all 37 measurements.

In the tensile and flexural results the difference between the mean values of the best and worst run is approximately 8 %.

The following comparison is made to determine whether the scatter results from the injection molding process or the measurement device. Dividing the mean values of the different runs of Fig 5.10 and Fig 5.11 by the mean value named "all runs" gives a standardization of the different runs. This standardization makes flexural and tensile measurements comparable. In Fig 5.12 these standardized values are shown.

The mean of "all runs" is plotted at last as reference with value 1. Run 1 and run 2 were produced at one production day. Series preliminary run, run 1 and run 2 were measured in a row. Run 3 is a replication of the preliminary run. The other runs were produced on several days and tested on different days.

From the first three runs (prelim. run, run 1 and run 2) a clear correlation of tensile and flexural results can be seen, concluding that there is a scatter in the injection

molding process. On the other days the scatter of the results might result from process scatter as well as the testing setup.

An ANOVA was carried out to test if there is a significant difference between the different days of production and testing, testing the different replicates of the standard weld line specimens, which were produced simultanously with the different insert head geometries. With a p-value of 0.004 a significant difference was found for tensile stress. This difference was found between the runs of insert type "prelim. run" and "run 4" by the Tukey method. The Fisher method gives more differences. The grouping can be seen in Tab 5.11, every run which is not in the same group differs significantly. All runs within one group share the same letter (A, B, C).

Concerning flexural strength a significant difference between the different production days was found as well with a p-value of 0.008. The grouping of the different runs can be seen in Tab 5.12.

The difference may result from a non steady state of production. Though the barrel was emptied and at least 10 specimens were rejected before taking specimens for inspection and testing the process was not in a steady state yet. To get there probably many more specimens would have to be rejected. Further explanations could be process fluctuation or fluctuation in material quality and the testing setup.

Nevertheless the scatter discussed here is in a range of 5 %, which is low enough to be tolerated within one material lot.

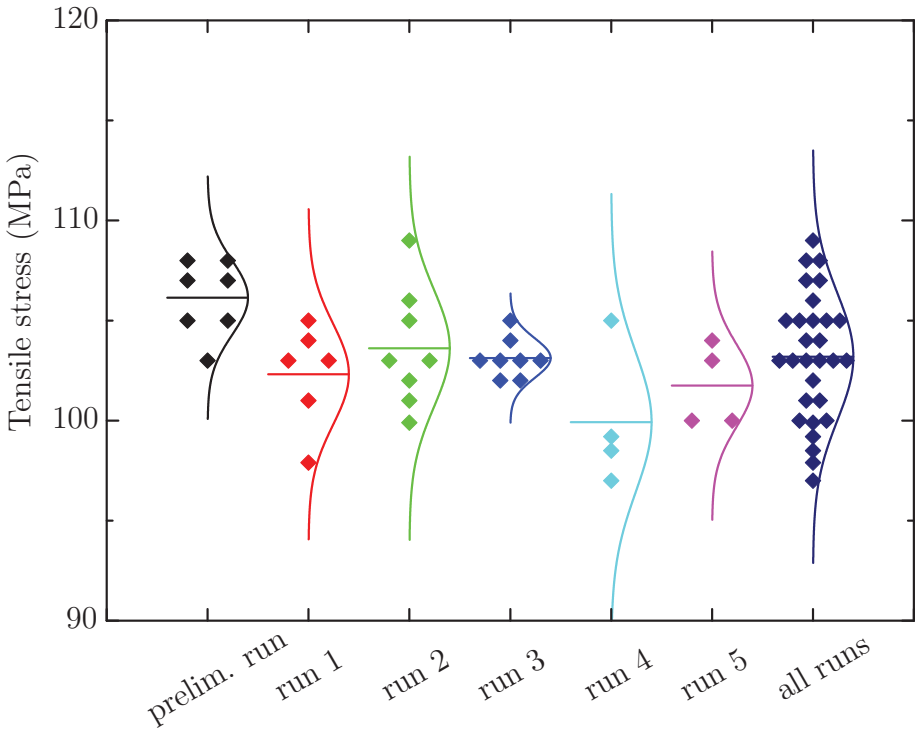


**Figure 5.10:** Tensile stress of standard weld lines manufactured on different days together with modified specimens. In the last column all data is reprinted to gain a mean value over six replicates.

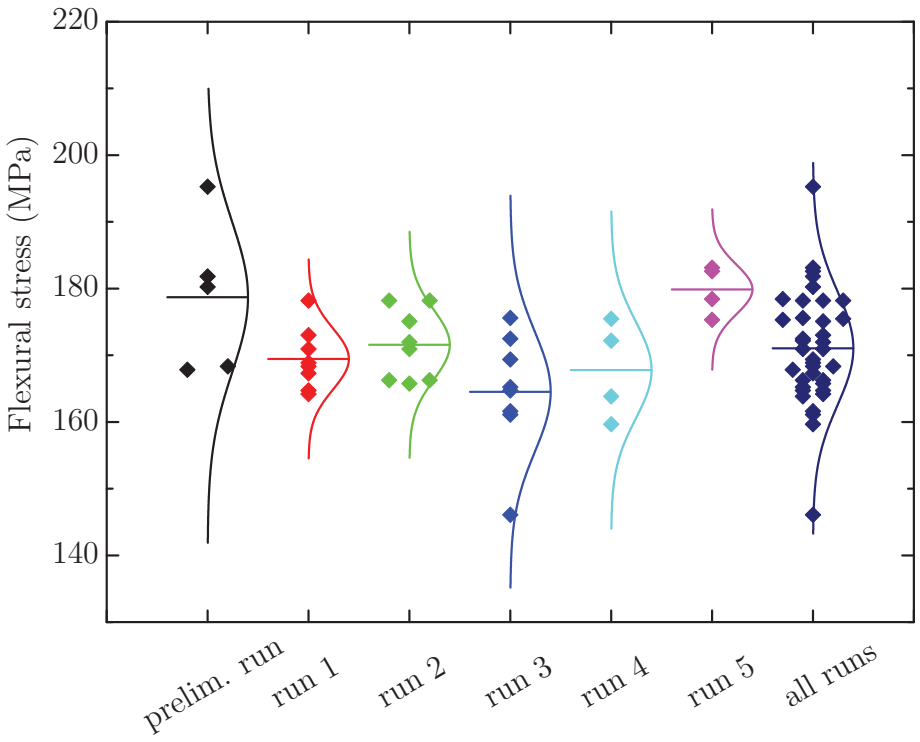


**Figure 5.11:** Flexural stress of standard weld lines manufactured on different days together with modified specimens. In the last column all data is reprinted to gain a mean value over six replicates.

**Table 5.11:** Grouping of the different production days of standard weld line specimens concerning tensile stress by the Fisher and the Tukey method. One group is one letter (A, B, C).

| **run number** | **tensile stress mean value** in MPa | **Tukey method** | **Fisher method** |
|---|---|---|---|
| prelim run | 106 | A | A |
| run 1 | 102 | A B | B C |
| run 2 | 104 | A B | A B |
| run 3 | 103 | A B | C |
| run 4 | 100 | B | B |
| run 5 | 102 | A B | B C |

**Table 5.12:** Grouping of the different production days of standard weld line specimens concerning flexural stress by the Fisher and the Tukey method. One group is one letter (A, B).

| run number | flexural stress mean value in MPa | Tukey method | Fisher method |
|---|---|---|---|
| prelim run | 179 | A | A |
| run 1 | 169 | A B | B |
| run 2 | 172 | A B | A B |
| run 3 | 165 | B | B |
| run 4 | 168 | A B | B |
| run 5 | 180 | A | A |

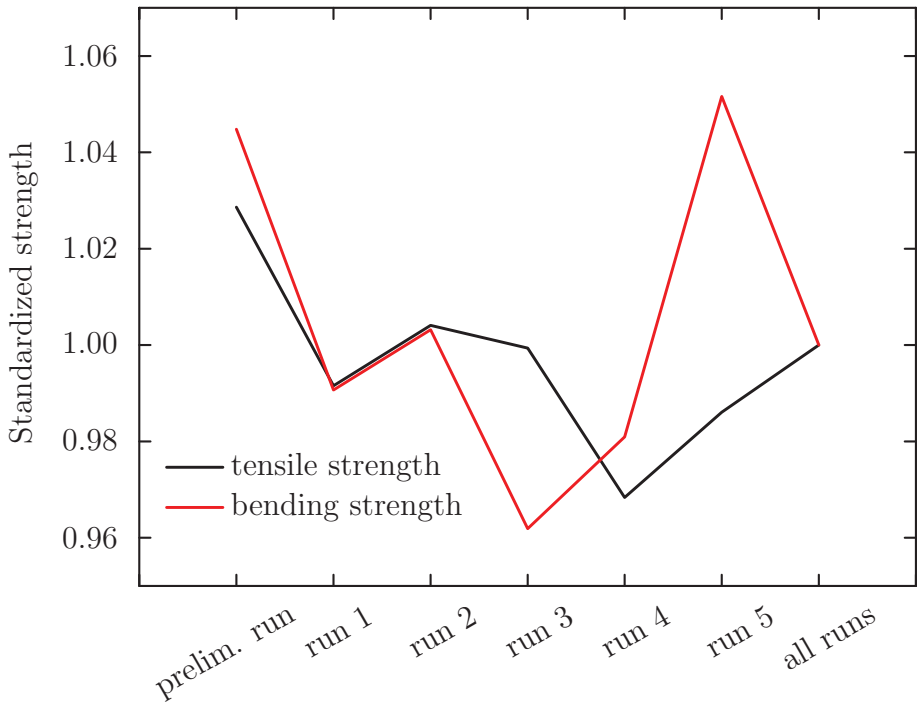


**Figure 5.12:** Standardized data of tensile and flexural strength of standard weld lines.

#### 5.1.5.1 Comparison of weld line types

In Fig 5.13 the tensile properties of the modified weld line specimens (Fig 5.8) and the standard weld line specimens (Fig 5.10) are compared, respectively the comparison for flexural strength is in Fig 5.14 (consisting of the data of Fig 5.9 and Fig 5.11). The standard weld line values are always below the modified strengths. This shows what could be achieved by modification of the weld line.

Although there is a difference of the mean values concerning Fig 5.13, half of the area of the normal curves is overlapping, which leads to the assumption that there is no significant difference between the different insert head geometries. Due to software failure the gained data of blade day 1 was lost and could not be restored. Therefore the blade geometry was reproduced on another day resulting in the series blade day 2.

To prove this assumption ANOVAs were carried out. The modified weld lines of each insert type performed significantly better in the tensile testing, with a p-value of 0.000 for every geometry. This proves a significant improvement of the weld line strength and the successful modification by any insert head geometry. This test was not repeated for bending testing because there the positive effect of the modification is more pronounced than in the tensile testing, compare Fig 5.13 and Fig 5.14.

The scatter of the mean values of tensile strength is in the range of 8.4 % and for flexural strength in the range of 5.0 %. For tensile testing the ANOVA finds significant differences between several inserts, with a p-value of 0.000. To find the differences, see Tab 5.13, where the grouping by Tukey method and by Fisher method of the different insert head geometries is shown.

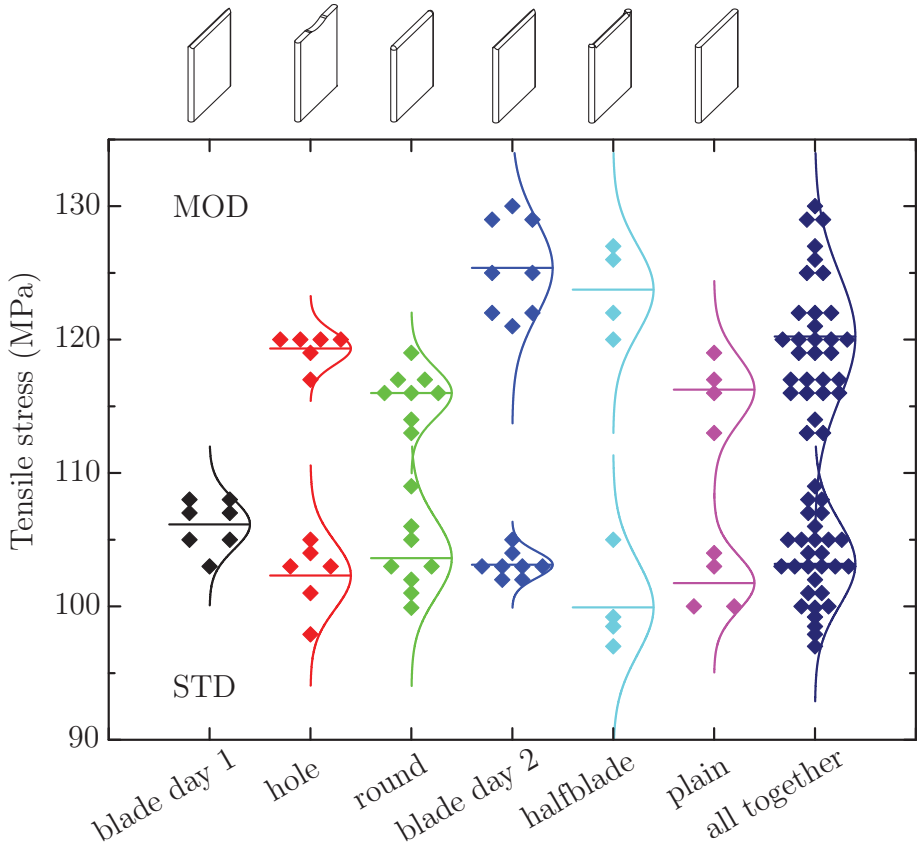


**Figure 5.13:** Tensile stress of standard and modified weld lines manufactured together. In the last column ("all together") all data is reprinted to gain a mean value over six replicates for the standard weld lines and a mean value for the modified specimens. This overlaying was done for the modified weld lines because the difference of the inserts is in the range of process scatter.

The ANOVA concerning flexural testing showed that the different insert head geometries do not significantly differ regarding the flexural strength of the modified weld lines, the p-value is 0.214.

Comparing the mean value of all standard to all modified specimens the achieved improvement by modification for tensile strength is 14 % from 103 to 120 MPa. Concerning flexural strength the improvement is from 171 MPa (standard weld line specimens) to 274 MPa (modified weld lines specimens), which is a significant improvement of 38 %.

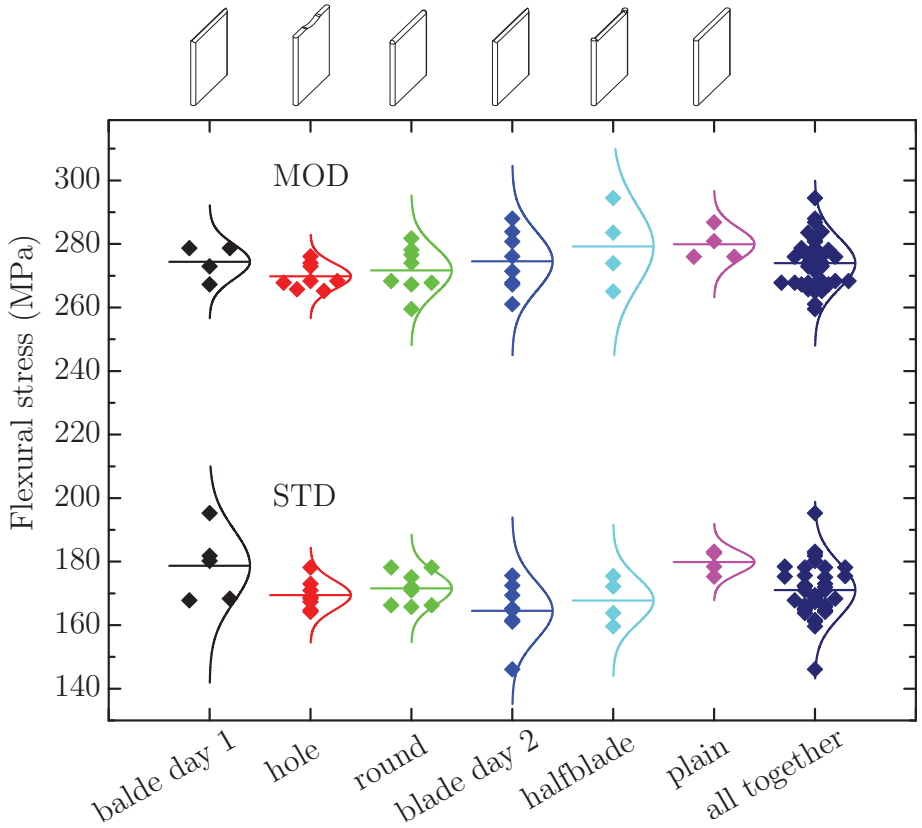


**Figure 5.14:** Flexural stress of standard and modified weld lines manufactured together. In the last column ("all together") all data is reprinted to gain a mean value over six replicates for the standard weld lines and a mean value for the modified specimens. This overlaying was done for the modified weld lines, too, because the difference of the inserts is in the range of process scatter.

**Table 5.13:** Grouping of the different insert head geometries of modified weld line specimens concerning tensile stress by the Fisher and the Tukey method. One group is one letter (A, B, C).

| **run number** | **flexural stress mean value** in MPa | **Tukey method** | **Fisher method** |
|---|---|---|---|
| blade | 125 | A | A |
| halfblade | 124 | A B | A |
| hole | 119 | B C | B |
| plain | 116 | C | B C |
| round | 116 | C | C |

**Interpretation**

In the previous chapters (section 5.1.4 to section 5.1.5.1) a mathematical analysis of the difference between standard weld lines and modified weld lines was performed. Every insert head geometry significantly improves the weld line strength concerning tensile and flexural strength. The ANOVAs performed show differences between the different insert head geometries for tensile testing only, but there was also significant difference between the different production days.

From a practical point of view the difference between the best and worst insert is hard to tell. The best performing inserts concerning tensile testing (blade and halfblade) shows 8 % more tensile strength than the worst (plain and round). Unfortunately specimens with the inserts blade or halfblade are hardest to produce, because the specimens tend to get stuck in the mold during ejection because of the protruding material.

The process scatter was only investigated for standard weld line specimens, where different days differed significantly from each other by approximately 4 %. Furtheron there is no significant difference between the insert head geometries concerning flexural testing. Considering these two facts the mathematically found significance between the differenc insert head geometries has no practical relevance. Compared to the difference between the strength of standard and modified weld lines the difference between the inserts is not as important as the modification itself.

## 5.2 Fracture behavior and fracture surface

In this section the fracture behavior is analyzed and interpreted using stress-strain diagrams and the corresponding fracture surface of the broken specimens. There are three types of specimens: a) specimens without weld lines, b) specimens with standard weld lines and c) specimens with modified weld lines. Tensile and flexural tests were investigated, especially the different fracture behavior in the flexural test between ejector side up and nozzle side up was examined.

The weld line is influenced asymmetrically, due to the movement of the flow obstacle. The insert is pushed out of the cavity when the mold is completely filled. It is assumed that the movement of the insert, respectively the melt, influences the modified weld line.

### 5.2.1 Fracture behavior

For non weld line and standard weld line specimens no big differences in the fracture surface occurs between tensile and flexural testing. In flexural testing the difference between ejector side configuration or nozzle side configuration is negligible, similar stress strain curves are obtained and the only possible influence on the result is the change in the tested profile due to the draft angle of 1 °.

For modified weld line specimens a big difference concerning fracture behavior can be noticed when flexural test curves are analyzed. The flow obstacle is pushed out of the cavity and this process works only into one way - from nozzle to ejector side. This causes asymmetric filling, which influences the breaking behavior. Altogether three examples of the results from flexural testing are shown in Fig 5.15 and Fig 5.16 for the insert head geometries halfblade, hole and plain. The other insert head geometries (blade and round) are similar to Fig 5.15.

Concerning Fig 5.15 no difference can be seen between the configurations for the standard weld line specimens. For the modified weld line specimens there is nearly no difference in bearable stress and strain, but in failure. All curves being tested nozzle side up start to crack, strain further and finally fail. This can be seen in the step(s) in each dark blue curve. The reason for that are the side weld lines which evolve because of the gap between mold wall and insert. For further information see the fracture surface analysis in section 5.2.2. These side weld lines seem to initiated the crack which leads to break. Whereas specimens tested in the ejector side up configuration break at the position of the loading edge.

In Fig 5.16 the bearable stress and strain of the modified weld line specimens type plain is reduced for nozzle side up compared to ejector side up. The explanation for that is the weld line which forms in the slit below the plain head surface of the insert. This behavior was found for the plain geometry only. The maximum strain is also dropping for nozzle side up. The first cracks start earlier compared to the other insert types,but are not that drastic.

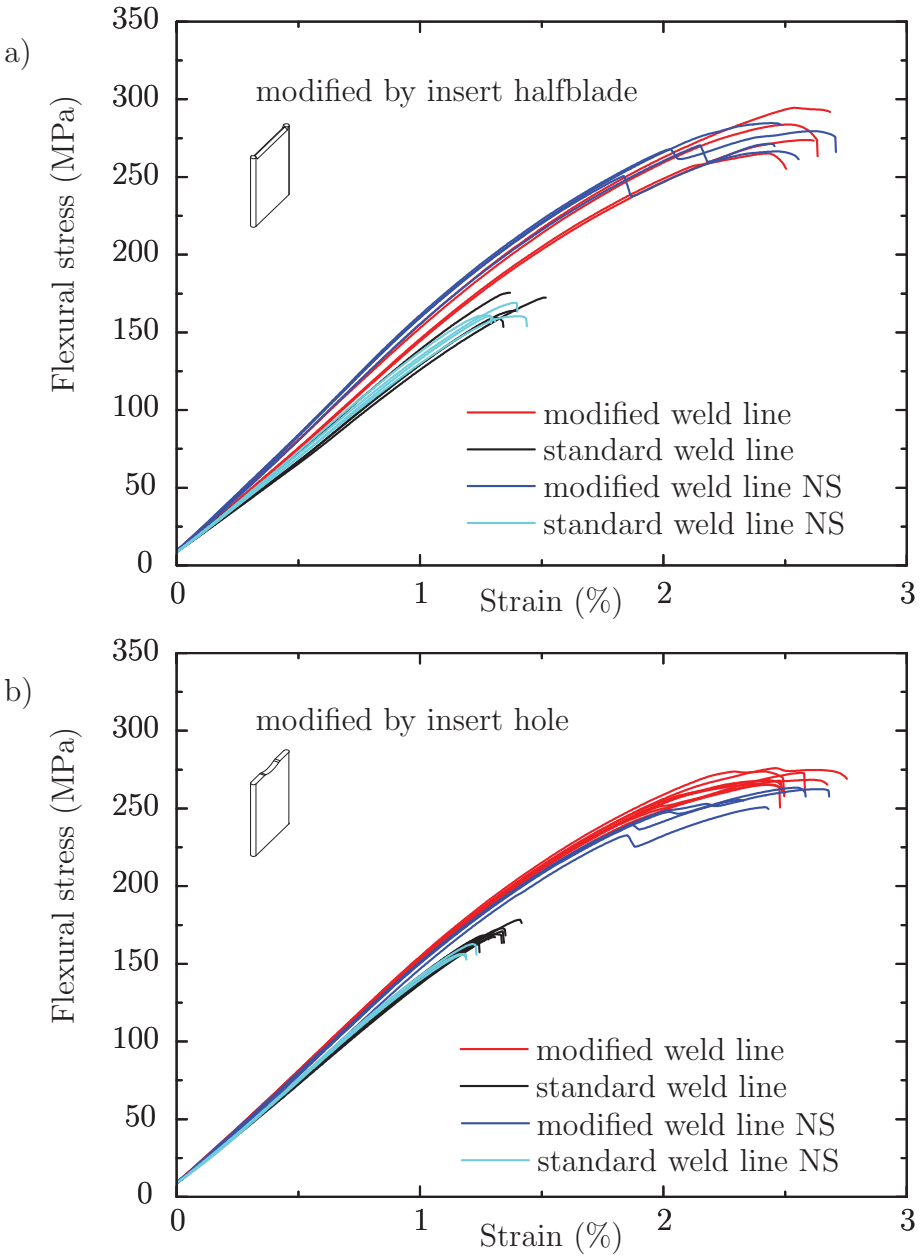


**Figure 5.15:** Comparison of flexural test results of the usual ejector side up and the nozzle side up configuration (marked with NS) of the insert halfblade in a) and of the insert hole in b). Furthermore, standard weld line specimens of the same production are tested.

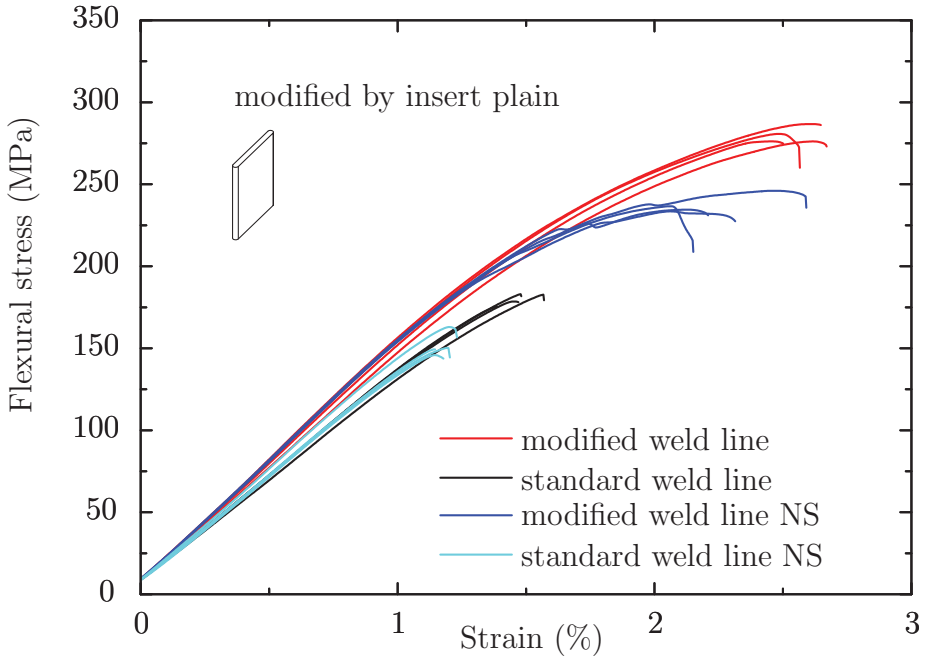


**Figure 5.16:** Comparison between the configurations ejector side up and nozzle side up for the insert plain.

### 5.2.2 Fracture patterns

The resulting fracture surface contains additional information about the specimen behavior. The three different groups of specimens (standard, modified and non weld line) showed different fracture surfaces. The non weld line specimens broke with a larger, rougher and more fissured surface than the standard weld line specimens, compare Fig 5.17 and Fig 5.18. The created surface of the standard weld line specimens was smooth.

For the modified weld line specimens testing conditions have an important influence on the fracture behavior. There is a difference between tensile and flexural tests. In the previous section 5.2.1 the difference between the stress-strain curves ejector side up or nozzle side up for flexural testing was already described. In the fracture surfaces these differences can be found as well, see Fig 5.19 to Fig 5.21. In the tensile testing (Fig 5.19) the modified weld line specimens break at a position of a side weld line. For flexural testing ejector side up (Fig 5.20) the modified weld line specimens break at the position of the loading edge, leaving a fissured fracture. The flexural testing configuration nozzle side up (Fig 5.21) shows a very smooth fracture pattern. Here the specimens break where the side weld lines are and where the modified weld line area is.

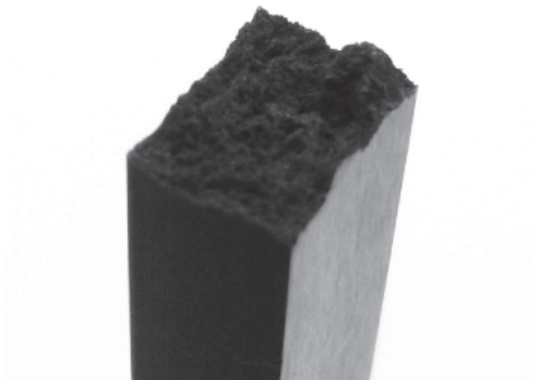

**Figure 5.17:** Fracture surface of a non weld line specimen. Generally the surface looks this way independent from the testing type. A highly three dimensional fracture surface can be observed. In this kind of specimens fibers are orientated in length direction of the specimen, leaving a fissured fracture surface. The area created during rupture is very large and its evolvement consumes much energy. This is an explanation why non weld line specimens bear very high loads.

a)

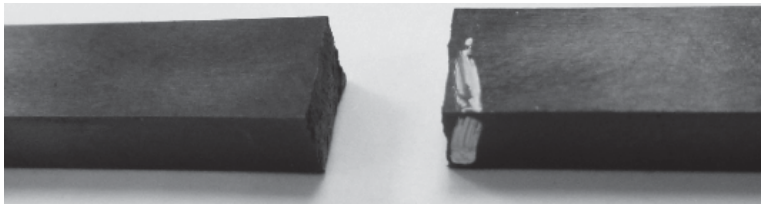

b)

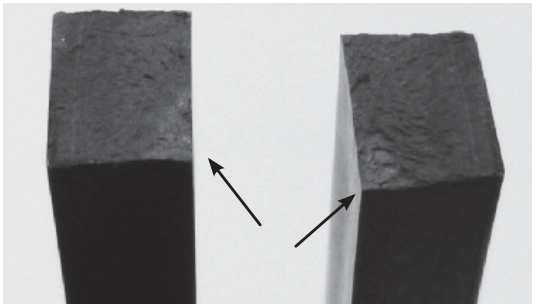

**Figure 5.18:** Fracture surface of a standard weld line specimen. The weld line is the weak spot of the specimen and weld line specimens always break there, independent from testing conditions.
In a) the assumed weld line position was marked with white paint before testing to position the specimen correctly for flexural testing.
In b) the plane fracture is shown. The edge where the crack is initiated is indicated with arrows. Due to the fiber orientation perpendicular to the flow direction (see section 2.2.4 and in section 5.3.1.1 Fig 5.26) the rupture is smooth in comparison to specimens without weld line.

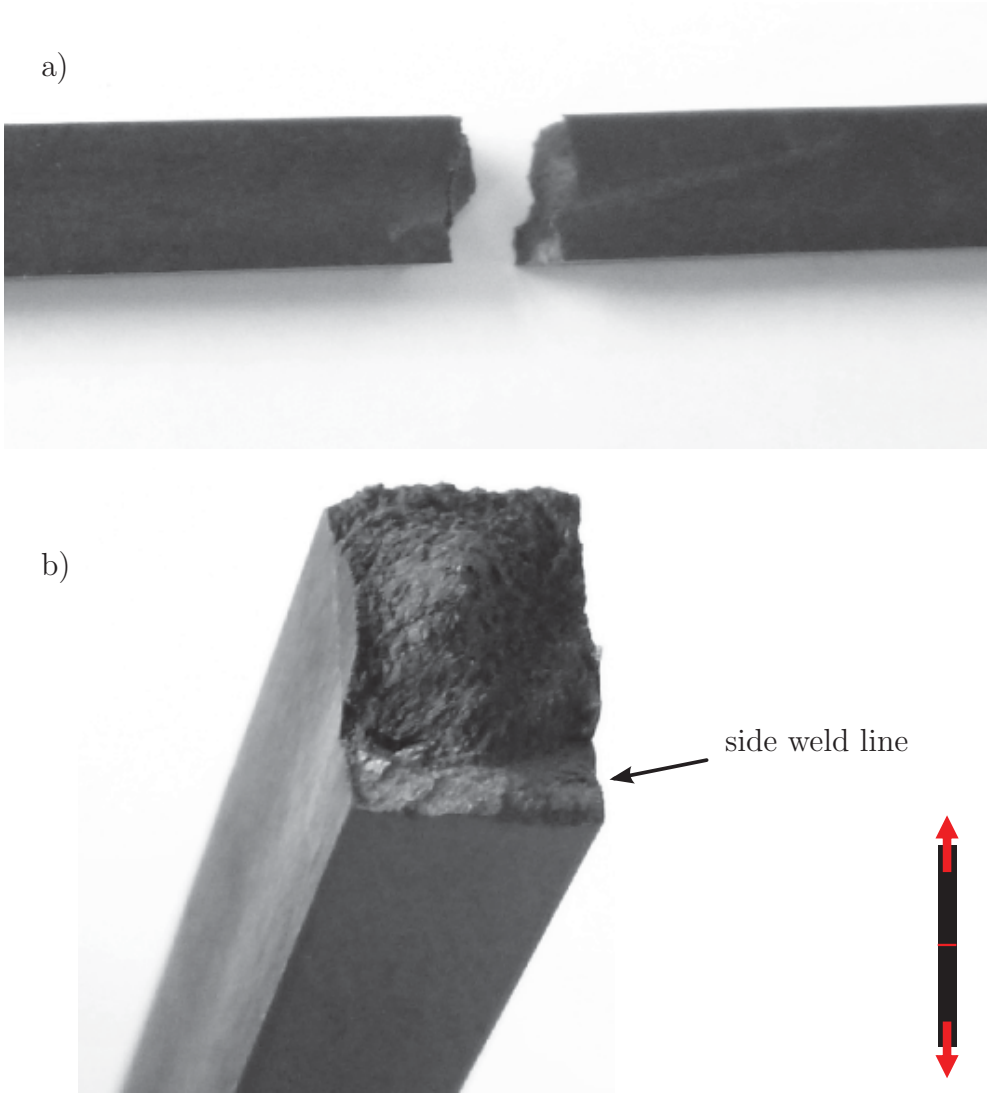


**Figure 5.19:** Fracture surface of a tensile tested specimen with a modified weld line. Similar to the non weld line specimens a very large surface is created during rupture.
In a) the nozzle side of the specimen is up, the blurry mark of the insert can be recognized. The fracture is not in the middle of the specimen. It occurs at one of the gaps between insert and mold where the side weld lines are formed. This can also be detected in b). The upper part of the specimen is fissured, but on the lower side there is a certain area where the fracture surface appearance changes. There the side weld line is located. It emerges because of the gap between insert and mold wall.

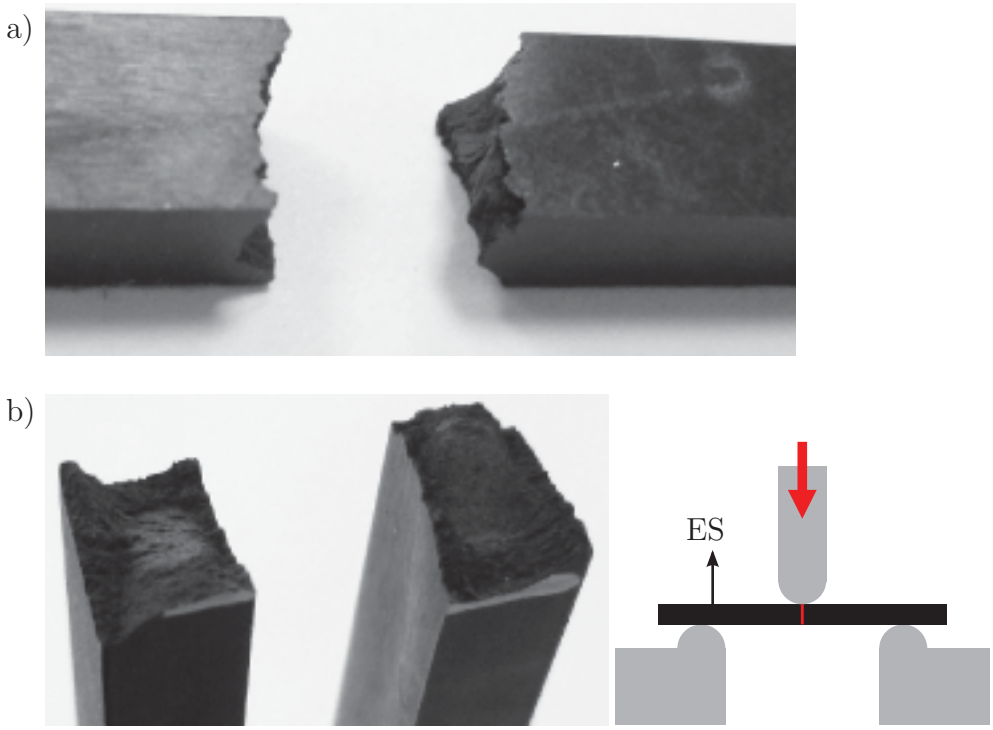


**Figure 5.20:** Fracture surface of a flexurally tested specimen with a modified weld line, ejector side is up. The fracture is in the middle of the insert. In b) again a highly complex fracture appears. Here a change of color can be recognized. In the middle of the specimen it appears brighter, to the edges darker. A possible explanation for that could be fiber orientation. While more fibers are aligned randomly in the middle of the specimen (brighter area), a strong orientation in flow direction can be found in the darker areas.

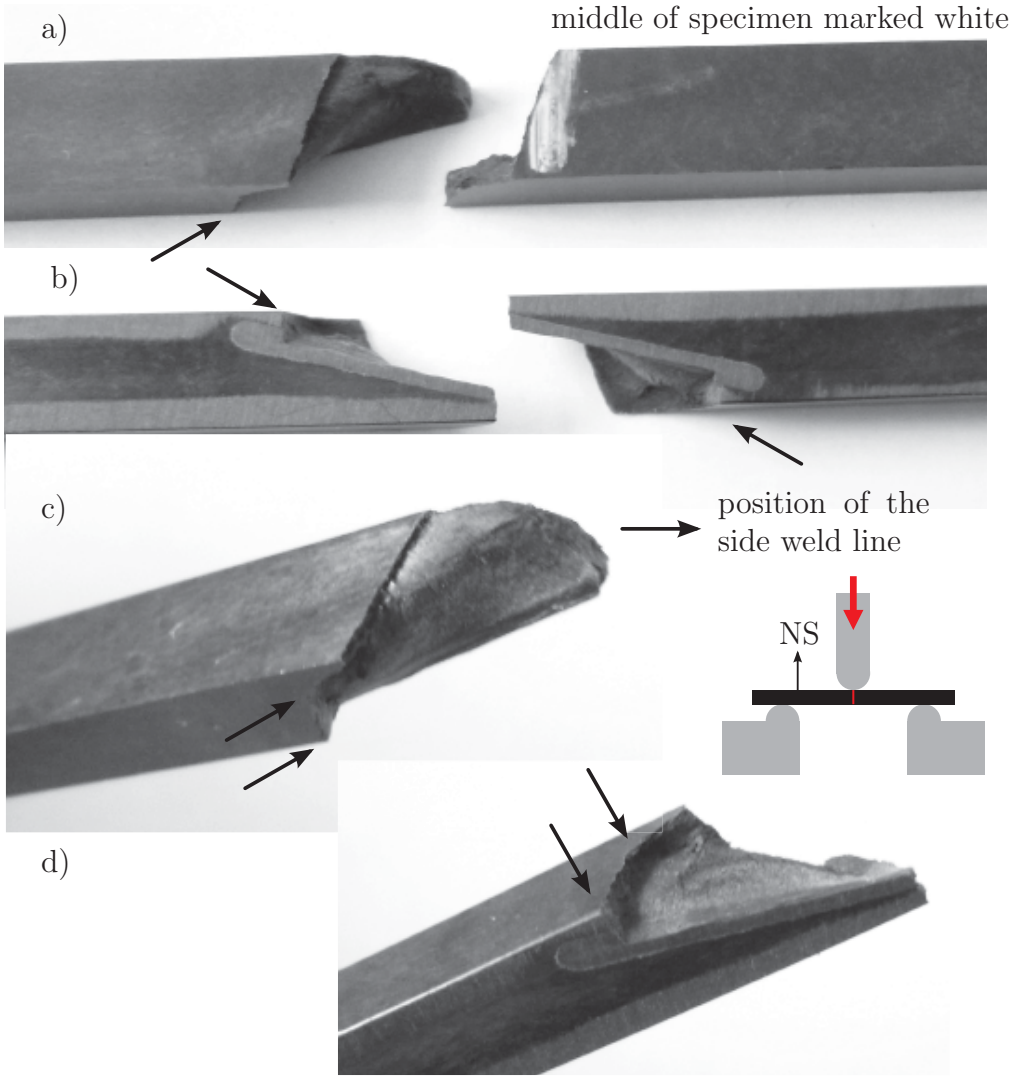


**Figure 5.21:** Fracture surface of a flexurally tested specimen with a modified weld line of the type blade, nozzle side is up. In this setting the fracture surface strongly differs from the ejector side up configuration. In a) the middle of the specimen and insert is marked with white paint on the nozzle side, where the loading edge is positioned. In b) the ejector side of the broken specimen is shown. Lapping removed protruding material and a bit of the specimen surface, these areas appear gray.
In c) and d) two different views on the fractured specimen are presented, showing again the start of rupture at the side weld lines. The difference to the other figures presented before is the rupture surface. When the nozzle side is up rupture starts at one (or both) side weld line(s), follows the modified weld line geometry and finally breaks. The side weld lines are marked with arrows. The appearance of the whole weld line is rather smooth, though. This leads to the assumption that the specimen broke directly at the modified weld line.

## 5.3 Microscopy

Using microscopy a model of the modified weld line shape could be created, the sample preparation and analysis is presented subsequently. Specimens were cut and investigated in several directions.

### 5.3.1 Sample-taking

#### 5.3.1.1 Cuts normal to the length direction

Specimens were cut with a saw, ground and polished for microscopy (polishing program is described in Tab 4.8). After a polish was photographed, it was ground and polished further to get an idea of the shape of the weld line over the length direction of a modified specimen. For better handling two specimens were needed to obtain enough information about the weld line shape, when cutting normal to the length direction. It was assumed that the two specimens are equal and their sides are symmetrical. Both specimens were cut and ground into different directions of the length axis. So a continuous image of the generated fiber orientation of the modified weld line can be generated over the whole insert length. The position of the cuts and the grinding directions are pictured in Fig 5.22. One specimen was cut between A and B and ground and polished into the direction of the arrows in the picture. The other cut was done between C and D.

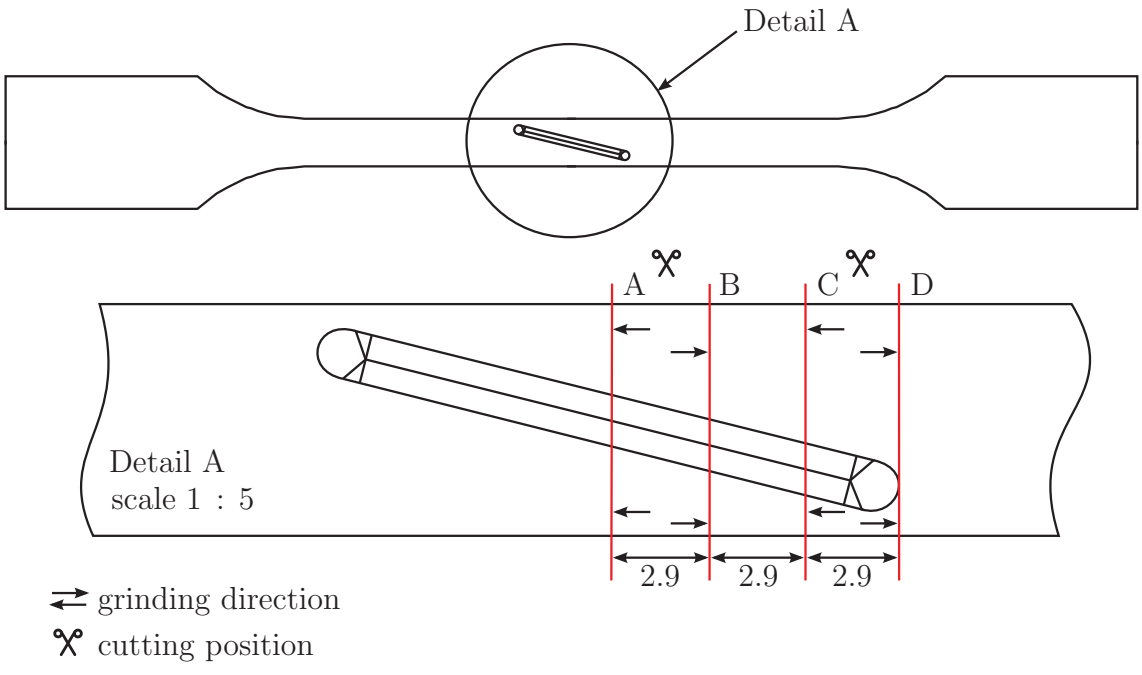


**Figure 5.22:** Preparation of polishes normal to the length direction of a specimen. Position of the cuts and grinding direction marked with arrows for the polish series (A to D). The distance between these cuts is approximately 2.9 mm. The real distances between the following polishes is shown in Tab 5.14 below.

After each polishing step the samples were analyzed by microscopy and photos were taken. In these pictures the real position was calculated from a notch positioned on top of the sample. The notch has the same angle to the side of the specimen as the insert has. So start and end point of the notch are defined and also the gradient, see schematic sketch Fig 5.23. A total of three polishing runs were performed, generating 12 polishes over the length of the modified insert. To determine the position of the cut equation (5.1) is used with x being the respective x-distance of the notch from the edge. The results of this calculation is presented in Tab 5.14.

Out of these polishes the shape of the modified weld line is determined over the specimens height with 20 equidistant points using the fiber orientation, which is perpendicular to the flow at the weld line. The distance between the points is 0.25 mm. An example of these measurements is shown in Fig 5.24c. Out of these generated points splines are created and put together to form a three dimensional weld area, which is shown and discussed subsequently.

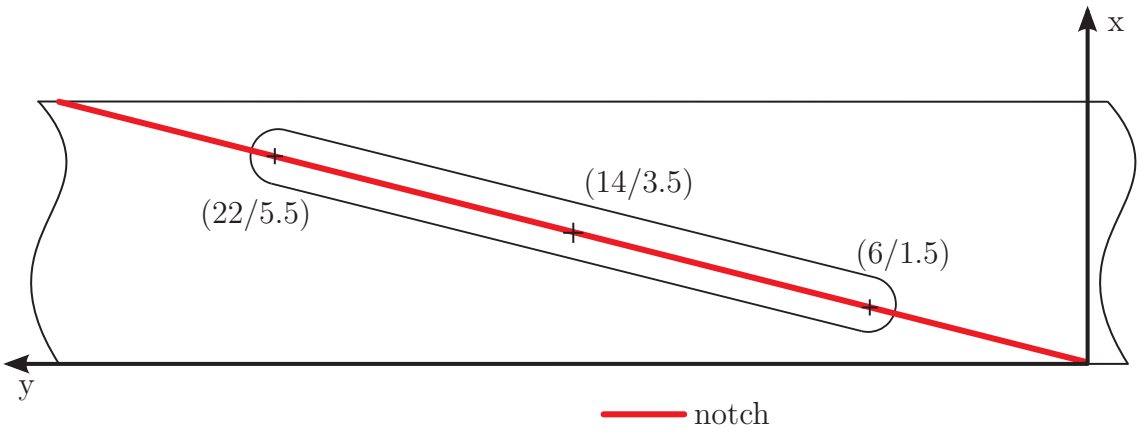


**Figure 5.23:** Preparation of polishes normal to the length of the specimens. The specimens were notched for the determination of the cut positions. The notch is painted red. Three points on the notch are already defined: the middle points of the radius in the end of the inserts and the middle point of the insert. The equation for the position determination of the cuts is shown in equation (5.1).

$$y = 4 * x \tag{5.1}$$

**Table 5.14:** Position determination of polishes $A_1$ to $D_3$. Unfortunately $D_1$ is closer to the the middle than $C_3$. While embedding not all samples remained vertically as positioned, so due to the embedding process this difference occurs. So unfortunately some samples where not exactly perpendicular to the polished surface. For each position (A, B, C and D) three polishes were manufactured which were numbered, e. g. for A: $A_1$, $A_2$ and $A_3$. These positions can be viewed in Fig 5.30.

| **position designation** | **x position** in mm | **calculated y position** in mm | **distance to middle** in mm |
|---|---|---|---|
| middle | 3.5 | 14 | 0 |
| $A_1$ | 3.092 | 12.37 | 1.63 |
| $A_2$ | 2.877 | 11.51 | 2.49 |
| $A_3$ | 2.707 | 10.83 | 3.17 |
| $B_1$ | 2.467 | 9.868 | 4.132 |
| $B_2$ | 2.286 | 9.144 | 4.856 |
| $B_3$ | 2.056 | 8.224 | 5.776 |
| $C_1$ | 1.856 | 7.424 | 6.576 |
| $C_2$ | 1.705 | 6.820 | 7.180 |
| $C_3$ | 1.480 | 5.920 | 8.080 |
| $D_1$ | 1.532 | 6.128 | 7.872 |
| end of insert | 1.5 | 5.25 | 8.75 |
| $D_2$ | 1.274 | 5.096 | 8.904 |
| $D_3$ | 1.069 | 4.276 | 9.724 |

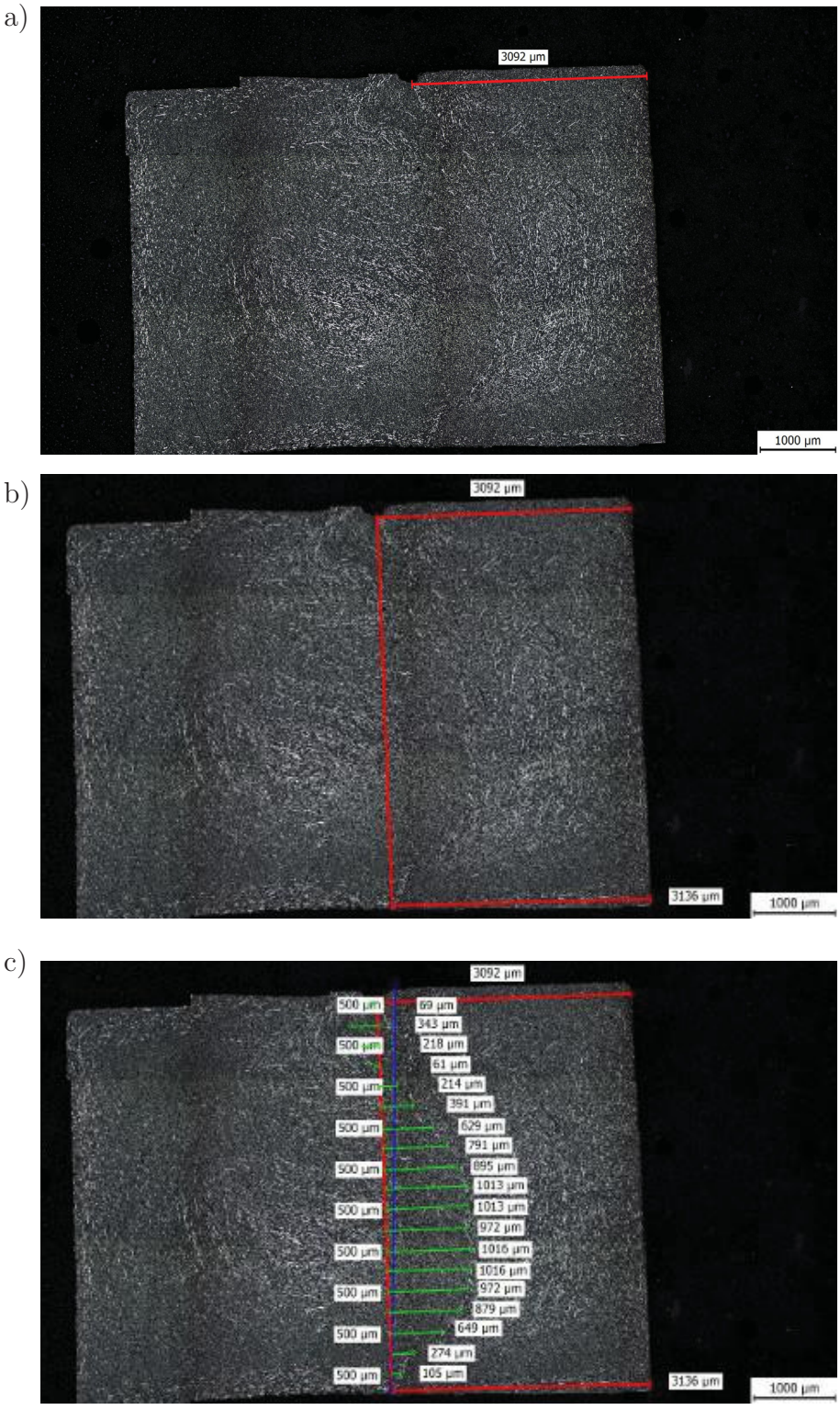


**Figure 5.24:** Polish of position $A_1$ from Fig 5.22. In a) the original picture, the distance of the notch is determined from the closer side of the specimen to the middle of the notch. In b) the insert position is marked with a vertical red line. In c) the assumed weld line is determined. 20 equidistant points are determined with the green horizontal measuring beams. The vertical distance between the points is 0.25 mm.

#### 5.3.1.2 Cuts normal to the specimen height

In the second part of microscoping, polishes were made over the height of the specimens of all different inserts as well as a specimen with a standard weld line. A sketch of the positions of polishes is shown in Fig 5.25. After satisfactory pictures had been taken, the height positions of the polishes were determined using a dial gauge. Then they were ground to the next position using several papers of grain size P320 and polished again.

The non standardized grinding results in irregular grinding depths. As an example the list of grinding positions for the insert type blade is shown in Tab 5.15.

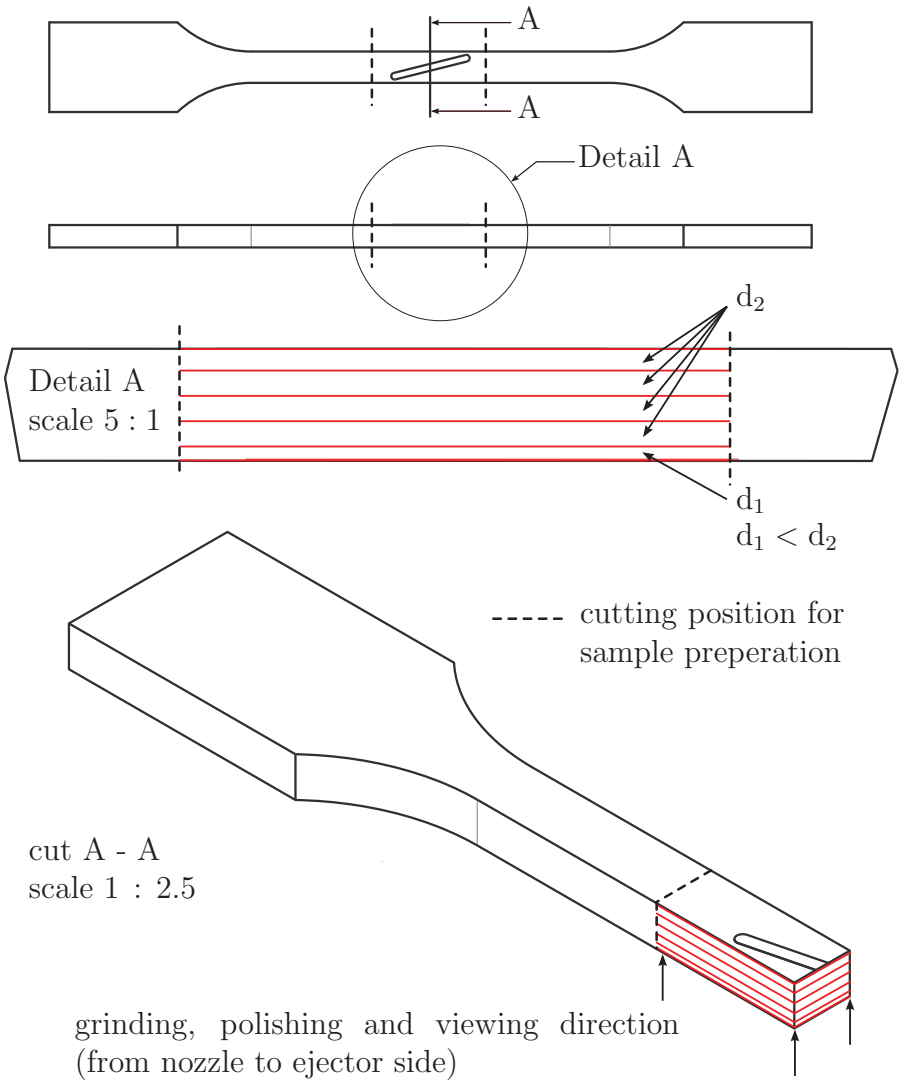


**Figure 5.25:** Sketch of the preparation of polishes over specimen height, positions of the cuts and grinding direction.
The first polish was made closely to the surface. The next polishes have a distance ($d_1$) of approximately 0.3 mm from the surface. Between all other polishes a greater distance ($d_2$) of 0.5 to 0.9 mm was chosen. In the schematic sketch only half of the polish positions are marked. Exact positions of the polishes can be found in Tab 5.15.

**Table 5.15:** Numbered positions of polishes in a modified specimen of type blade. The distance from nozzle to ejector side is smaller here than 5 mm due to shrinkage.

| **number** | **position of polishes over specimen height** in mm |
|---|---|
| | 0 = nozzle side surface |
| 0 | 0.03 |
| 1 | 0.34 |
| 2 | 0.65 |
| 3 | 1.35 |
| 4 | 1.76 |
| 5 | 2.54 |
| 6 | 3.29 |
| 7 | 3.86 |
| 8 | 4.67 |
| | 4.8 to 4.9 = ejector side surface |

### 5.3.2 Polishes of standard weld lines

Literature in section 2.2.4 states several layers over part thickness and different shrinkage at the weld line due to fiber orientation. The weld line appears visibly because of different fiber orientation, see Fig 5.26 and Fig 5.27. In these figures standard weld lines are examined and the differences in fiber orientation are marked. The fiber orientation is random in the bulk, but orientated perpendicular to the flow at the weld line.

Fig 5.26 shows the fiber orientation of a standard weld line. There the fiber orientation is marked shematically by arrows. Fig 5.27 shows a series of polishes made with different distance to a standard weld line. The change in fiber orientation can be viewed. The greater the distance to the weld line the more fibers are orientated randomly, especially in the center of the polished sample. Furthermore, voids can be seen in $G_1$ and $H_1$ as black specks in the middle of the images. These voids appear only in the middle of the bulk of the specimens and not at the weld line.

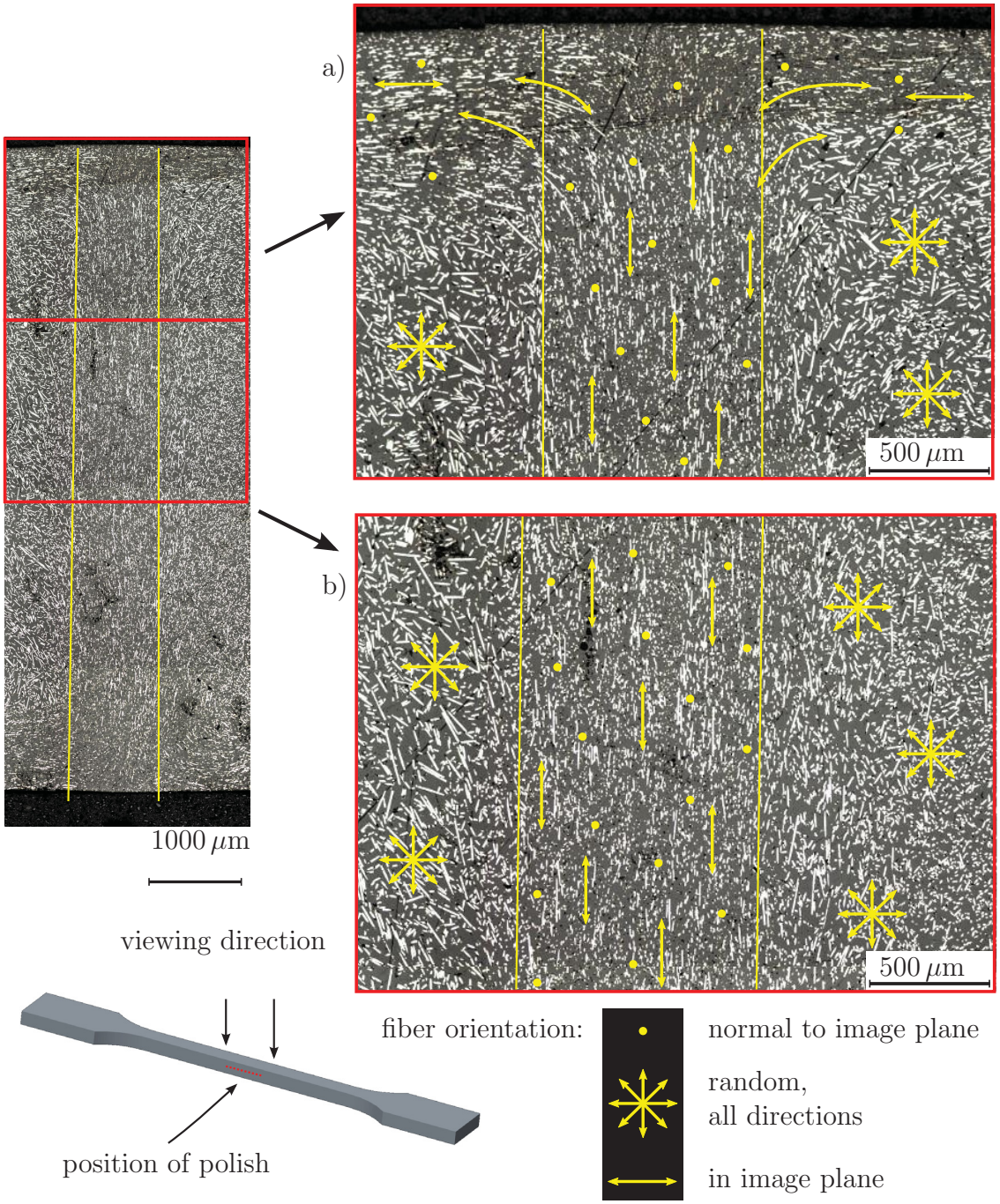


**Figure 5.26:** In this picture the fiber orientation at a standard weld line is explained schematically. The cut is approximately in the middle of the specimen height. The fiber orientation is drawn as yellow arrows in the image plane and as yellow dots out of the image plane. The weld line can be distinguished from the bulk easily, and is located between the yellow lines.
Two parts of the weld line are enlarged. In a) and b) fibers from the bulk are orientated in the image plane, easily recognizable by their oval or fiberlike shape. In a) the fiber orientation changes from an alignment top to bottom to left to right near the surface, this is due to material flow.

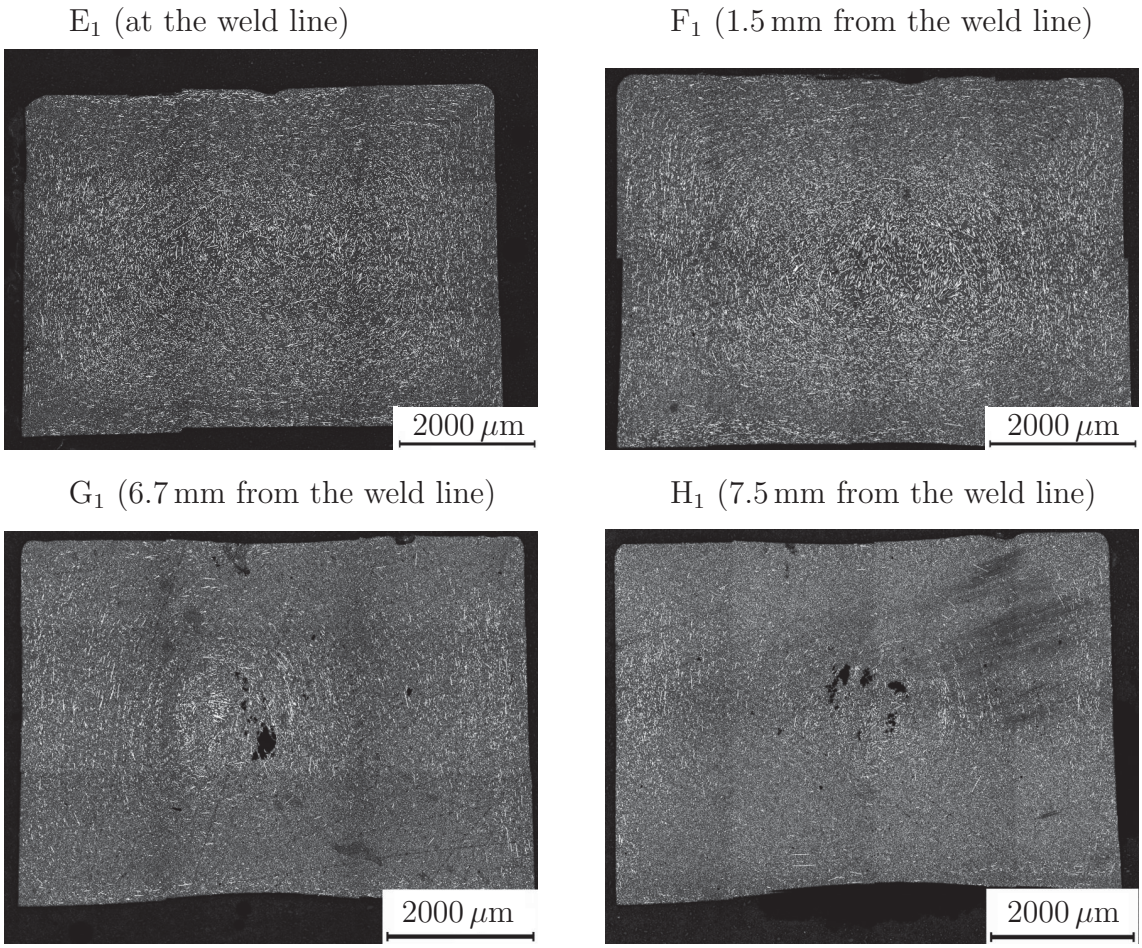


**Figure 5.27:** These pictures were made from standard weld line specimens, analogous to the described procedure in section 5.3.1.1, polishes normal to the specimen length direction. The positions E, F, G, H are equal to A, B, C, D in Fig 5.22. $E_1$ is at the weld line, $F_1$ in a distance of 1.5 mm, $G_1$ 6.7 mm and $H_1$ is 7.5 mm away.
A change in fiber orientation can be recognized from $E_1$ to $H_1$, which dramatically influences shrinkage. In $E_1$ the fibers are orientated perpendicularly to the flow in the image plane, which is parallel to the "weld plane", nearly no shrinkage is detectable, whereas in $H_1$ the fibers are aligned in flow direction and in viewing direction shrinkage is easily recognizable at the bottom of the image.
Furthermore, voids can be seen in $G_1$ and $H_1$ as black specks in the middle of the images.

### 5.3.3 Polishes of the modified weld lines

Polishes of the modified weld lines were made from two directions: a) normal to the specimen length (see section 5.3.3.1) and b) normal to the specimen height (see section 5.3.3.3). In both cases a series of polishes was produced, so the weld line shape can be analyzed a) over the specimen height and b) over the specimen length. The analysis of

point a) enabled the generation of a three dimensional model of a modified weld line. Polishes normal to the specimen height show the side weld lines more clearly.

#### 5.3.3.1 Polishes normal to the specimen length

Using incident light microscopy, all polishes normal to the specimen length were investigated. The preparation and analysis method of these polishes is explained in section 5.3.1.1. The multistep pictures of the modified weld line type halfblade are shown in Fig 5.28 and Fig 5.29. From the fiber orientation of these pictures the position and shape of the modified weld line can be imagined. The modified weld area is curved. The side weld lines can be found in Fig 5.29, where many fibers area orientated in the picutre plane.

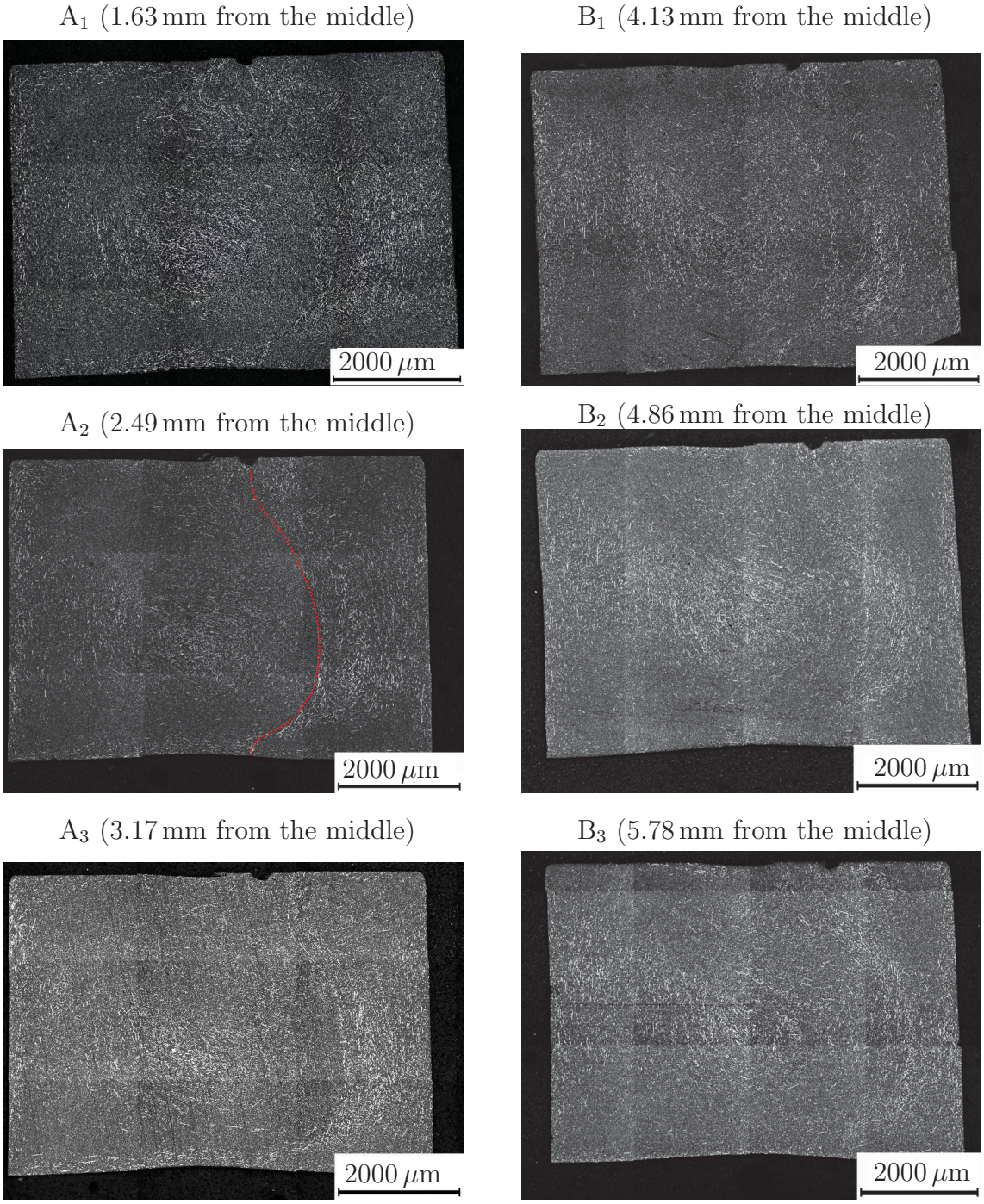


**Figure 5.28:** Two series of polishes in the length direction of a modified weld line of the insert type halfblade. $A_1$ is closest to the middle of the flow obstacle, $B_3$ about half the way between middle and edge of the insert. For further information about the positioning see Tab 5.14. In all pictures a change of fiber orientation can be seen as a line. This visible line is the weld line. Easiest to identify is this line/band in $A_3$ and $B_1$. Interesting is the shape of the weld line. It is not straight form top to bottom but curved. As an example this line is marked with a dotted red line in $A_2$.

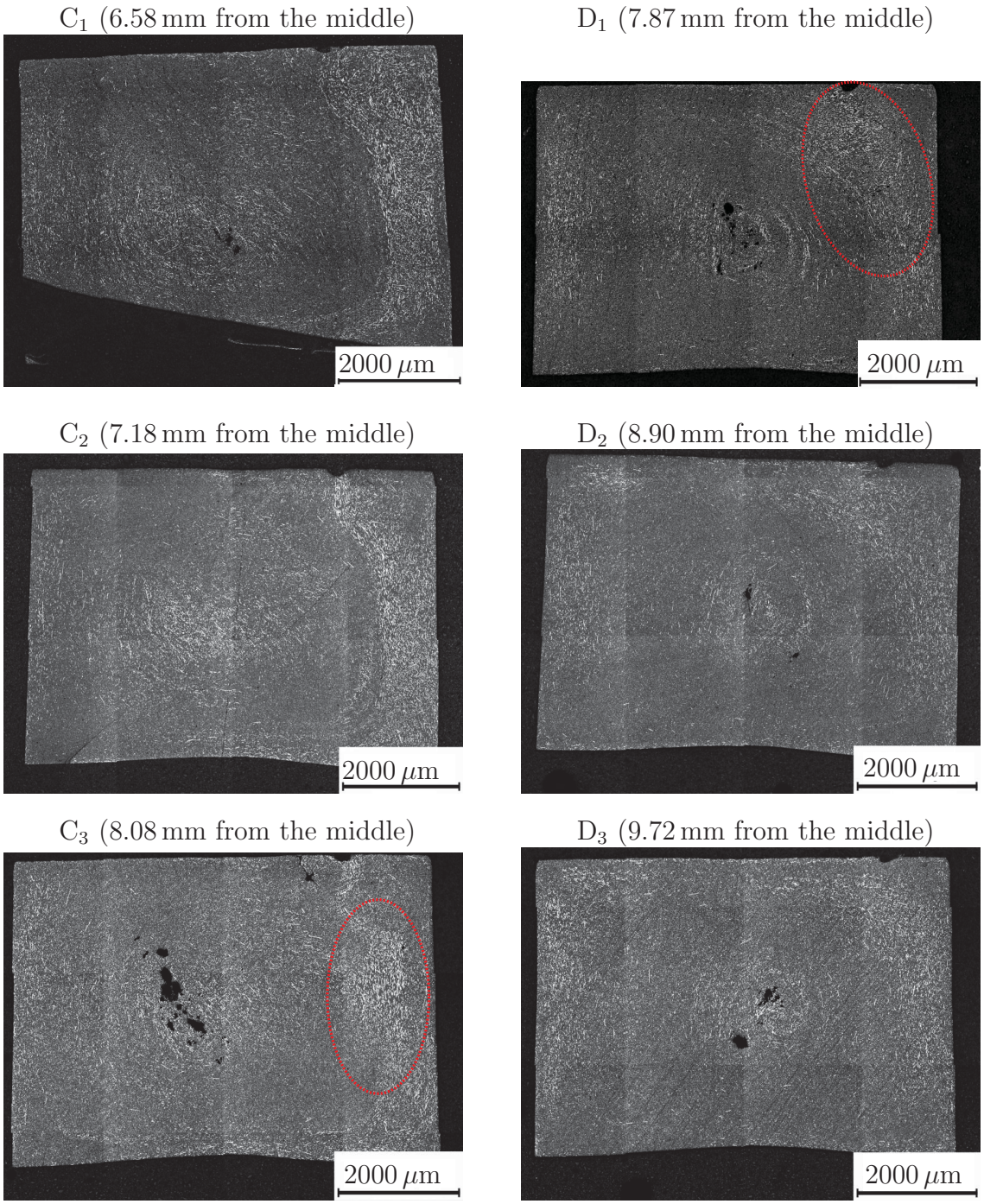


**Figure 5.29:** Further polishes of a modified weld line of the insert type halfblade. $C_1$ and $C_2$ show the same curved line that seems to separate two areas of orientation, as described in Fig 5.28. In $C_3$ and $D_1$ the position of the side weld line which occurs at the gap between the insert and mold wall is reached. The areas with fibers orientated in the image plane are circled with dotted red lines. Here the line differs and many fibers are orientated in the weld plane (identical with image plane). Important to mention is that $D_1$ is located further in the middle than $C_3$, see Tab 5.14. This results from the position of the cut and grinding direction.

#### 5.3.3.2 3D model of a modified weld line

The cuts of the previous section 5.3.3.1 of a specimen with a modified weld line type halfblade were used for the creation of splines. The procedure of data generation is explained in Fig 5.24. These splines were mirrored to generate a model over the whole insert. This model is pictured in Fig 5.31 below. The shape of the assumed modified weld line is definitely not as straight as the flow obstacle.

The dislocations from the position of the insert might be a bit irregular, but over all in agreement with series Fig 5.32 to Fig 5.41, which also show a bended weld line shape (red). Additionally the side weld lines (green) are pictured as simple planes, compare Fig 5.32. This model gives an insight of the formed modified weld line, but it has to be mentioned that it has flaws. There is a tiny offset between $A_3$ and $B_1$, see Fig 5.30, resulting most likely from imperfect notching and usage of different polishes. The second flaw is the linear assumption at the middle, the flexion between $A_1$ and middle is overdrawn, due to the spline method.

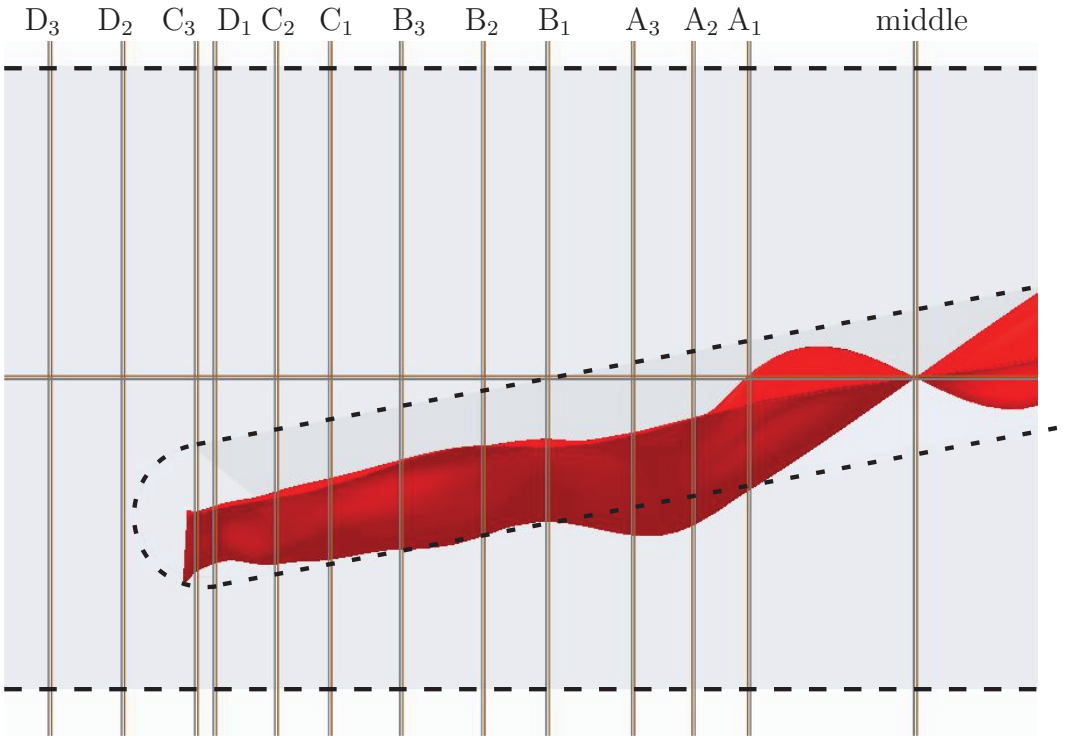


**Figure 5.30:** All positions of the polishes are indicated in one half of the flow obstacle, plus one more in the middle of the insert. In the middle no curved spline was used but a straight line from top to bottom. This assumption causes overshooting near the middle position.

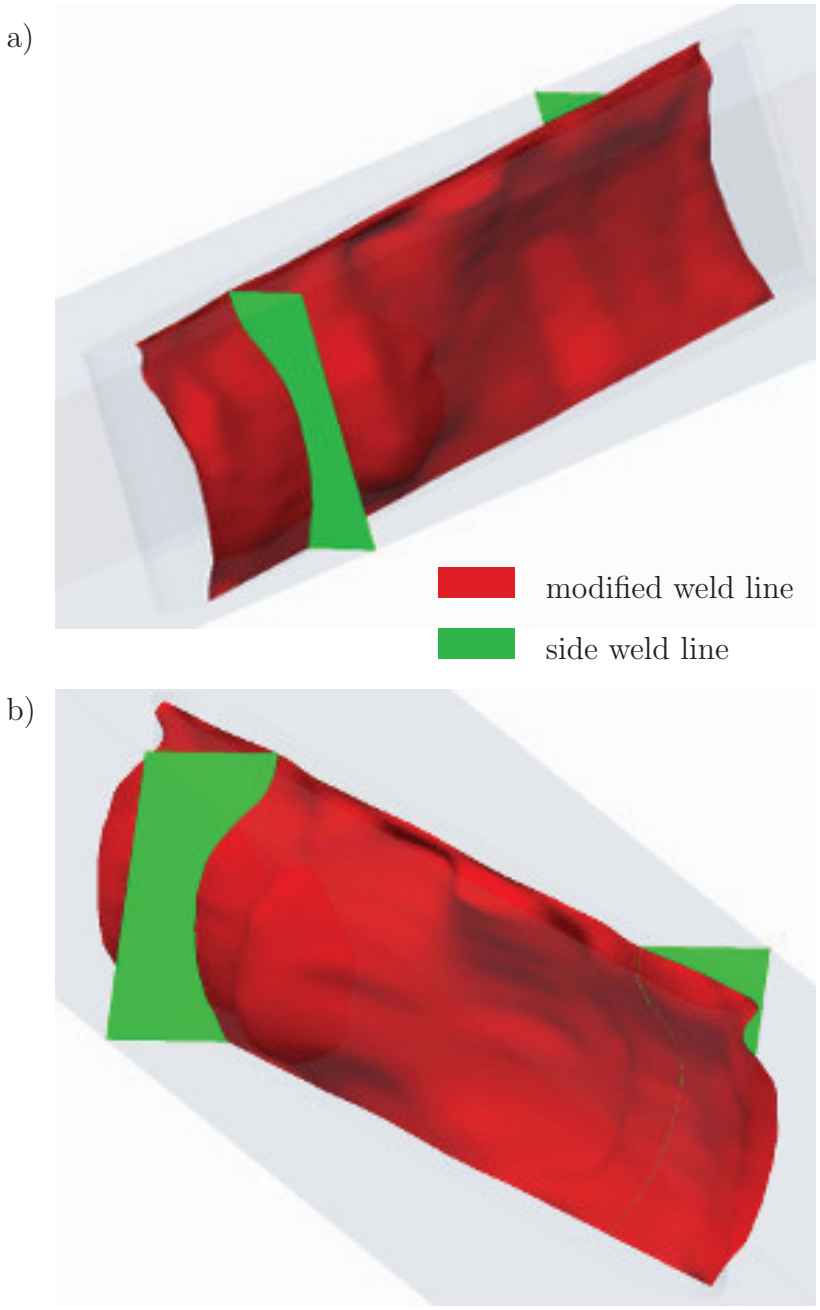


**Figure 5.31:** In a) and b) two different views on the three dimensional model are shown, modified weld line (red) and side weld lines (green).

#### 5.3.3.3 Cuts normal to the specimen height

A series of nine polishes of the insert type blade was made, the preparation was performed as described in section 5.3.1.2. The polish numbers are 0 to 8 and their positions are summarized in Tab 5.15. In this table the distance between nozzle and ejector side is only 4.8 mm, although the cavity hight is 5 mm. The reason for this difference is shrinkage, which depends on the position in the length direction, see Fig 5.33. The

profile of the specimen was measured two times using equation (5.1) for position determination. No notch was needed because the protrusion created from the blade was not lapped away and positioned right were the notch would have to be, see Fig 5.33.

This series was performed by means of dark field microscopy. Fig 5.32 and Fig 5.34 to Fig 5.41 show the photographed polishes of the insert type blade. Generally fibers which are cut in direction of their axes appear as white ellipsoids. So brighter areas inherit more fibers in the image plane. The darker an area is the more fibers are orientated perpendicularly to the image plane. So the weld line area appears dark especially on the borders of the specimen. In the middle of the specimen the fibers are randomly orientated so finding the actual weld line is hard, see Fig 5.35 to Fig 5.38. In the middle of the specimen voids are present, as white specks, Fig 5.36 to Fig 5.38. These voids were not further investigated because they appeared in the bulk area and not at the position of the geometric modification through the insert.

In Fig 5.32 the modified weld line and the side weld lines can be identified. The insert forms the line which crosses the picture from lower left to upper right. The two side weld lines evolve, which are formed like standard weld lines and are orientated top to bottom in the image. These side weld lines are formed due to the fact, that molten material passes through the gap between the insert and the mold wall and the melt flow of the opposite sides is reunited. This is shown in the filling study Fig 4.1. The white speck on the left side of the picture is a rest of injection molded surface of the specimen, which has not been ground and polished off jet. This shows how close to the specimen surface this polish is positioned and that the specimen does not have a plane surface, see Fig 5.33.

In Fig 5.33 the profile of this specimen is not rectangular any more. Furthermore, shrinkage differs greatly between height (5 mm) and width (7 mm). Only the height direction is examined due to stronger shrinkage and polishing direction.
The position of a) is 12.4 mm meaning a distance of 1.6 mm to the middle of the insert. Shrinkage in the middle of the profile is 0.1 mm.
In b) the position is 8.2 mm, so nearly 3 mm away from the end of the flow obstacle. Here shrinkage is even greater than in a) leaving a height of only 4.77 mm in the middle. The following images each consist of more than 35 single photos.

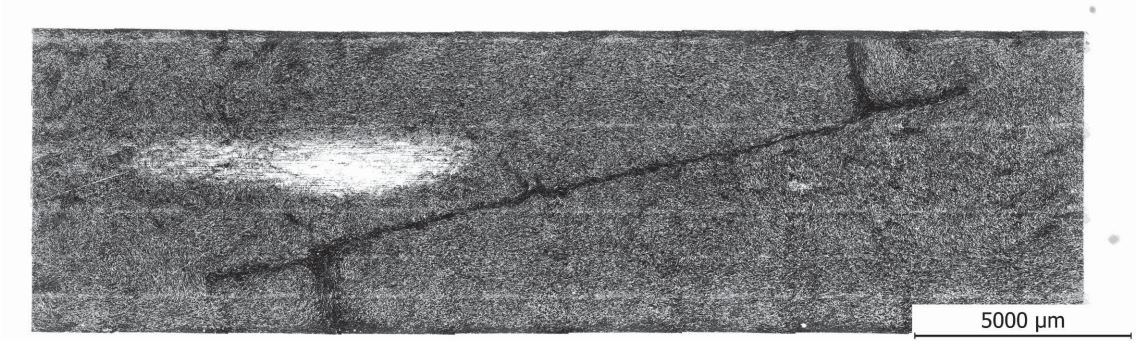


**Figure 5.32:** Polish number 0 of the insert type blade, position 0.03 mm from nozzle side. The weld line can be easily identified as black line, where the fibers are orientated out of the image plane.

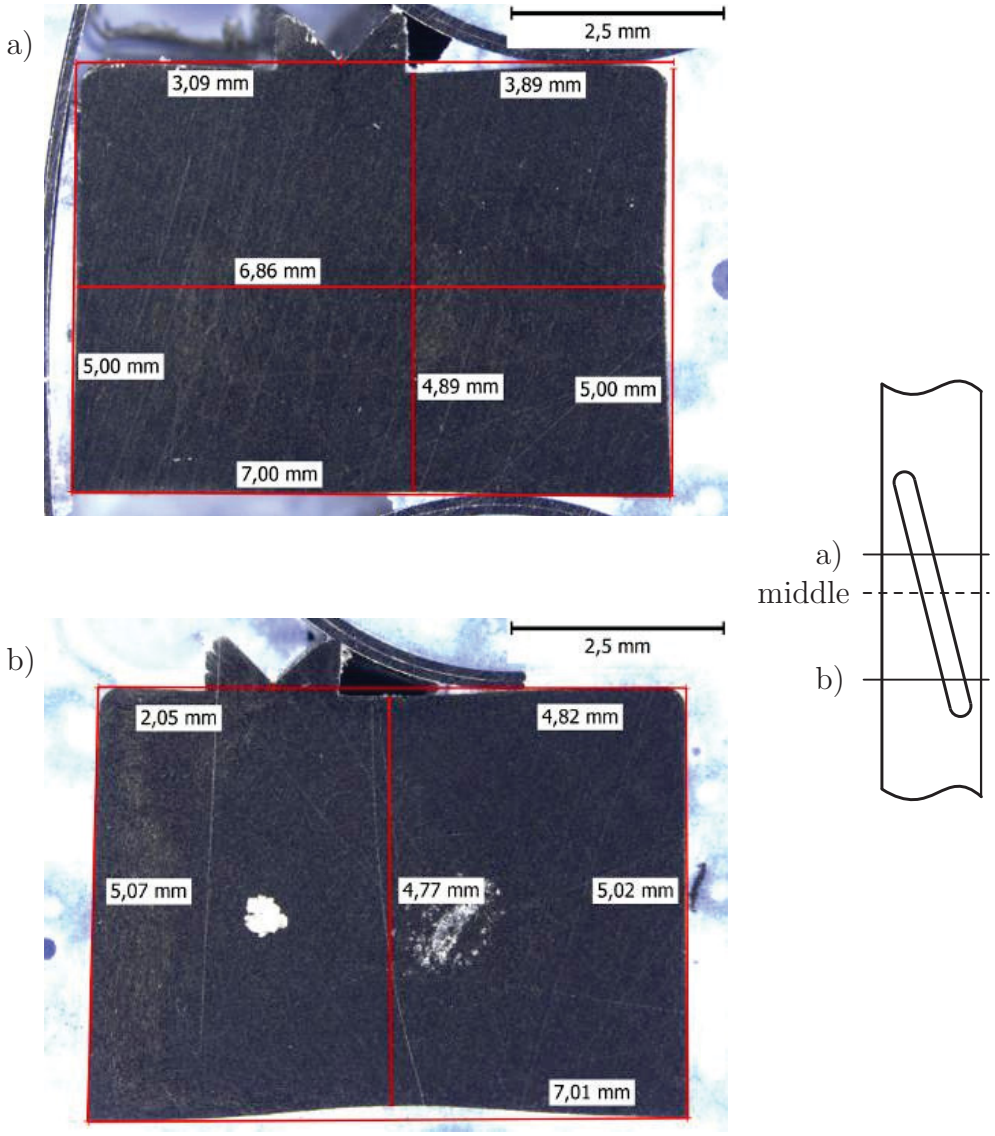


**Figure 5.33:** Profile of a modified weld line to measure shrinkage. The positions of a) and b) are shown on shematically on the right.

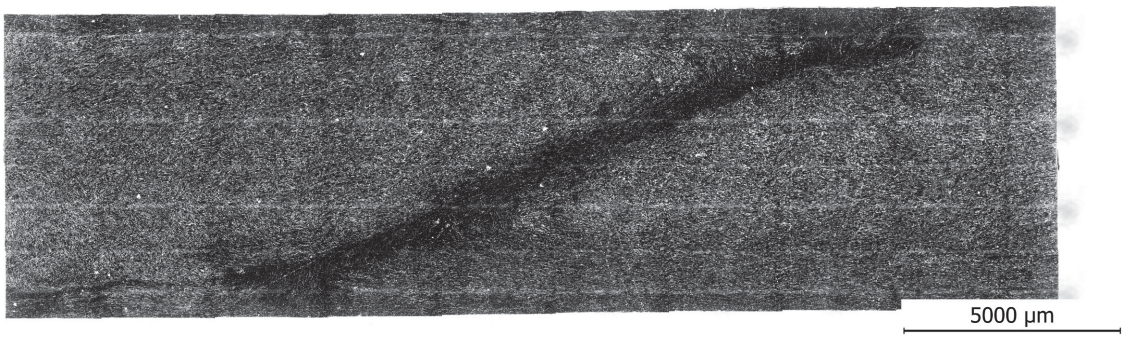


**Figure 5.34:** Polish number 1 of the insert type blade, position 0.34 mm from nozzle side. Pushing the insert back the weld line area grows broader.
The side weld lines described in Fig 5.32 also grow wider and become hard to distinguish from the modified part of the weld line.

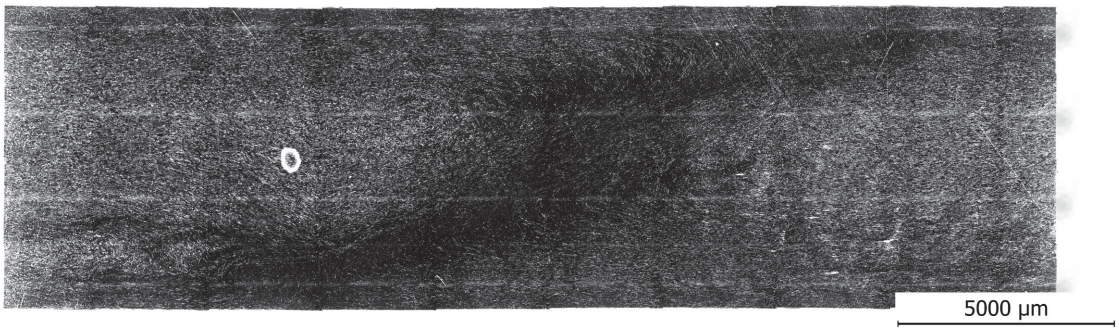


**Figure 5.35:** Polish number 2 of the insert type blade, position 0.65 mm from nozzle side. At this position the weld line becomes broader and it becomes hard to distinguish between bulk and the weld line area.


**Figure 5.36:** Polish number 3 of the insert type blade, position 1.35 mm from nozzle side. Here the weld line can hardly be found, describing a double bended curve. Furthermore, fiber orientation of the melt streaming close to the flow obstacle becomes visible.
The white specks in the middle of the specimen are voids.

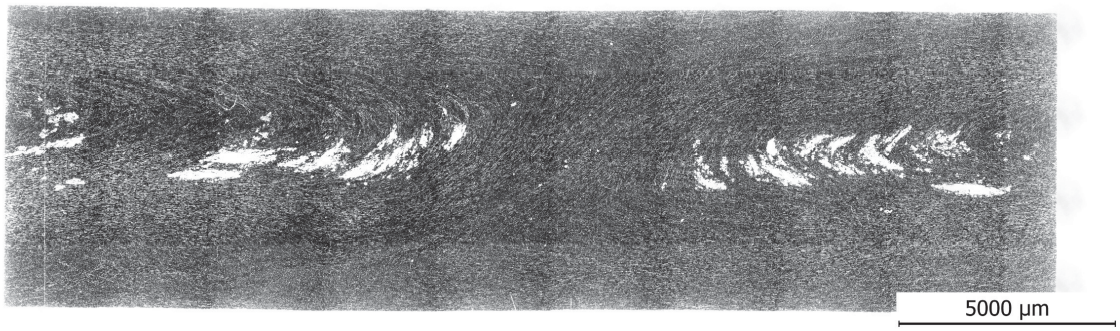


**Figure 5.37:** Polish number 4 of the insert type blade, position 1.76 mm from nozzle side. Fiber orientation due to melt movement is clearly recognizable. The weld line shape is no straight line any more but double curved. Again the white specks are voids, which occur in the middle of the specimen.

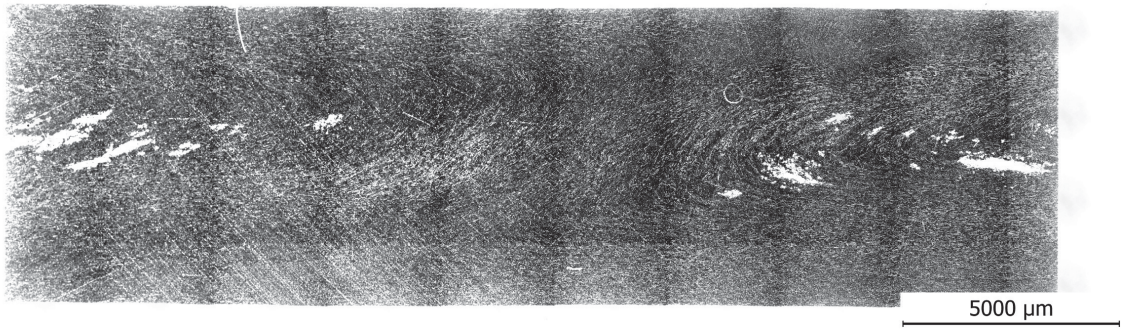


**Figure 5.38:** Polish number 5 of the insert type blade, position 2.54 mm from nozzle side. Fiber orientation due to melt flow is clearly visible and voids occur. The weld line is barely recognizable as double curved line.

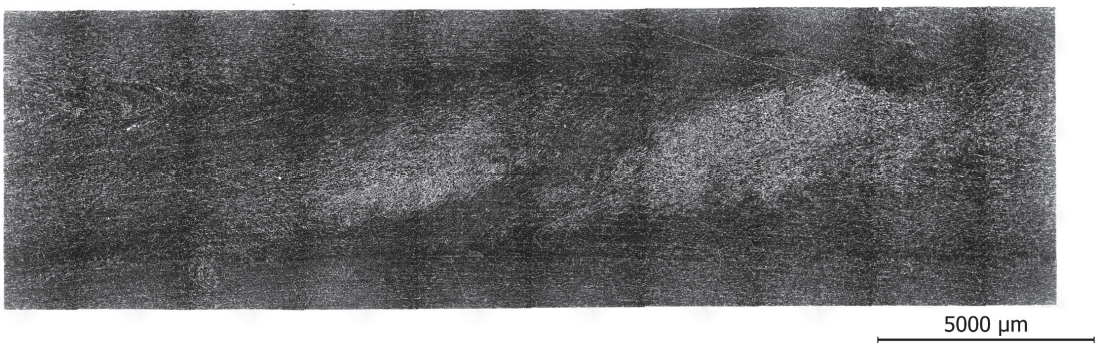


**Figure 5.39:** Polish number 6 of the insert type blade, position 3.29 mm from nozzle side. Moving further away from the middle of the specimen the fiber orientation turns into the picture plane again. So the middle of the modified weld line is pictured clearly.

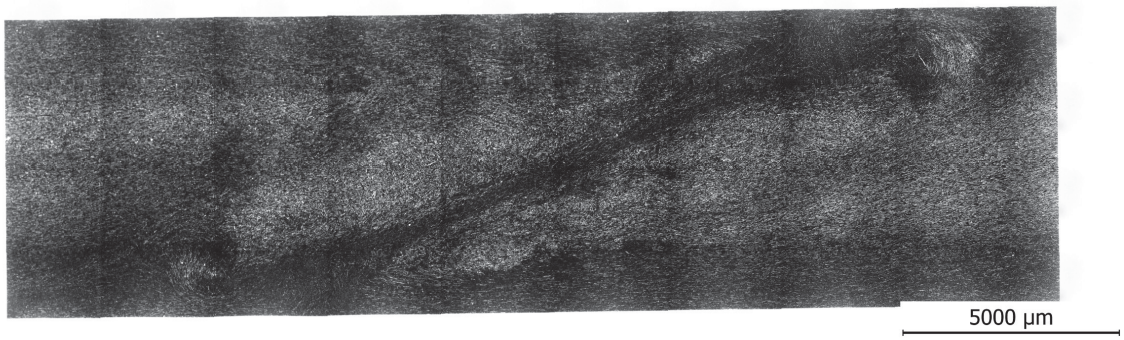


**Figure 5.40:** Polish number 7 of the insert type blade, position 3.86 mm from nozzle side. Only about 1 mm from the surface the weld line becomes clearly visible again.

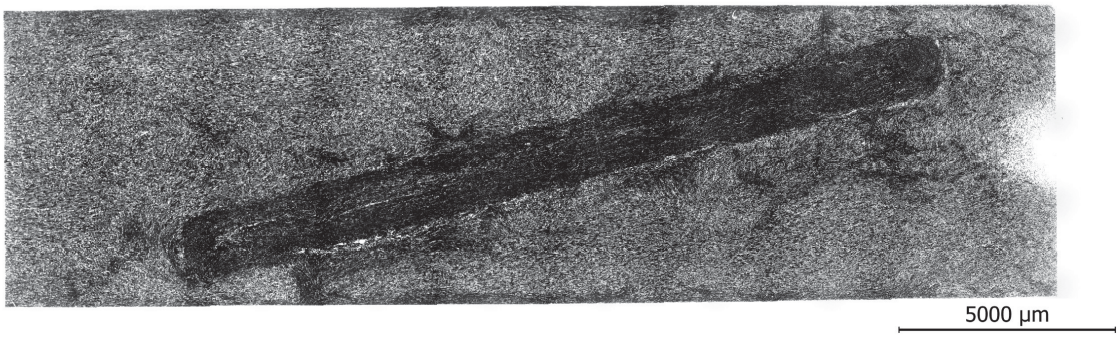


**Figure 5.41:** Polish number 8 of the insert type blade, position 4.67 mm from nozzle side. Close to the surface of the ejection side the form of the flow obstacle is clearly visible. This results from the flow of melt which pushes the flow obstacle out of the cavity and forms the protrusion.

# Chapter 6

# Summary

The existence of weld lines weakens specimens drastically. Standard weld lines halve bearable stress and strain in comparison to specimens without weld lines out of CF reinforced PEEK.

The aim of this thesis was to improve weld lines considering two possibilities: a) processing parameters and b) a geometric modification of the weld line.

No significant improvements were be obtained by changing the processing parameters holding pressure and injection speed. The only parameter having significant influence was the melt temperature, but only for the already improved modified weld line specimens.

A great improvement in weld line strength was obtained by a modification of the specimen with a movable flow obstacle. Thereby the weld line factor improved from 0.45 to 0.58 for tensile stress and from 0.36 to 0.47 for tensile strain. Concerning flexural properties the weld line factor rose from 0.49 to 0.82 for flexural stress and from 0.62 to 1.09 for flexural strain. This achievement comes presumable from the enlargement of the weld line area (which doubles) and favorable fiber orientation which is produced by redirecting the melt flow with the insert.

Five inserts with different head geometries were tested and compared. The specimens were manufactured at the center point level of the DOE giving the possibility to adjust parameters in both directions if necessary. Tensile and flexural properties were investigated resulting in following fact: There difference between the insert types, but only for tensile testing, further this difference is in the same range as the scatter of the investigated injection molding process. A comparison for different flexural configurations was made resulting in a favorable loading condition. If possible the load on modified weld lines shall be applied on the side where the insert is pushed out (here: the ejector side). The analysis of the fracture surface and fracture behavior of the tested specimens showed how specimens failed depending on loading and that there was a negative influence of the side weld line formed by a gap between the insert and mold wall.

It is worth mentioning that although all inserts achieve similar weld line quality they differ in easiness in production. The inserts halfblade and blade create protrudings which tend to make the produced specimen stick in the cavity at the location of the insert. A disadvantage of the plain head geometry is the slit which is used when producing specimens to give the possibility of pressing the insert out of the cavity. The

height of the slit has to be adjusted manually. Especially when many of these inserts are used this can be disadvantageous. Furthermore, the plain flow obstacle performs worse of all inserts at flexural testing configuration nozzle side up because of the (standard) weld line which is formed in the slit. The advantage of the head geometry plain is that the insert lines up precisely with the mold wall, leaving no protruding material. Out of these thoughts the inserts hole and round are favorable because they allow production without a slit and are easy to handle during production.

Polishes of the specimens were made and examined. Additionally, a possible three dimensional model of the modified weld line surface including the side weld lines was created. The model shows that the modified weld line shape does not always follow the insert. It is assumed that the melt pressure at the modified weld line dislocates it from the original position.

# Chapter 7

# Perspectives/Outlook

These studies could be the basics for further investigations of weld line modification. Following ideas could be investigated:

- One idea is that the flow obstacle is enlarged in length direction. This leads to a complete barrier for the flowing melt, so no more side weld lines are created because of a gap between the insert and mold wall.
- Another idea is that the angle of the modifying insert is adjustable to find the best angle for modification.
- Furthermore, a process capability as well as a machine capability could be determined to gather further information about reasons for the process scatter.

# Bibliography


[1] Akay, M.; Barkley, D.; Fibre orientation and mechanical behaviour in reinforced thermoplastic injection mouldings; Journal of Materials Science; (26), 1991, 2731–2742.

[2] Anonymus; CAMPUS Datenbank; URL `http://www.campusplastics.com/d`; last checked: 31.10.2012.

[3] Anonymus; Kunststoffe - Bestimmung der Zugeigenschaften - Teil 1: Allgemeine Grundsätze (ISO 527-1:1012).

[4] Anonymus; Minitab Statistical Software 16: Stat Guide, Key word: p-value.

[5] Anonymus; Zeus Focus on PEEK; URL `http://www.zeusinc.com/`; last checked: 31.10.2012.

[6] Anonymus; VICTREX PEEK 650CA30, Apr 2012; URL `http://www.victrex.com/docs/datasheets-docs/Victrex_TDS_650CA30.pdf`; last checked: 21.06.2013.

[7] Anonymus; Standard Practice for Design of Molds for Test Specimens of Plastic Molding Materials, Reapproved 1981.

[8] Barbosa, S.E.; Kenny, J.M.; Analysis of the Relationship between Processing Conditions, Fiber Orientation and Final Properties in Short Fiber Reinforced Polypropylene; Journal of Reinforced Plastics and Composites; 18 (5), 1999, 413–420.

[9] Boundy, R.H.; Boyer R. F.; Styrene: Its Polymers, Copolymers and Derivatives; Book Division, Reinhold Publishing Corporation, New York 36 and U. S. A., 1952.

[10] Bown, J.; Injection moulding of plastic components: A guide to efficiency, fault diagnosis and cure; McGraw-Hill Book Co., London and New York, 1979.

[11] Brunotte, R.; Kühnert, I.; Mennig, G.; Einfluss von pulsierendem Nachdruck auf die Festigkeit von Bindenähten; Technomer 2003. Fachbeitrge: 18. Fachtagung ber Verarbeitung und Anwendung von Polymeren, 2003.

[12] Chang, T.C.; Faison, E.; Optimization of Weld Line Quality in Injection Molding Using an Experimental Design Approach; Journal of Injection Molding Technology; 3 (2), June 1999, 61–66.

[13] Cloud, P.J.; McDowell, F.; Gerakaris S.; Reinforced Thermoplastics: Understanding Weld-Line Integrity; Plastics Technology; (August), 1976.

[14] Criens, R.M.; Moslé, H.G.; On the influence of knit-lines on the mechanical behavior of injection molded structural elements; ANTEC, 1982, 22–24.

[15] Criens, R.M.; Moslé, H.G.; The Influence of Knit-Lines on the Tensile Properties of Injection Molded Parts; Polymer Engineering & Science; 23 (10), 1983, 591–596.

[16] Dairanieh, I.S.; Haufe, A.; Wolf, H.J.; Mennig, G.; Computer Simulation of Weld Lines in Injection Molded Poly(Methyl Methacrylate); Polymer Engineering & Science; 36 (15), 1996, 2050–2057.

[17] Dickson, R.F.; Jones, C.J.; Harris, B.; Leach, D.C.; Moore, D.R.; The environmental fatigue behaviour of carbon fibre reinforced polyether ether ketone; Journal of Materials Science; 20 (1), 1985, 60–70.

[18] Ehrenstein, G.; Polymer-Werkstoffe: Struktur - Eigenschaften - Anwendung; 3 edition; Carl Hanser Verlag, München, 2010.

[19] Elsner, P.; Eyerer, P.; Hirth, T.; Domininghaus - Kunststoffe: Eigenschaften und Anwendungen; Springer, 2007.

[20] Fellahi, S.; Meddad, A.; Fisa, B.; Favis, B.D.; Weldlines in Injection-Molded Parts: A Review; Advances in Polymer Technology; 14 (3), 1995, 169–195.

[21] Fisa, B.; Rahmani, M.; Weldline Strength in Injection Molded Glass Fiber-Reinforced Polypropylene; Polymer Engineering & Science; 31 (18), 1991, 1330–1336.

[22] Gardner, G.; Cross, C.; The Effect of a Heated Core Pin on the Weld Strength of PP; Plastics Engineering; February, 1993, 29–31.

[23] Hamada, H.; Maekawa, Z.; Horino, T.; Lee, K.; Tomari, K.; Improvement of Weld Line Strength in Injection Molded FRTP Articles; Int. Polym. Process; (2), 1988, 131–136.

[24] Hobbs, S.Y.; Some Observations on the Morphology and Fracture Characteristics of Knit Lines; Polymer Engineering & Science; 14 (9), 1974, 621–626.

[25] Janko M.; BWZ weld line strength PC_v00r02_Lit: First run of the new weld-line mold (BWZ) with PC ( Hoerbiger standard PEEK CF20); Hoerbiger Internal Report, 2012.

[26] Janko M.; Project Agreement; Hoerbiger Internal Report, 2012.

[27] Kaiser, W.; Kunststoffchemie für Ingenieure: Von der Synthese bis zur Anwendung; 3 edition; Carl Hanser Verlag, München, 2011.

[28] Kazmer, D.O.; Roe, D.S.; Exploiting Melt Compressibility to Achieve Improved Weld Line Strengths; Plastics, Rubber and Composites Processing and Applications; (27), 1998, 272–278.

[29] Kenig, S.; Fiber Orientation Development in Molding of Polymer Composites; Polymer Composites; 7 (1), 1986, 50–55.

[30] Kim, J.K.; Song, J.H.; Chung, S.T.; Kwon, T.H.; Morphology and mechanical properties of injection molded articles with weld-lines; Polymer Engineering & Science; 37 (1), 1997, 228–241.

[31] Kobayashi, Y.; Teramoto, G.; Kanai, T.; The Unique Flow of Polypropylene at the Weld Line Behind an Obstacle in Injection Molding; Polymer Engineering & Science; 51 (3), 2011, 526–531.

[32] Liu, S.J.; Lin, K.Y.; Tsai, S.K.; Improving weldline strengths of injection moulded parts by ultrasonic oscillation; Plastics, Rubber and Composites; 37 (1), 2008, 23–28.

[33] Liu, S.J.; Wu, J.Y.; Chang, J.H.; Hung, S.W.; An Experimental Matrix Design to Optimize the Weldline Strength in Injection Molded Parts; Polymer Engineering & Science; 40 (5), 2000, 1256–1262.

[34] Malguarnera, S.; Weld Lines in Polymer Processing; Polymer-Plastics Technology and Engineering; 18 (1), 1982, 1–45.

[35] Malguarnera, S.; Manisali, A.; The Effects of Processing Parameters on the Tensile Properties of Weld Lines in Injection Molded Thermoplastics; Polymer Engineering & Science; 21 (10), 1981, 586–593.

[36] Malguarnera, S.; Manisali, A.I.; Riggs, D.C.; Weld Line Structures and Properties in Injection Molded Polypropylene; Polymer Engineering & Science; 21 (17), 1981, 1149–1155.

[37] Meddad, A.; Fisa, B.; Weldline Strength in Glass Fiber Reinforced Polyamide 66; Polymer Engineering & Science; 35 (11), 1995, 893–901.

[38] Menges, G.; Schacht, T.; Einfluss der Verarbeitungsparameter auf die mechanischen Eigenschaften von Bindenähten; Kunststoffberater; (4), 1988, 54–57.

[39] Mennig, G.; Die Bindenaht in der Kunststoffverarbeitung; Materialwissenschaft und Werkstofftechnik; 19 (11), 1988, 383–390.

[40] Mennig, G.; Zum Einfluss des Molekulargewichts auf die makroskopische Grenzfläche Bindenaht; Die Angewandte Makromolekulare Chemie; (185/86), 1991, 179–188.

[41] Michel, S.A.; Kieselbach, R.; Martens, H.J.; Fatigue strength of carbon fibre composites up to the gigacycle regime (gigacycle-composites); International Journal of Fatigue; 28 (3), 2006, 261–270.

[42] Montgomery, D.C.; Design and analysis of experiments; 8 edition; John Wiley, Hoboken (N.J.), 2013.

[43] Moslé, H.G.; Brüller, O.S.; Dick, H.; On the influence of the geometry and processing parameters on the mechanical properties of injection molded plastics; ANTEC; (26), 1980, 290–296.

[44] Moslé, H.G.; Criens, R.M.; Zur Festigkeit von Bindenähten in spritzgegossenen Polycarbonat-Plattenkörpern mit Durchbrüchen; Kunststoffe; (4), 1982, 222–227.

[45] Moslé, H.G.; Criens, R.M.; Dick, H.; On the Strength of Knit-Lines in Injection Molded Parts; ANTEC, 1984, 772–776.

[46] Moslé, H.G.; Dick, H.; Erarbeitung von Kennwerten für das kunststoffgerechte Konstruieren; Westdeutscher Verlag, Opladen [Germany - West], 1980.

[47] Ozcelik, B.; Kuram, E.; Topal, M.M.; Investigation the effects of obstacle geometries and injection molding parameters on weld line strength using experimental and finite element methods in plastic injection molding; International Communications in Heat and Mass Transfer; 39 (2), 2012, 275–281.

[48] Patcharaphun, S.; Investigation on Weldline Strength of Short-glass-fiber Reinforced Polycarbonate Manufactured through Push-Pull-processing Technique; Journal of Reinforced Plastics and Composites; 25 (4), 2005, 421–435.

[49] Patcharaphun, S.; Jariyatammanukul, P.; The Effect of Thickness on the Weld-Line Strength of Injection-Molded Thermoplastic Composites: Polymer-Plastics Technology and Engi- neering; Polymer-Plastics Technology and Engineering; 49 (13), 2010, 1305–1309.

[50] Patel, P.; Hull, T.R.; McCabe, R.W.; Flath, D.; Grasmeder, J.; Percy, M.; Mechanism of thermal decomposition of poly(ether ether ketone) (PEEK) from a review of decomposition studies; Polymer Degradation and Stability; 95 (5), 2010, 709–718.

[51] Saib, K.S.; Evans, W.J.; Isaac, D.H.; The role of microstructure during fatigue crack growth in poly(aryl ether ether ketone) (PEEK); Polymer; 34 (15), 1993, 3198–3203.

[52] Sanschagrin, B.; Gauvin, R.; Fisa, B.; Vu-Khanh, T.; Weldlines in Injection Molded Polypropylene: Effect of Filler Shape; Journal of Reinforced Plastics and Composites; 9 (2), 1990, 194–208.

[53] Savadori, A.; Pelliconi, A.; Romanini, D.; Weld line resistance in polypropylene composites; Plastics, Rubber Processing and Applications; (3), 1983, 215–221.

[54] Schambron, T.; Lowe, A.; McGregor, H.V.; Effects of environmental ageing on the static and cyclic bending properties of braided carbon fibre/PEEK bone plates; Composites Part B: Engineering; 39 (7–8), 2008, 1216–1220.

[55] Seldén, R.; Effect of Processing on Weld Line Strength in Five Thermoplastics; Polymer Engineering & Science; 37 (1), 1997, 205–218.

[56] Tomari, K.; Harada, T.; Fracture Toughness of Weldlines in Thermoplastic Injection Molding; Polymer Engineering & Science; 33 (15), 1993, 996–1001.

[57] Tomari, K.; Takashima, H.; Hamada, H.; Improvement of Weldline Strength of Fiber Reinforced Polycarbonate Injection Molded Articels Using Simultaneous Composite Injection Molding; Advances in Polymer Technology; 14 (1), 1995, 25–34.

[58] Tomari, K.; Tonogai, S.; Harada, T.; The V-Notch at Weld Lines in Polystyrene Injection Moldings; Polymer Engineering and Science; 30 (15), 1990, 931–936.

[59] Vaxman, A.; Narkis, M.; Siegmann, A.; Kenig, S.; Weld-Line Characteristics in Short Fiber Reinforced Thermoplastics; Polymer Composites; 12 (3), 1991, 161–168.

[60] Wu, C.H.; Liang, W.J.; Effects of Geometry and Injection-Molding Parameters on Weld-Line Strength; Polymer Engineering & Science; 45 (7), 2005, 1021–1030.

[61] Yokoi, H.; Murata, Y.; Watanabe, H.; Oka, K.; Visual Analysis of Weld Line Vanishing Process by Glass-Inserted Mold; ANTEC, 1991, 367–371.

[62] Zhang, T.; Breidt, C.; Chang, L.; Friedrich, K.; Wear of PEEK composites related to their mechanical performances; Tribology International; 37 (3), 2004, 271–277.

[63] Zhou, Y.; Mallick, P.K.; Fatigue Performance of an Injection-Molded Short E-Glass Fiber-Reinforced Polyamide 6,6. I. Effects of Orientation, Holes and Weld Line; Polymer Composites; 27 (2), 2006, 230–237.

# Chapter 8

# Appendix

## Material

**Table 8.1:** Recommended processing conditions for PEEK 650CA30 [6].

| **recommended processing conditions** | **conditions** |
|---|---|
| drying temperature/time | 150 °C / 3 h or 120 °C / 5 h |
| temperature settings | 390 / 400 / 405 / 410 / 415°C (nozzle) |
| hopper temperature | not greater than 100°C |
| mold temperature | 180 °C − 210 °C (max. 250 °C ) |
| runner | die / nozzle > 3 mm; manifold > 3.5 mm |
| gate | > 2 mm 0.5 x part thickness |

**Table 8.2:** Shrinkage and spiral flow of PEEK 650CA30 [6].

| **mould shrinkage and sprial flow** | | | | | | |
|---|---|---|---|---|---|---|
| | nozzle | tool | | method | unit | value |
| spiral flow | 415 °C | 200 °C | 1 mm thick section | Victrex | mm | 80 |
| | | | 3 mm thick section | | | 375 |
| mold shrinkage | 415 °C | 200 °C | along flow | ISO 294-4 | % | 0.1 |
| | | | across flow | | | 0.5 |

**Table 8.3:** Material properties for PEEK 650CA30 from Victrex data sheet [6] - part A.

| data | conditions | test method | units | value |
|---|---|---|---|---|
| **mechanical data** | | | | |
| tensile strength | break, 23 °C | ISO 527 | MPa | 250 |
| | break, 125 °C | | | 125 |
| | break, 175 °C | | | 85 |
| | break, 275 °C | | | 50 |
| tensile elongation | break, 23 °C | ISO 527 | % | 2.2 |
| tensile modulus | 23 °C | ISO 527 | GPa | 27 |
| flexural strength | 23 °C | ISO 178 | MPa | 370 |
| | 125 °C | | | 250 |
| | 175 °C | | | 120 |
| | 275 °C | | | 60 |
| flexural modulus | 23 °C | ISO 178 | GPa | 23 |
| compressive strength | 23 °C | ISO 604 | MPa | 280 |
| | 120 °C | | | 180 |
| | 200 °C | | | 60 |
| charpy impact strength | notched, 23 °C | ISO 179/1eA | kJ $m^2$ | 10.5 |
| | unnotched, 23 °C | ISO 179/1U | | 60 |
| izod impact strength | notched, 23 °C | ISO 180/A | kJ $m^2$ | 12 |
| | unnotched, 23 °C | ISO 180/U | | 60 |
| **thermal data** | | | | |
| melting point | | ISO 11357 | °C | 343 |
| glas transition $T_g$ | onset | ISO 11357 | °C | 143 |
| specific heat capacity | 23 °C | DSC | kJ $kg^{-1}$ °C $^{-1}$ | 1.8 |
| coefficient of thermal expansion | along flow below $T_g$ | ISO 11359 | ppm $K^{-1}$ | 6 |
| | average below $T_g$ | | ppm $K^{-1}$ | 50 |
| | along flow above $T_g$ | | ppm $K^{-1}$ | 6 |
| | average above $T_g$ | | ppm $K^{-1}$ | 135 |
| heat deflection temperature | 1.8 MPa | ISO 75-f | °C | 333 |
| thermal conductivity | 23 °C | ISO 22007-4 | W $m^{-1}$ $K^{-1}$ | 0.95 |

**Table 8.4:** Material properties for PEEK 650CA30 from Victrex data sheet [6] - part B.

| data | conditions | test method | units | value |
|---|---|---|---|---|
| **miscellaneous** | | | | |
| melt viscosity | 420 °C | ISO 11443 | Pa.s | 775 |
| density | crystalline | ISO 1183 | $g\,cm^{-3}$ | 1.40 |
| water absorption (3.2 mm thick tensile bar) | 24 h, 23 °C | ISO 62-1 | % | 0.04 * |
| (by immersion) | equilibrium, 23 °C | | | 0.3 [1] |
| volume resistivity | 23 °C 1 V | ASTM D4496 | Ω cm | $10^{5}$ [1] |

*result based on similar product

# Design of inserts

On the next page the designs of four inserts is shown. The only missing modified geometry is type plain. It has no modifications and has a plane top, all other dimensions are the same as for the four shown inserts.

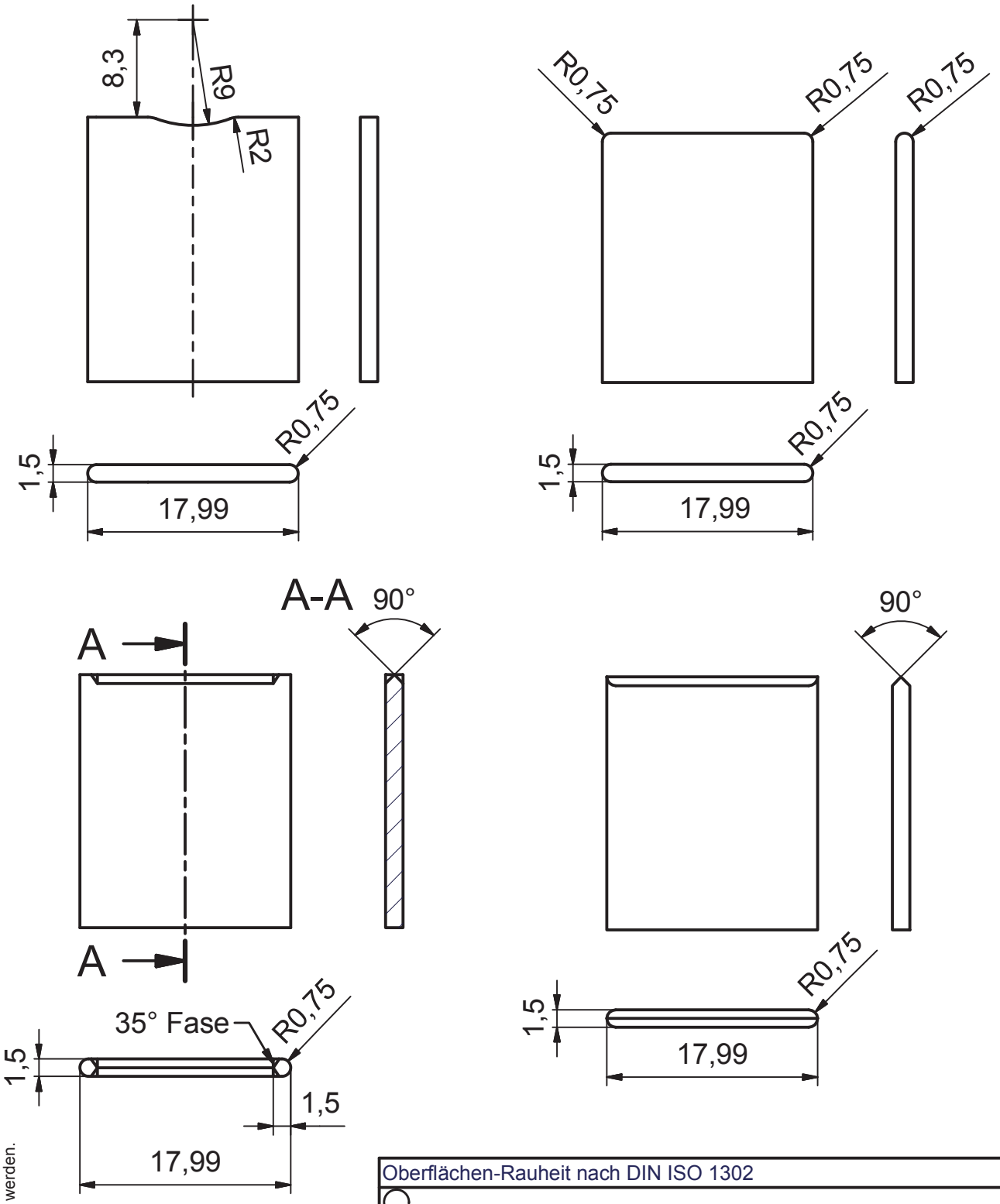




Oberflächen-Rauheit nach DIN ISO 1302

HOERBIGER

HOERBIGER VENTILWERKE GmbH & Co KG
Braunhubergasse 23 · A-1110 Vienna, Austria

| | Tag | Zch. |
|---|---|---|
| gez. | 10.08.2012 | u1ac_jm |
| gepr. | | |
| ngepr. | | |

Freimaßtoleranz nach DIN ISO 2768-1 Längenmaß

| 0,5 bis 6 | über 6 bis 30 | über 30 bis120 | über120 bis400 | über400 bis1000 |
|---|---|---|---|---|
| ± 0,1 | ± 0,2 | ± 0,3 | ± 0,5 | ± 0,8 |

Werkstoff

Maßstab —

Gewicht [kg]

Grundzeichnung Nr.

Modell Nr.
Schnitt Nr.
Vorrichtungs Nr.

M351-Einsatz-1

Blatt Nr. 1

Stücklisten Nr.

A4

# Acronyms

| | |
|---|---|
| ABS | acrylonitrile butadiene styrene |
| ANOVA | analysis of variance |
| CF | carbon fibers |
| DOE | design of experiments |
| EPDM | ethylen/propylene/diene terpolymere |
| ES | ejector side |
| GF | glass fibers |
| HDPE | high density polyethylene |
| MOD | modified |
| NS | nozzle side |
| PA6 | polyamide 6 |
| PAEK | polyaryl ether ketone |
| PC | polycarbonate |
| PE | polyethylne |
| PEEK | polyether ether ketone |
| PP | polypropylne |
| PPS | polyphenylne sulfide |
| PS | polystyrene |
| PTFE | polytetrafluroethylene |
| STD | standard |

# Symbols

| Symbol | Unit | Meaning |
|---|---|---|
| $T_g$ | $°C$ | glass transition temperature |
| $T_m$ | $°C$ | melting temperature |
| l | mm | length dimension of a filler |
| b | mm | width dimension of a filler |
| d | mm | height/diameter of a filler |
| $\sigma_b$ | $N/mm^2$ | flexural stress |
| $F$ | N | load |
| $L$ | mm | specimen length |
| $B$ | mm | specimen width |
| $H$ | mm | specimen height |
| $\epsilon_b$ | % | flexural strain/edge fibre elongation |
| $\delta$ | mm | displacement of traverse |
| $\sigma_t$ | $N/mm^2$ | tensile stress |
| $\epsilon_t$ | % | tensile strain |
| $\delta_t$ | mm | displacement of the extensiometer |
| $L_0$ | mm | distance of fixed support in flexural testing |
| $l_0$ | mm | distance between the arms of the extensiometer at the beginning |

# List of Figures

# List of Tables